

Knot polynomials from 1-cocycles

Thomas Fiedler

December 14, 2024

pour Séverine

Abstract

Let M_n be the topological moduli space of all parallel n -cables of long framed oriented knots in 3-space. We construct in a combinatorial way for each natural number $n > 1$ a 1-cocycle R_n which represents a non trivial class in $H^1(M_n; \mathbb{Z}[x_1, x_2, \dots, x_1^{-1}, x_2^{-1}, \dots])$, where the number of variables x_i depends on n . To each generic point in M_n we associate in a canonical way an arc *scan* in M_n , such that $R_n(\text{scan})$ is already a polynomial knot invariant. We show that $R_3(\text{scan})$ detects the non-invertibility of the knot 8_{17} in a very simple way and without using the knot group.

There are two well-known canonical loops in M_n for each parallel n -cable of a long framed knot K : Gramain's loop *rot* and the Fox-Hatcher loop *fh*. The calculation of R_n is of at most quartic complexity for these loops with respect to the number of crossings of K for each fixed n . It follows from results of Hatcher that K is not a torus knot if the rational function $R_n(fh(K))/R_n(rot(K))$ is not constant for each $n > 1$.

$\oplus_n R_n$ is a natural candidate in order to separate all classes in $H_1(M_1; \mathbb{Q}) \cong H_1(M_n; \mathbb{Q})$, and in particular to distinguish all knot types $\pi_0(M_1)$.

1

¹2000 *Mathematics Subject Classification*: 57M25 *Keywords*: polynomial valued 1-cocycles, non-invertibility of knots, global tetrahedron equations

Contents

1	Introduction	2
2	Main results	12
2.1	The 1-cocycle R_1 in $M \setminus \Sigma_{trans-cusp}^{(2)}$	12
2.2	The 1-cocycle R_n in M for $n > 1$	19
3	First applications, questions and conjectures	21
3.1	Applications of the 1-cocycle R_1 in $M \setminus \Sigma_{trans-cusp}^{(2)}$. Detecting the non-invertibility of string links with two components . . .	21
3.2	Applications of the 1-cocycle R_n in M for $n > 1$. Detecting the non-invertibility of knots	32
4	Proof	43
4.1	Generalities and reductions by using singularity theory	43
4.2	Reidemeister II moves in a cusp and in a flex	50
4.3	Simultaneous Reidemeister moves	51
4.4	Refined tetrahedron equation for string links	54
4.5	Cube equations	75
4.6	Moving cusps and scan-property	88
4.7	Invariance of R_n^i for $n > 1$	96

1 Introduction

This paper contains infinitely many new knot polynomials which

- can distinguish the orientations of knots
- can be calculated with a smaller degree of complexity than the Alexander polynomial
- can distinguish homology classes of loops in the space of all long knots
- carry topological and perhaps even geometrical information about knots
- distinguish perhaps all classical knots in 3-space.

They have their origin in a slight change of the subject: we study 1-parameter families of knots instead of individual knots.

The topological moduli space of a knot is the infinite dimensional space of all smooth knots isotopic to the given knot. Our philosophy is that *finite type invariants should be sufficient in general to separate all topological objects of a given kind if and only if each component of the topological moduli space of*

these objects is a contractible space. An example are braids. It is well known that the topological moduli space of each braid, seen as a tangle in the 3-ball, is a contractible space, and indeed e.g. Bar-Natan has proven that finite type invariants separate all braids [2]. (An exception to our philosophy are closed 2-braids. They are evidently distinguished by the unique finite type invariant of degree 1. However, in this case closed braids are isotopic if and only if the braids are already isotopic.) On the other hand the moduli spaces of closed braids in the solid torus (besides for the closed 1-braid) and of knots in the 3-sphere are never contractible spaces. Hatcher has proven e.g. that for the oriented trivial knot the moduli space deformation retracts onto the Grassmannian of oriented 2-planes in 4-space. It is not known whether finite type invariants can detect the non-invertibility of closed braids and of knots in 3-space, but it is known that quantum invariants can definitely not. Again, if we consider oriented tangles of two non-closed components in the 3-ball and such that the complement does not contain an incompressible torus then each component of the moduli space is a contractible space. And indeed Duzhin and Karev [13] have found a finite type invariant of degree 7, which can sometimes detect the non-invertibility of such a tangle (and it follows from results of Bar-Natan that there are no such invariants of degree smaller than 7, see [3], [1]).

The topology of moduli spaces of knots was much studied in [23], [7], [8], [9], [10]. It seems that the Teiblum-Turchin 1-cocycle v_3^1 and its lift to \mathbb{R} by Sakai were the only known 1-cocycles for long knots which represent a non trivial cohomology class. The Teiblum-Turchin 1-cocycle is an integer valued 1-cocycle of degree 3 in the sense of Vassiliev's theory [39]. Its reduction mod 2 has a combinatorial description and can be calculated, see [40] and [38]. Sakai has defined a \mathbb{R} valued version of the Teiblum-Turchin 1-cocycle via configuration space integrals [36]. We have found a very complicated formula for an integer extension of $v_3^1 \bmod 2$ in [16]. The most beautiful formula for an integer valued 1-cocycle for long knots which extends $v_3^1 \bmod 2$ and which probably coincides with v_3^1 was found by Mortier [31], [32].

The idea is now to construct polynomial valued 1-cocycles and to apply them to canonical loops in the components of the topological moduli space in order to obtain polynomial knot invariants. Following this philosophy we had constructed integer valued finite type 1-cocycles for closed braids in [15]. (In fact, these invariants have a completely evident deformation quantization to polynomial valued invariants, which are no longer of finite type but still calculable with polynomial complexity. We will come back to this in a new

version of [15].) A refinement of these 1-cocycles, which uses in addition some local system by giving names to the crossings of the closed braids, can indeed detect sometimes the non-invertibility of a closed braid (that is the non-invertibility of the link in S^3 which consists of the closed braid together with the closure of the braid axis), when it is applied to the loop generated by the rotation of the solid torus around its core, compare [15]. Since then we have tried to find such 1-cocycles for long knots in the 3-space.

It is well known that if a knot K in the 3-sphere is not a satellite then its topological moduli space is a $K(\pi, 1)$ with π a finite group (in fact $\pi = \text{Aut}(\pi_1(S^3 \setminus K), \partial)$, where ∂ is the peripheral system of the knot K , see [41], [25], [24]). Consequently, in this case there can't exist any non-trivial 1-cocycles with values in a torsion free module. However, it is well known that the components of the moduli space of knots in the 3-sphere are in a natural 1 – 1 correspondence with the components of the moduli space of long knots in 3-space. Hatcher has proven that for long knots in 3-space the situation is much better. There are always two canonical non-trivial loops in the component of the topological moduli space of a long knot K if it is not the trivial knot: Gramain's loop, denoted by $\text{rot}(K)$, and the Fox-Hatcher loop, denoted by $\text{fh}(K)$. *Gramain's loop* is induced by the rotation of the 3-space around the long axis of the long knot [20]. *Fox-Hatcher's loop* is defined as follows: one puts a pearl (i.e. a small 3-ball B) on the closure of the long framed knot K in the 3-sphere. The part of K in $S^3 \setminus B$ is a long knot. Pushing B once along the knot with respecting the framing induces the Fox-Hatcher loop, see [23] and also [19]. The homology class of $\text{rot}(K)$ does not depend on the framing of K and changing the framing of K adds multiples of $\text{rot}(K)$ to $\text{fh}(K)$. Notice that the Fox-Hatcher loop has a canonical orientation induced by the orientation of the long knot. The same loops are still well defined and non-trivial for those n -string links which are n -cables of a framed non-trivial long knot. It follows from results of Hatcher [23] and Budney [10] that these two loops are linearly dependent in the rational homology if and only if the knot is a torus knot (compare also Lemma 1 in Section 3.2). Moreover, Hatcher has shown that the topological moduli space of a long hyperbolic knot deformation retracts onto a 2-dimensional torus. Hence it follows from Künneth's formula that it is sufficient to construct just 1-cocycles in this case.

We had constructed a 1-cocycle for long knots with values in a module generated by singular long knots in [17]. Its construction is correct but the examples in [17] are wrong. We can prove now that this 1-cocycle is in reality

a 1-coboundary and it is not interesting.

The present paper contains the first polynomial valued 1-cocycle R_n for the topological moduli space of all oriented string links of n components for $n > 1$, and which is not a 1-coboundary, see Theorem 2 in Section 2.2. It leads to the first knot polynomials which can detect the orientation of a classical knot by applying R_n to n -cables of a framed long knot, see Examples 4 and 5 in Section 3.2. An important point is that we do not make any explicit use of the knot group (thus avoiding the usual problems in group theory). Moreover, our invariants are calculable with complexity of degree at most 4 with respect to the number of crossings for each fixed $n > 1$.

The goal of this paper is to construct these invariants, to calculate first examples and to give first applications. The development of the general theory of these invariants as well as perhaps a proof that they eventually distinguish all classical knots will probably be the subject of a long term research.

(Notice that our invariants can not be generalized for virtual knots in contrast to most other known knot invariants in dimension 3. This comes from the fact that each non-trivial loop contains necessarily forbidden moves. However, $R_n(\text{scan})$ could perhaps be generalized for welded knots because the scan-arc contains only one type of forbidden moves.)

Definition 1 *We fix a orthogonal projection $pr : \mathbb{C} \times \mathbb{R} \rightarrow \mathbb{C}$. A long knot K is an oriented smoothly embedded copy of \mathbb{R} in $\mathbb{C} \times \mathbb{R}$ which coincides with a fixed straight line (e.g. the real axis in $\mathbb{C} \times 0$) outside a compact set. A (parallel) n -cable of a framed long knot is a n -component link with fixed endpoints where each component is parallel to the framed long knot with respect to the blackboard framing given by pr . A n -string link T is a n -component link with fixed endpoints where each component is parallel to a long knot in $\mathbb{C} \times 0$ outside some compact set.*

It is convenient for calculations to represent a long knot K as a closed braid with just one strand opened to go to infinity.

Let M be the topological moduli space of all oriented smooth string links in $\mathbb{C} \times \mathbb{R}$ (in particular $M_n \subset M$).

It follows from Thom-Mather singularity theory that each component of the infinite dimensional space M has a natural *stratification with respect to pr* :

$$M = \Sigma^{(0)} \cup \Sigma^{(1)} \cup \Sigma^{(2)} \cup \Sigma^{(3)} \cup \Sigma^{(4)} \dots$$

Here, $\Sigma^{(i)}$ denotes the union of all strata of codimension i .

The strata of codimension 0 correspond to the usual generic *diagrams of knots*, i.e. all singularities in the projection are ordinary double points. So, our *discriminant* is the complement of $\Sigma^{(0)}$ in M . Notice that this discriminant of non-generic diagrams is very different from Vassiliev's discriminant of singular knots [39].

The three types of strata of codimension 1 correspond to the *Reidemeister moves*, i.e. non generic diagrams which have exactly one ordinary triple point, denoted by $\Sigma_{tri}^{(1)}$, or one ordinary self-tangency, denoted by $\Sigma_{tan}^{(1)}$, or one ordinary cusp, denoted by $\Sigma_{cusp}^{(1)}$, in the projection pr . We call the triple point together with the under-over information (i.e. its embedded resolution) a *triple crossing*. We distinguish self-tangencies for which the orientation of the two tangents coincide, called $\Sigma_{tan+}^{(1)}$, from those for which the orientations of the tangents are opposite, called $\Sigma_{tan-}^{(1)}$.

Proposition 1 *There are exactly six types of strata of codimension 2. They correspond to non generic diagrams which have exactly either*

- (1) *one ordinary quadruple point, denoted by $\Sigma_{quad}^{(2)}$*
- (2) *one ordinary self-tangency with a transverse branch passing through the tangent point, denoted by $\Sigma_{trans-self}^{(2)}$*
- (3) *one ordinary self-tangency in an ordinary flex ($x = y^3$), denoted by $\Sigma_{self-flex}^{(2)}$*
- (4) *two singularities of codimension 1 in disjoint small discs (this corresponds to the transverse intersection of two strata from $\Sigma^{(1)}$, i.e. two simultaneous Reidemeister moves at different places of the diagram)*
- (5) *one ordinary cusp ($x^2 = y^3$) with a transverse branch passing through the cusp, denoted by $\Sigma_{trans-cusp}^{(2)}$*
- (6) *one degenerate cusp, locally given by $x^2 = y^5$, denoted by $\Sigma_{cusp-deg}^{(2)}$*

We show these strata in Fig. 1.

For a proof as well as for all other necessary preparations from singularity theory see [18] (and also [11] and references therein).

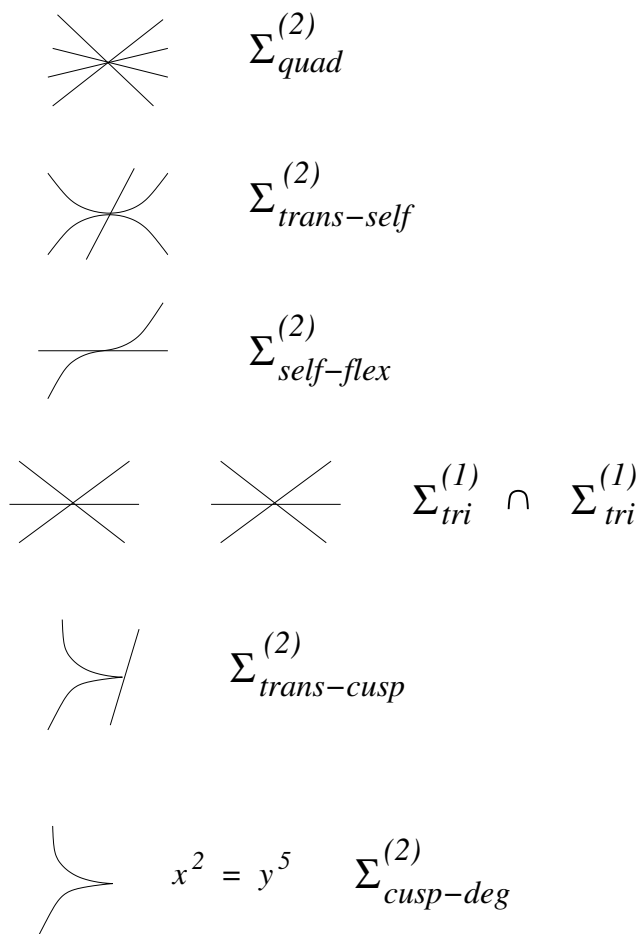


Figure 1: The strata of codimension 2 of the discriminant of non generic projections

Our strategy is the following: for an oriented generic loop or arc in M we associate some polynomial to the intersection with each stratum in $\Sigma^{(1)}$, i.e. to each Reidemeister move, and we sum up over all Reidemeister moves in the arc. We have to prove now that this sum is 0 for each meridian of strata in $\Sigma^{(2)}$. This is extremely complex but we use strata from $\Sigma^{(3)}$ in order to reduce the proof to a few strata in $\Sigma^{(2)}$. It follows that our sum is invariant under generic homotopies of arcs (with fixed endpoints). But it takes its values in an abelian ring and hence it is a 1-cocycle.

The construction of R_n is now in two steps. First we construct a 1-cocycle R_1 which represents a non-trivial class only in $H^1(M \setminus \Sigma_{trans-cusp}^{(2)}; \mathbb{Z}[x, x^{-1}])$, see Theorem 1 in Section 2.1. In order to make it a 1-cocycle without taking out $\Sigma_{trans-cusp}^{(2)}$ we have to use cables. We refine R_1 by using *admissible colorings of the 1-cocycle* coming from colorings of the components of the n -cable. The number of admissible colorings increases rapidly with n . Each admissible coloring i on R_1 leads to a 1-cocycle R_n^i which represents an element now in $H^1(M_n; \mathbb{Z}[x_i, x_i^{-1}])$ and R_n is the sum over all admissible colorings of R_1 . We can apply R_n^i to the loops *rot* and *fh* in M_n . But let T be a tangle of n non-closed components in the 3-ball or equivalently a *string link* and such that there is no incompressible torus in its complement. Then of course $[R_n] = 0$. But it is remarkable that we can nevertheless extract non trivial information from the 1-cocycle R_n . Let us add a small positive curl (possibly linked with the other components of T) to an arbitrary component of T near to the boundary ∂T of T at infinity.

Definition 2 *The scan-arc $scan(T)$ in M is the regular isotopy which makes the small curl big under the rest of T up to being near to infinity, compare Fig. 2.*

It turns out that $R_n(scan(T))$ is an isotopy invariant of T for all $n > 0$. It can detect sometimes the orientation of a knot, at least starting from 3-cables of the long knot, and conjecturally $R_1(scan(T))$ can detect sometimes with cubical complexity that a 2-component tangle T is not a 2-cable of any long knot (compare Section 3.1).

We could see the *scan-arc* in the following way. Given a framed knot in S^3 we transform it first into a long knot. We add then a long longitude and we glue a meridian of the knot as a curl to the longitude. We push now the knot together with its longitude half way through the attached meridian and calculate R_n on this arc in the knot space. *Hence $R_n(scan)$ is a combinatorial way to make explicit use of the peripheral system of a knot without*

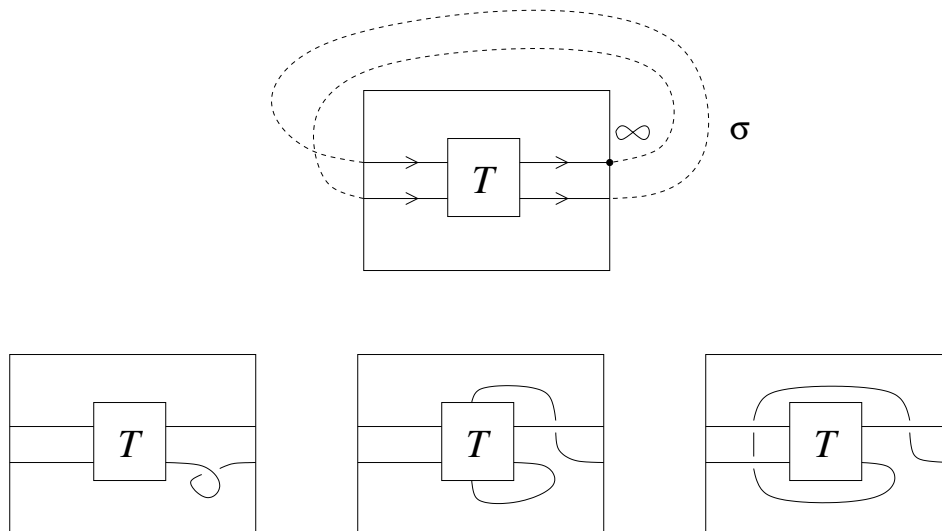


Figure 2: a scan-arc for a string link T

making explicit use of the knot group (compare [41] for the definition of the peripheral system and its application to knot theory). This seems to be the reason that our invariant can detect the orientation of a knot in contrast to all other known knot invariants which make no explicit use of the knot group too: invariants of polynomial complexity as (the known) Vassiliev invariants, the Alexander polynomial, the Rozansky polynomials and invariants of exponential complexity as the Jones polynomial, the HOMFLYPT polynomial, the Kauffman polynomial and so on as well as their categorifications. Notice that even the A-polynomial, which uses representations of the knot group into $SL(2, \mathbb{C})$, does not distinguish the orientations of knots, compare e.g. [12].

The paper is organized as follows: in Section 2 we give a self-contained definition of R_n in its most compact form. The interested reader could already write a computer program and calculate lots of examples. The calculation of R_n is of complexity of degree 4 for the Fox-Hatcher loop (however the leading coefficient is already rather big for $n = 2$) and it is of degree 3 for Gramain's loop and for the scan-arc with respect to the number of crossings of a long knot for fixed n . So, a priori it is even better than the Alexander polynomial (which can be calculated with complexity of degree 4, thanks to Dror Bar-Natan for the information) and it could be calculated for knots

with thousands of crossings.

In Section 3 we give first applications of R_n and we formulate conjectures and open questions.

Section 4 contains the proof that R_n is indeed a 1-cocycle. Showing that $R_1 = 0$ for the meridians of $\Sigma_{quad}^{(2)}$ is by far the hardest part. This corresponds to finding a new solution of the tetrahedron equation. Consider four oriented straight lines which form a braid and such that the intersection of their projection into \mathbb{C} consists of a single point. We call this an *ordinary quadruple crossing*. After a generic perturbation of the four lines we will see now exactly six ordinary crossings. We assume that all six crossings are positive and we call the corresponding quadruple crossing a *positive quadruple crossing*. Quadruple crossings form smooth strata of codimension 2 in the topological moduli space of lines in 3-space which is equipped with a fixed projection pr . Each generic point in such a stratum is adjacent to exactly eight smooth strata of codimension 1. Each of them corresponds to configurations of lines which have exactly one ordinary triple crossing besides the remaining ordinary crossings. We number the lines from 1 to 4 from the lowest to the highest (with respect to the projection pr). The eight strata of triple crossings glue pairwise together to form four smooth strata which intersect pairwise transversally in the stratum of the quadruple crossing, see e.g. [18]. The strata of triple crossings are determined by the names of the three lines which give the triple crossing. For shorter writing we give them names from P_1 to P_4 and \bar{P}_1 to \bar{P}_4 for the corresponding stratum on the other side of the quadruple crossing. We show the intersection of a normal 2-disc of the stratum of codimension 2 of a positive quadruple crossing with the strata of codimension 1 in Fig. 3. The strata of codimension 1 have a natural coorientation, compare the next section. We could interpret the six ordinary crossings as the edges of a tetrahedron and the four triple crossings likewise as the vertices's or the 2-faces of the tetrahedron. For the classical tetrahedron equation one associates to each stratum P_i some operator (or some R-matrix) which depends only on the names of the three lines and to each stratum \bar{P}_i the inverse operator. The tetrahedron equation says now that if we go along the meridian then the product of these operators is equal to the identity. Notice, that in the literature, see e.g. [28], one considers planar configurations of lines. But this is of course equivalent to our situation because all crossings are positive and hence the lift of the lines into 3-space is determined by the planar picture. Moreover, each move of the lines in the plane which preserves the transversality lifts to an isotopy of the lines

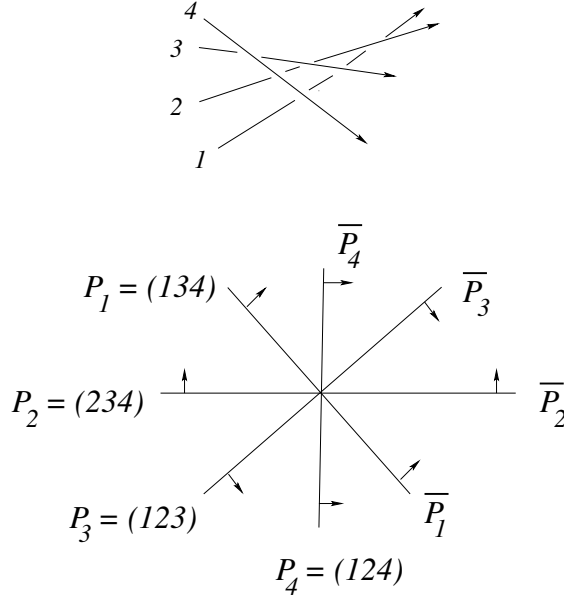


Figure 3: intersection of a normal 2-disc of a positive quadruple crossing with the strata of triple crossings

in 3-space. The tetrahedron equation has many solutions, the first one was found by Zamolodchikov, see e.g. [28].

However, the solutions of the classical tetrahedron equation are not well adapted in order to construct 1-cocycles for moduli spaces of knots. First of all there is no natural way to give names to the three branches of a triple crossing in an arbitrary knot isotopy besides in the case of closed braids. But it is not hard to see that in the case of braids Markov moves would make big trouble (see e.g. [5] for the definition of Markov moves and Markov's theorem). As well known, a Markov move leads only to a normalization factor in the construction of 0-cocycles, see e.g. [26]. However, the place in the diagram and the moment in the isotopy of a Markov move become important in the construction of 1-cocycles (as already indicated by the lack of control over the Markov moves in Markov's theorem). Secondly, a local solution of the tetrahedron equation is of no use for us because as already pointed out there are no integer polynomial valued 1-cocycles for knots in the 3-sphere. We have to replace them by long knots and we have to use the point at infinity on the knot. Therefore we have to consider *twenty four* different positive tetrahedron equations, corresponding to the six different abstract closures

of the four lines to a circle and to the four different choices of the point at infinity in each of the six cases. One easily sees that there are exactly *forty eight* local types of quadruple crossings (analog to the eight local types of triple crossings). Each of the six involved crossings appears in exactly four of the triple crossings. In order to obtain polynomial valued 1-cocycles instead of a integer valued one we have to keep track of the six crossings individually and we have to split the tetrahedron equation further into *six* equations: for each of the six crossings the contributions of the four corresponding strata of triple crossings have already to sum up to 0. Consequently, our tetrahedron equation splits into $24 \times 48 \times 6 = 6912$ equations! Surprisingly, it has an interesting solution, which is constructed combinatorially by using relative finite type invariants of degrees 1 and 2 with respect to couples: a Reidemeister move of a knot diagram together with a crossing in the move. Our solution is *not local* in contrast to all other solutions which come from representation theory of the Yang-Baxter or the tetrahedron equation, i.e. the contribution of the move is not determined by the three lines alone but uses the whole Gauss diagram of the long knot.

Acknowledgments

I wish to thank Ryan Budney and Victor Turchin for patiently explaining to me the topology of moduli spaces of knots, and Hugh Morton for his observation that the graph in what has become the cube equations is indeed the 1-skeleton of a cube. I'm especially grateful to Dror Bar-Natan for first observing a telescoping effect which implies that all my previous 1-cocycles for long knots were actually 1-coboundaries. The present paper has grown out from trying to avoid this telescoping effect. Finally, let me mention that without Séverine, who has created all the figures, this paper wouldn't exist.

2 Main results

2.1 The 1-cocycle R_1 in $M \setminus \Sigma_{trans-cusp}^{(2)}$

To each Reidemeister move of type III corresponds a diagram with a *triple crossing* p : three branches of the knot (the highest, middle and lowest with respect to the projection $pr : \mathbb{C} \times \mathbb{R} \rightarrow \mathbb{C}$) have a common point in the projection into the plane. A small perturbation of the triple crossing leads to an ordinary diagram with three crossings near $pr(p)$.

Definition 3 *We call the crossing between the highest and the lowest branch*

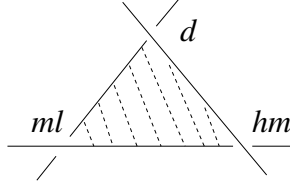


Figure 4: The names of the crossings in a R III move

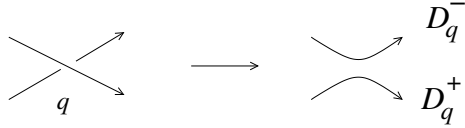


Figure 5: Two ordered knot diagrams associated to a crossing q

of the triple crossing p the distinguished crossing of p and we denote it by d . The crossing between the highest branch and the middle branch is denoted by hm and that of the middle branch with the lowest is denoted by ml , compare Fig. 4. Smoothing a crossing c with respect to the orientation splits the closure of K into two oriented and ordered circles. We call D_c^+ the component which goes from the under-cross to the over-cross at c and by D_c^- the remaining component, compare Fig. 5.

In a Reidemeister move of type II both new crossings are considered as distinguished and we often identify them.

A Gauss diagram of a long knot K is an oriented circle with oriented chords and a marked point corresponding to the point at ∞ .

String links are always oriented from the left to the right, i.e. near to infinity each component of T projects orientation preserving onto the oriented x -axis. We have to chose an abstract closure of T to a circle and we have to chose a point at infinity in the closure (we could see this as adding at infinity a pointed virtual permutation braid which represents in the symmetric group a n -cycle). We denote the closed diagram still by T .

Our 1-cocycle will of course depend on these two choices. There exists an orientation preserving diffeomorphism from the oriented line to the closed oriented string link T such that each chord connects a pair of points which are mapped onto a crossing of $pr(T)$ and infinity is mapped to the marked point. The chords are oriented from the preimage of the under crossing to the preimage of the over crossing (here we use the orientation of the \mathbb{R} -

factor). The circle of a Gauss diagram in the plane is always equipped with the counter-clockwise orientation.

A *Gauss diagram formula* of degree k is an expression assigned to the diagram of a closed string link T , which is of the following form:

$$\sum_{\text{configurations}} \text{function}(\text{ writhes of the crossings})$$

where the sum is taken over all possible choices of k (unordered) different crossings in the diagram such that the chords arising from these crossings in the diagram of T build a given sub-diagram with given marking. The marked sub-diagrams are called *configurations*. If the function is (as usual) the product of the writhes of the crossings in the configuration, then we will denote the sum shortly by the configuration itself. As usual, the writhe of a positive crossing is $+1$ and the writhe of a negative crossing is -1 .

Definition 4 *An ordinary crossing c in a diagram T is of (homological) type 1 if $\infty \in D_c^+$ and is of (homological) type 0 otherwise, denoted by $[c] = 1$ respectively $[c] = 0$.*

Let T be a generic diagram with a triple crossing or a self-tangency p and let d be the distinguished crossing for p . In the case of a self-tangency we identify the two distinguished crossings.

Definition 5 *Let c be a crossing of type 1. Then the linear weight $W_1(c)$ is defined as the sum of the writhes $w(r)$ of the crossings r in T which form one of the configurations shown in Fig. 6. These crossings r , which are of type 0 are called r -crossings of c .*

Notice that we do not multiply here $W_1(c)$ by the writhe $w(c)$.

Definition 6 *Let c be a crossing of type 0. Then the quadratic weight $W_2(c)$ is defined by the Gauss diagram formula shown in Fig. 7. The crossings f , which are of type 1, are called f -crossings of c .*

The second (degenerate) configuration in Fig. 7 can of course not appear for a self-tangency but only for a triple crossing.

$$W_I(c) = \begin{array}{c} \text{Diagram 1} \end{array} + \begin{array}{c} \text{Diagram 2} \end{array}$$

Figure 6: The linear weight $W_I(c)$ for c of type 1

$$W_2(c) = \sum w(f) W_I(f) + \sum w(f) W_I(f)$$

$$\begin{array}{c} \text{Diagram 1} \end{array} \quad \begin{array}{c} \text{Diagram 2} \end{array}$$

$$+ \sum w(f) W_I(f) + \sum w(f) W_I(f)$$

$$\begin{array}{c} \text{Diagram 3} \end{array} \quad \begin{array}{c} \text{Diagram 4} \end{array}$$

Figure 7: The quadratic weight $W_2(c)$ for c of type 0

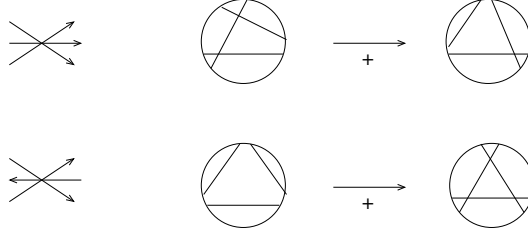


Figure 8: The coorientation for Reidemeister III moves

Definition 7 We consider the Gauss diagrams for the crossings involved in the move. The coorientation of a self-tangency is the direction from no crossings to the diagram with two new crossings. For a triple crossing the coorientation is the direction from two intersection points of the corresponding three arrows to one intersection point and of no intersection point of the three arrows to three intersection points, compare Fig. 8. (We will see later in the cube equations for $\Sigma_{\text{trans-self}}^{(2)}$ that the two coorientations for triple crossings fit together for the strata of $\Sigma_{\text{tri}}^{(1)}$ which come together in $\Sigma_{\text{trans-self}}^{(2)}$.) Evidently, our coorientation is completely determined by the corresponding planar curves. We call the side of the complement of $\Sigma_{\text{tri}}^{(1)}$ in M into which points the coorientation, the positive side of $\Sigma_{\text{tri}}^{(1)}$.

Reidemeister moves of type I do not contribute at all.

Each transverse intersection p of an oriented arc with $\Sigma^{(1)}$ has now an intersection index $+1$ or -1 , called $\text{sign}(p)$, by comparing the orientation of the arc with the coorientation of $\Sigma^{(1)}$.

Definition 8 The integer linking number $l(c)$ of an ordinary crossing c is defined as the sum of the writhe of all crossings between D_c^+ and D_c^- (hence in the case of a long knot it is twice the usual linking number of the oriented 2-component link).

Definition 9 The linking number $l(p)$ for $p \in \Sigma_{\text{tan-}}^{(1)}$ is defined as $l(d^+) = l(d^-)$ where d^+ is the new positive crossing and d^- is the new negative crossing. The linking number $l(p)$ for $p \in \Sigma_{\text{tan+}}^{(1)}$ is defined as $l(d^+) + 1 = l(d^-) - 1$ (in other words, only the arrows in the Gauss diagram which cut the double arrow $d^+ = d^-$ contribute to $l(p)$).

Let $p \in \Sigma_{\text{tri}}^{(1)}$ and let c be an ordinary crossing from the triple crossing. Then the linking number $l(c)$ is defined as $l(c)$ taken on the positive side of

$\Sigma_{tri}^{(1)}$. (For $c = ml$ and $c = hm$ the side of $\Sigma_{tri}^{(1)}$ doesn't matter for $l(c)$ but it changes by $+2$ or -2 for $c = d$.)

Definition 10 Let $p \in \Sigma_{tri}^{(1)}$. Then $\eta(p) = 1$ if $[d] = 1$ and $\eta(p) = -1$ if $[d] = 0$.

The following correction term is needed in the definition of R_1 , it will disappear in the definition of R_n for $n > 1$ in the case of a non-degenerate coloring (compare the next subsection).

Definition 11 Let $p \in \Sigma_{tri}^{(1)}$. Then $\epsilon(p) = 1/2$ if $[d] = 0$ and $[hm] = 1$ and $\epsilon(p) = 0$ otherwise.

We are now ready to define R_1 . There are $8 \times 6 = 48$ different types of Reidemeister III moves for long knots and they contribute almost all in a different way to R_1 . Luckily, we have managed to encode the contributions in a single formula.

Definition 12 (The 1-cocycle R_1)

Let s be an oriented generic smooth closed arc in M (s is in general position with respect to the stratification $\Sigma^{(i)}$, i.e. its endpoints are in $\Sigma^{(0)}$, it intersects $\Sigma^{(1)}$ transversally in a finite number of points, called p , and it does not intersect $\Sigma^{(i)}$ for $i > 1$). We consider the crossings d , ml and hm for each $p \in \Sigma_{tri}^{(1)}$ and we identify the two crossings d for each $p \in \Sigma_{tan}^{(1)}$. Then $R_1(s) \in \mathbb{Z}[x, x^{-1}]$ is defined by

$$\begin{aligned}
R_1(s) = & \sum_{p \in \Sigma_{tri}^{(1)}, [d]=0} sign(p) 4l(d) x^{W_2(d) + \epsilon(p)w(hm)(w(ml) - w(d))} \\
& + \sum_{p \in \Sigma_{tri}^{(1)}, [ml]=0} sign(p) \eta(p) w(hm) (l(ml) - w(ml))^2 \times \\
& (x^{W_2(ml) + w(hm)W_1(hm) + \epsilon(p)w(hm)(w(ml) - w(d))} - x^{W_2(ml)}) \\
& + \sum_{p \in \Sigma_{tan-}^{(1)}, [d]=0} sign(p) 4l(d) x^{W_2(d)} \\
& + \sum_{p \in \Sigma_{tan+}^{(1)}, [d]=0} sign(p) 8l(d) x^{W_2(d)}
\end{aligned}$$

In other words, we associate to a Reidemeister move p some monomial if and only if the distinguished crossing d is of type 0 and we associate some binomial if and only if the crossing ml is of type 0. Notice that in the latter case we have to consider only Reidemeister III moves with $[ml] = 0$ and $[hm] = 1$. Indeed, the binomial is 0 if $[hm] = 0$ too because both $W_1(hm) = 0$ and $\epsilon(p) = 0$. But it can happen that d and ml contribute both for the same move.

Remark 1 *The main difference with our previous 1-cocycles [17] are the linking numbers $l(d)$ and $l(ml)$. A fixed crossing can contribute to $R_1(s)$ as a d -crossing and hence with linear coefficient $4l(d)$. Moving further in the arc s the same crossing could the next time contribute as a ml -crossing and hence with a quadratic coefficient $(l(ml) - w(ml))^2$. This makes a cancellation of monomials in the two contributions (the "telescoping effect") rather unlikely, because the linking number l of a crossing can only change by $+2$ or -2 when the crossing contributes as a d -crossing! But notice that it is of crucial importance that we associate to a crossing ml a binomial and not just a monomial. One of the monomials in the binomial corresponds to the weight of ml just before the RIII move and the other corresponds to the weight of ml just after the RIII move. Hence, by moving further on the arc s the weight of the crossing has changed now and can not cancel out with the previous*

contribution as a ml -crossing. It is this combinatorial structure of quadratic versus linear linking number and binomial versus monomial for the same crossing in different moves which makes the whole thing working!

But R_1 is not a 1-cocycle in M because of the strata $\Sigma_{trans-cusp}^{(2)}$. In the unfolding of $\Sigma_{trans-cusp}^{(2)}$ we see one crossing which appears from the cusp and exactly one triple crossing. Let $\Sigma_{trans-cusp, cusp=[ml]=0, [d]=1}^{(2)}$ be the union of all strata of one ordinary cusp ($x^2 = y^3$) with a transverse branch passing through the cusp in the projection, and such that in its unfolding the crossing which appears from the cusp becomes the crossing ml of type 0 in the triple crossing and the distinguished crossing d in the triple crossing is of type 1. This implies of course that the transverse branch moves *over* the cusp in the unfolding and hence intersections with strata of type $\Sigma_{trans-cusp, cusp=[ml]=0, [d]=1}^{(2)}$ can not appear in $scan(K_t)$ for any isotopy $K_t, t \in [0, 1]$, of a long knot K_0 , because the branch moves *under* the rest of the knot, compare Section 4.6.

Theorem 1 R_1 represents a non-trivial cohomology class in

$H^1(M \setminus \Sigma_{trans-cusp, cusp=[ml]=0, [d]=1}^{(2)}; \mathbb{Z}[x, x^{-1}])$ for each choice of an abstract closure of T to a circle and for each choice of a point at infinity in ∂T . Moreover, for each generic point T in M (i.e. $T \in \Sigma^{(0)}$) the Laurent polynomial $R_1(scan(T))$ is an isotopy invariant of T .

2.2 The 1-cocycle R_n in M for $n > 1$

We consider R_1 , which was defined in the previous subsection, and we take $n > 1$. Remember that we have chosen an abstract closure of $T \in M$ to a circle and we have chosen a point at infinity in the closure. We start at the point at infinity and we go along the circle. This defines an ordering on the set of components of $T : C_1, C_2, \dots, C_n$, called the *coloring* of the components. Notice that we can obtain more colorings by identifying the colors of several components. A *coloring* of R_1 is now a restriction in the definition of R_1 to only those crossings d , ml , f and r with fixed colorings of the undercross and the overcross, denoted by undercross \rightarrow overcross: $C_i \rightarrow C_j$.

Definition 13 A coloring of R_1 for $n > 1$ by

d in $\Sigma_{tri}^{(1)}$ as well as in $\Sigma_{tan}^{(1)}$ and ml in $\Sigma_{tri}^{(1)} : C_{i_1} \rightarrow C_{i_2}$

$f: C_{i_2} \rightarrow C_{i_2} \text{ or } C_{i_2} \rightarrow C_{i_3}$
 $r: C_{i_3} \rightarrow C_{i_2} \text{ or } C_{i_3} \rightarrow C_{i_3}$
 is called admissible if
 $C_{i_1} \neq C_{i_2} \text{ and } C_{i_2} \neq C_{i_3}$.

We enumerate for each fixed n the admissible colorings of R_1 by natural numbers i .

Definition 14 (*The 1-cocycle R_n^i*)

The degenerate case: $C_{i_1} = C_{i_3}$.

Let i be a degenerate admissible coloring of R_1 . Then R_n^i is defined as R_1 but where only the crossings with prescribed colorings in i contribute and moreover $[ml] = 0$ in a Reidemeister III move contributes only if the overcross of d in this move has the color C_{i_2} or $C_{i_1} = C_{i_3}$. We replace now the variable x in the values of R_n^i by the new variable x_i .

The non-degenerate case : $C_{i_1} \neq C_{i_3}$.

Let i be a non-degenerate admissible coloring of R_1 . Then R_n^i is defined as R_1 without the correction term $\epsilon(p)w(hm)(w(ml) - w(d))$, but where only the crossings with prescribed colorings in i contribute. (If $W_1(hm) = 0$ then $[ml] = 0$ in a Reidemeister III move does not contribute because there is no correction term. $W_1(hm) = 0$ automatically if the overcross of d in this move has not the color C_{i_2} or C_{i_3} .) We replace now the variable x in the values of R_n^i by the new variable x_i .

R_n is defined as $\sum_i R_n^i$ over all admissible colorings i .

Notice that an admissible coloring for $n = 2$ is evidently degenerate. We take always $C_1 = \text{black}$ and $C_2 = \text{red}$ (and hence $\infty = \text{red-}\infty$ is always the end of the red component). Then R_2 is just R_1 with the admissible coloring $C_{i_1} = \text{red}$ and $C_{i_2} = \text{black}$. Indeed, the other choice would lead to d and ml of homological type 1.

We consider the virtual closure $\sigma_1\sigma_2$ and the colors $C_1 = \text{black}$, $C_2 = \text{green}$, $C_3 = \text{red}$ for $n = 3$. We consider in this paper only the following non-degenerate admissible coloring, called 1, which turns out to contribute non-trivially to R_3 in the case of $\text{red-}\infty$: $C_{i_1} = \text{red}$, $C_{i_2} = \text{black}$, $C_{i_3} = \text{green}$.

It is convenient for calculations (see the next section) to introduce *potential f-crossings* and *potential r-crossings*.

Definition 15 *A crossing in a generic diagram is called a potential f-crossing for an admissible coloring if it is of (homological) type 1 and of (colored) type*

$C_{i_2} \rightarrow C_{i_2}$ or $C_{i_2} \rightarrow C_{i_3}$. A crossing is called a potential r-crossing if it is of type 0 and of type $C_{i_3} \rightarrow C_{i_2}$ or $C_{i_3} \rightarrow C_{i_3}$.

The following theorem is the main result of this paper.

Theorem 2 R_n^i represents a cohomology class in $H^1(M; \mathbb{Z}[x_i, x_i^{-1}])$ for each $n > 1$ and for each admissible coloring i . The 1-cocycle $R_n = \sum_i R_n^i$ is not always a 1-coboundary.

Moreover, for each generic point T in M the Laurent polynomial $R_n^i(\text{scan}(T))$ is an isotopy invariant of T . It can be calculated with cubic complexity with respect to the number of crossings of T and it can sometimes detect the non-invertibility of a knot.

Remark 2 All our definitions are very non-symmetric. In fact, if we apply our definitions to mirror images or to reversed orientations of knots then in general our 1-cocycles become new "dual" 1-cocycles. To break these symmetries was an important point together with the combinatorial structure (compare Remark 1) in order to get 1-cocycles which are not 1-coboundaries.

3 First applications, questions and conjectures

3.1 Applications of the 1-cocycle R_1 in $M \setminus \Sigma_{trans-cusp}^{(2)}$. Detecting the non-invertibility of string links with two components

Let K be a long knot up to regular isotopy (i.e. isotopy without Reidemeister moves of type I). Then Gramain's loop $rot(K)$ has a nice representative: with a Reidemeister I move we add a small positive curl at the right end, then we perform the scan, we slide the knot along the curl, we perform an "over-scan" (i.e. the branch moves over the knot) and at the end we eliminate the small curl again with a Reidemeister I move (compare Fig. 9). If K and K' are regularly isotopic then evidently $[rot(K)] = [rot(K')]$ in $H_1(M \setminus \Sigma_{trans-cusp}^{(2)}; \mathbb{Z})$ for the above representatives, because no branch moves over the two cusps in any homotopy in M , which connects the two loops and which consists only of regular isotopies.

Proposition 2 Let K be a long knot and let $v_2(K)$ be its Vassiliev invariant of degree 2 (normalized to be 1 on the trefoil).

Then $R_1(rot(K)) = x^{v_2(K)} - 1$.

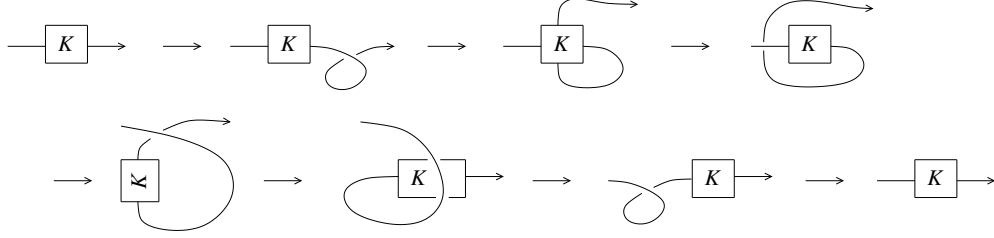


Figure 9: Nice realization of Gramain's loop

Proof. Let K and K' be long knots and let $K \sharp K'$ be the long knot which is their connected sum. Pushing K' through the positive curl at the right adds $x^{v_2(K)} R_1(\text{rot}(K'))$ as contribution to $R_1(\text{rot}(K \sharp K'))$. Indeed, the knot K appears just after the point at infinity and hence each crossing of type 1 of K is a f-crossing for each crossing d or ml of K' which contributes to $R_1(\text{rot}(K \sharp K'))$. No crossing of K is ever a r-crossing for a crossing in K' and vice-versa. It follows now from the *Polyak-Viro Gauss diagram formulas for $v_2(K)$* , compare [34] and Fig. 10, that K adds $v_2(K)$ to each weight W_2 and consequently, it adds the factor $x^{v_2(K)}$ to each contribution to $R_1(\text{rot}(K \sharp K'))$ of the crossings d and ml of K' .

Pushing now K through the positive curl adds only $R_1(\text{rot}(K))$ to

$R_1(\text{rot}(K \sharp K'))$. Indeed, the knot K' appears just before the point at infinity and hence no crossing of K' is ever a f-crossing for a crossing of type d or ml of K which contributes to $R_1(\text{rot}(K \sharp K'))$. It follows that

$R_1(\text{rot}(K \sharp K')) = x^{v_2(K)} R_1(\text{rot}(K')) + R_1(\text{rot}(K))$. But the connected sum of long knots is commutative, i.e. $K \sharp K'$ is even regularly isotopic to $K' \sharp K$. Consequently, $R_1(\text{rot}(K \sharp K')) = x^{v_2(K')} R_1(\text{rot}(K)) + R_1(\text{rot}(K'))$ too. It follows that $(x^{v_2(K)} - 1) R_1(\text{rot}(K')) = (x^{v_2(K')} - 1) R_1(\text{rot}(K))$ for a given knot K and an arbitrary knot K' . Hence, we have the alternative

either $R_1(\text{rot}(K)) = 0$ for each knot K
or $R_1(\text{rot}(K)) = x^{v_2(K)} - 1$ for each knot K .

A direct calculation for the positive trefoil shows that the second possibility is the right one.

□

It follows from the proposition that $dR_1(\text{rot}(K))/dx|_{x=1} = \alpha_3^1(\text{rot}(K)) = v_2(K)$, where α_3^1 is the Mortier 1-cocycle. Notice that for $x = 1$ the crossings ml do no longer contribute to R_1 , as follows immediately from its definition.

One easily sees that the more interesting information of $R_1(\text{rot}(K))$ is

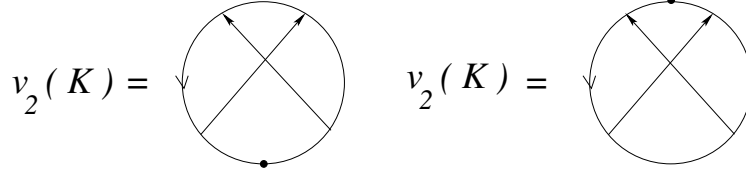


Figure 10: Polyak-Viro formulas for the Vassiliev invariant v_2 . For each of the two configurations $v_2(K)$ is the sum of the product of the writhe of all couples of crossings with the given configuration.

concentrated in $R_1(scan(K))$, because the "over-scan" part of the loop contributes only a constant to R_1 . Indeed, in the "over-scan" part ml does never contribute and for each contribution of d the weight $W_2(d) = 0$, because there is never an undercross on the arc from ∞ to the overcross of d and hence there are no f-crossings at all.

Let $M_K^{reg} \subset M_K$ be the subspace of all *regular* long knots, i.e. long knots for which the projection pr into the plane is an immersion. R_1 is evidently a 1-cocycle in M_K^{reg} . Thus, in order to calculate $R_1(fh(K))$ it is sufficient to approximate the loop $fh(K)$ in M_K by a loop in M_K^{reg} . It is easy to see that this can always be done by using Whitney tricks, see e.g. [14]. However, this approximation is not unique at all. In order to have $R_1(fh(K))$ as an invariant of framed knots, we would need that the following question has a positive answer.

Question 1 *Let $in : M_K^{reg} \rightarrow M_K$ be the inclusion. Is $in_* : H_1(M_K^{reg}, \mathbb{Q}) \rightarrow H_1(M_K, \mathbb{Q})$ injective? If not so, does R_1 annihilate the kernel of in_* ?*

Notice that the analogue is certainly not true for knots in the 3-sphere because we could slide a small curl all along the knot.

It seems to us that R_1 in M_K^{reg} is a *deformation quantization* of the Teiblum-Turchin or Mortier 1-cocycle, i.e. if we set $x = 1 + q$ and develop the invariant in q then the coefficient of the linear term is equal to the value of the Teiblum-Turchin or Mortier 1-cocycle. If the answer to the above question is positive, then a calculation of Mortier [31] would suggest that $dR_1(fh(K))/dx|_{x=1} = \alpha_3^1(fh(K)) = 6v_3(K) - w(K)v_2(K)$. (Here, $w(K)$ is the writhe of the framed knot K and $v_3(K)$ is the unique Vassiliev invariant of degree 3 normalized to be 1 on 3_1^+ and -1 on 3_1^- .)

The proposition shows also that already $R_1(rot(K))$ is *not* multiplicative for the connected sum of two knots.

Morally, the proposition tells us that for long knots we have to add long longitudes in order to get something really interesting. On one hand we want a 1-cocycle for the whole space M_T without taking out any strata in $\Sigma^{(2)}$ and on the other hand, adding a local knot on a component of the string link T should not lead to a formula which already calculates the invariant as in Proposition 2.

Remark 3 *We will achieve both goals with R_n for $n > 1$ because by definition the colors of the foot and of the head are always different for the crossings d , ml and there are no f -crossings of type $C_{i_3} \rightarrow C_{i_3}$ and no r -crossings of type $C_{i_2} \rightarrow C_{i_2}$. There can be f -crossings $C_{i_2} \rightarrow C_{i_2}$ and r -crossings $C_{i_3} \rightarrow C_{i_3}$ but $C_{i_2} \neq C_{i_3}$. It follows immediately that the crossing ml in $\Sigma_{trans-cusp, cusp=[ml]=0, [d]=1}^{(2)}$ does never contribute (because ml is just the crossing of the small curl) and that there are no contributions to W_2 by crossings only in a local knot on a component. Consequently, adding a local knot K to a component of the string link does not lead to just a multiplication of the invariant by $x^{v_2(K)}$.*

Let us replace now the framed knot K by its parallel 2-cable determined by the framing, which we denote by $2 - cable(K), w(K)$. Here as usual the framing is encoded in the writhe $w(K)$ of the diagram, i.e. the algebraic number of crossings with respect to the fixed projection pr . It turns out that there is a first splitting of R_1 into several 1-cocycles (compare Section 4.4): we take into account only the crossings d and ml which are in addition of a given colored type e.g. $red \rightarrow red$ or $red \rightarrow black$.

We take always $red - \infty$ as the end of the red component and $black - \infty$ as the end of the black component.

The corresponding 1-cocycles are denoted by $R_1(red - red, red - \infty)$, $R_1(red - red, black - \infty)$, $R_1(red - black, red - \infty)$ and so on. These splittings do not yet correspond to admissible colorings because we do not care about the colors for the f - and the r -crossings.

We have calculated the following examples, where we use the standard notations for knots from the *knot atlas*. Let the knot 8_{17} be the standard closure of the 3-braid $\sigma_2\sigma_2\sigma_1^{-1}\sigma_2\sigma_1^{-1}\sigma_2\sigma_1^{-1}\sigma_1^{-1}$ oriented as usually from the left to the right.

We show the arc $scan(2 - cable(3_1^+), w = 3)$ in Fig. 11 as an example.

Example 1

$$R_1(red - red, red - \infty)(scan(2 - cable(3_1^+), w = 3)) = x^{14} - 49x^{13}$$

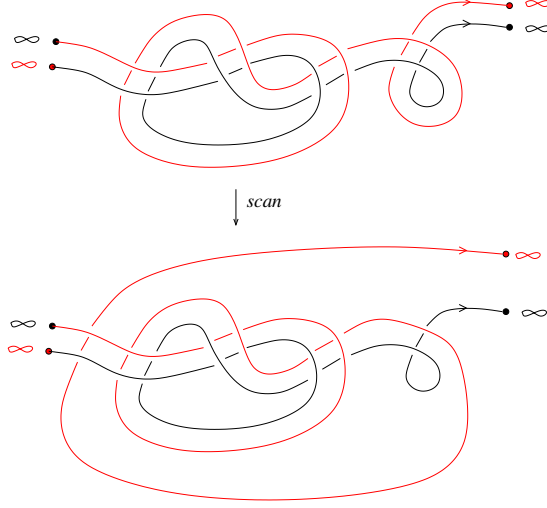


Figure 11: scan of the 2-cable of the positive trefoil

$$R_1(\text{red} - \text{black}, \text{red} - \infty)(\text{scan}(2 - \text{cable}(3_1^+), w = 3)) = -8x^6 + 36x^{12}$$

$$R_1(\text{red} - \text{red}, \text{black} - \infty)(\text{scan}(2 - \text{cable}(3_1^+), w = 3)) = x^9 - 49$$

$$R_1(\text{red} - \text{red}, \text{red} - \infty)(\text{scan}(2 - \text{cable}(4_1), w = 0)) = x^{-1} - 1$$

$$R_1(\text{red} - \text{red}, \text{red} - \infty)(\text{scan}(2 - \text{cable}(8_{17}), w = 0)) = x^{-1} - 1$$

$$R_1(\text{red} - \text{red}, \text{red} - \infty)(\text{scan}(2 - \text{cable}(-8_{17}), w = 0)) = x^{-1} - 1$$

It is easy to see that $R_1(\text{red} - \text{black}, \text{black} - \infty)(\text{scan}(2 - \text{cable}(K))) = 0$ as well as $R_1(\text{black} - \text{black}, \text{black} - \infty)(\text{scan}(2 - \text{cable}(K))) = 0$ for each knot K because no crossing at all can contribute for a moving red arc under the rest of the knot.

Conjecture 1 (*Fewnomials*)

The values of the 1-cocycles $R_1(\text{red} - \text{red}, \text{red} - \infty)(\text{scan}(2 - \text{cable}(K, w)))$, $R_1(\text{red} - \text{red}, \text{black} - \infty)(\text{scan}(2 - \text{cable}(K, w)))$ and $R_1(\text{red} - \text{red}, \text{black} - \infty)(\text{scan}(2 - \text{cable}(K, w)))$ are completely determined by the Vassiliev invariants $w(K)$ of degree 1 for (framed) knots and $v_2(K)$ of degree 2 and each value is at most a binomial.

It seems likely that e.g. if $w(K) = 0$ then always

$$R_1(\text{red} - \text{red}, \text{red} - \infty)(\text{scan}(2 - \text{cable}(K, w = 0))) = x^{v_2(K)} - 1,$$

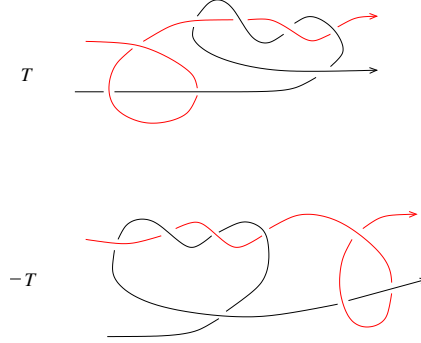


Figure 12: The 2-tangle T and its inverse

but we have no proof for this. (Notice that $R_1(\text{red-red}, \text{red}-\infty)(\text{scan}(2\text{-cable}(K, w)))$ could be 0 for $w(K) = 0$ and $v_2(K) = 0$ and it could be a monomial for $w(K) \neq 0$ and $v_2(K) = 0$.)

The above conjecture looks like bad news: $R_1(\text{scan})$ is not interesting for 2-cables of long knots neither. However, it turns out to be extremely interesting for 2-tangles other than 2-cables.

Example 2 Let T be the 2-tangle shown in Fig. 12 and let $-T$ be its inverse. Each of the components is a long trivial knot. We add to each of the two tangles a crossing σ_1 at the right end. Then

$$R_1(\text{black} - \text{black}, \text{red} - \infty)(\text{scan}(T\sigma_1)) = -49 + x^{-1}$$

$$R_1(\text{black} - \text{black}, \text{red} - \infty)(\text{scan}(-T\sigma_1)) = -49 - 39x^{-1} + 40x^{-2}$$

Notice that the two Laurent polynomials have the same value at $x = 1$.

For the convenience of the reader and in order to get a bit familiar with the new invariants we give the calculation of $R_1(\text{black} - \text{black}, \text{red} - \infty)(\text{scan}(-T\sigma_1))$ in some detail below.

There are exactly six different *global types* of triple crossings with a point at infinity. For shorter writing we give names to them and show them in Fig. 13. (Here "r" indicates that the crossing between the middle and the lowest branch goes to the right and "l" indicates that it goes to the left.) It follows from the definitions that d can contribute only for the triple crossings of the types r_a , r_b , l_b . The crossing ml can contribute only for the types r_a and l_c .

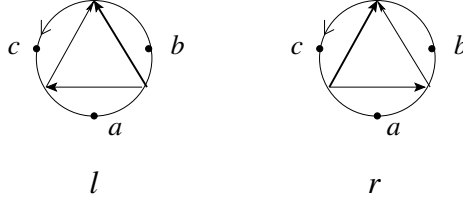


Figure 13: The six global types of triple crossings

The abstract closure of $T\sigma_1$ and $-T\sigma_1$ to a circle is now by the trivial 2-braid because we have already added a σ_1 . The arc of the diagram which moves under the tangle in *scan* is now black.

There are exactly 10 Reidemeister moves which can contribute to $R_1(\text{black-black}, \text{red} - \infty)(\text{scan}(-T\sigma_1))$. We give numbers to them in Fig. 14. We show the corresponding Gauss diagrams together with the calculation of the contributions to R_1 in Fig. 15 and Fig. 16. We draw the crossing d always by a bold arrow for better visualizing the global type of the move.

The calculation gives now:

- move 1: $+l_c$, $w(ml) = w(d)$, $W_1(hm) = 0$, no contribution
- move 2: $+r_b$, $l(d) = -2$, $W_2(d) = -1$, contribution $4(-2)x^{-1}$
- move 3: $-l_c$, $\eta = -1$, $\epsilon = 0$, $w(ml) = 1$, $w(hm) = -1$, $l(ml) = -2$, $W_1(hm) = 1$, $W_2(ml) = 0$, contribution $(-3)^2(x^{-1} - 1)$
- move 4: $+tan^+$, $l(d) = -5$, $W_2(d) = -1$, contribution $8(-5)x^{-1}$
- move 5: $+r_b$, $l(d) = -2$, $W_2(d) = -2$, contribution $4(-2)x^{-2}$
- move 6: $-r_a$, $w(ml) = w(d) = 1$, $l(d) = -2$, $W_2(d) = 0$, contribution $-4(-2)x^0$, $w(hm) = 1$, $\eta = -1$, $l(ml) = -6$, $W_1(hm) = -2$, $W_2(ml) = 0$, contribution $(-7)^2(x^{-2} - 1)$
- move 7: $+l_c$, $w(ml) = w(hm) = -1$, $l(ml) = -2$, $W_1(hm) = -1$, $W_2(ml) = -2$, contribution $(-1)^2(x^{-1} - x^{-2})$
- move 8: $+r_b$, $l(d) = 0$, no contribution
- move 9: $+l_c$, $w(ml) = w(hm) = -1$, $l(ml) = 0$, $W_1(hm) = -1$, $W_2(ml) = -1$, contribution $(+1)^2(1 - x^{-1})$
- move 10: $-tan^-$, $l(d) = 0$, no contribution.

Consequently, $R_1(\text{black-black}, \text{red} - \infty)(\text{scan}(-T\sigma_1)) = -8x^{-1} + 9(x^{-1} - 1) - 40x^{-1} - 8x^{-2} + 8 + 49(x^{-2} - 1) + (x^{-1} - x^{-2}) + (1 - x^{-1}) = -49 - 39x^{-1} + 40x^{-2}$.

It turns out that for $R_1(\text{black-black}, \text{red} - \infty)(\text{scan}(T\sigma_1))$ no Reidemeister move at all contributes with a term of degree -2 .

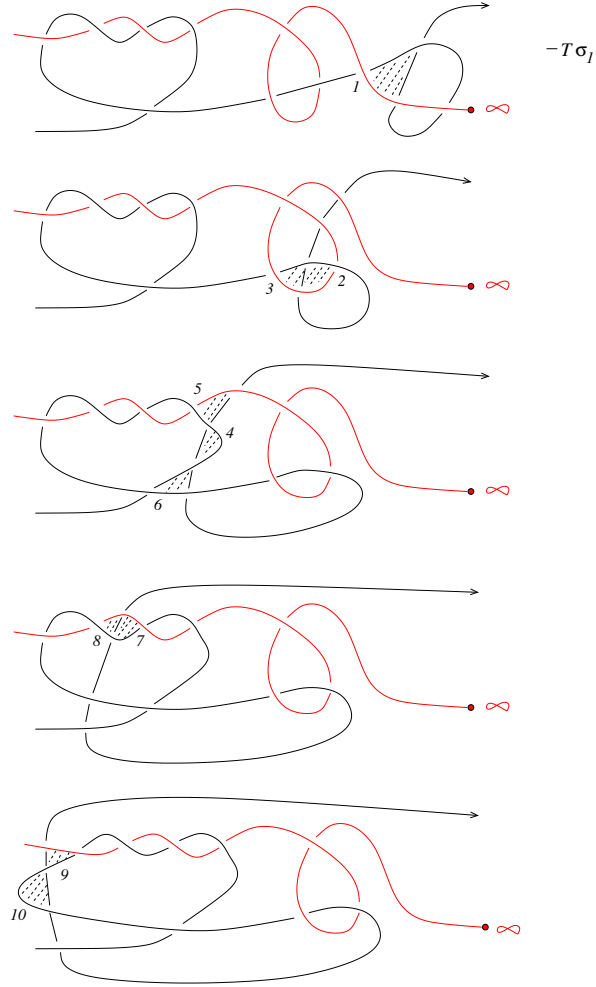
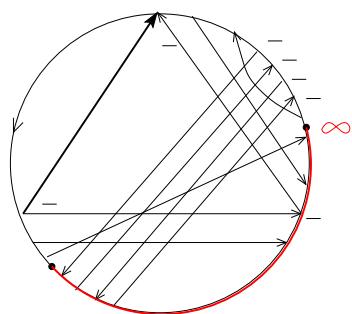
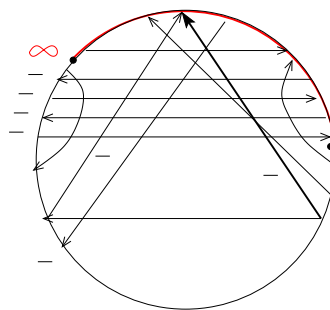


Figure 14: The Reidemeister moves in $scan(-T\sigma_1)$

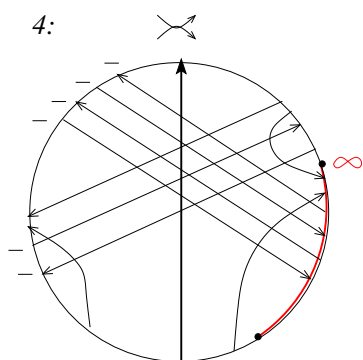
2:



3:



4:



5:

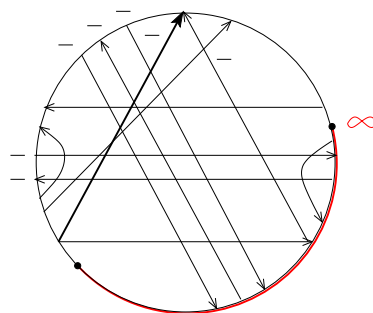


Figure 15: The Gauss diagrams for the moves in $scan(-T\sigma_1)$

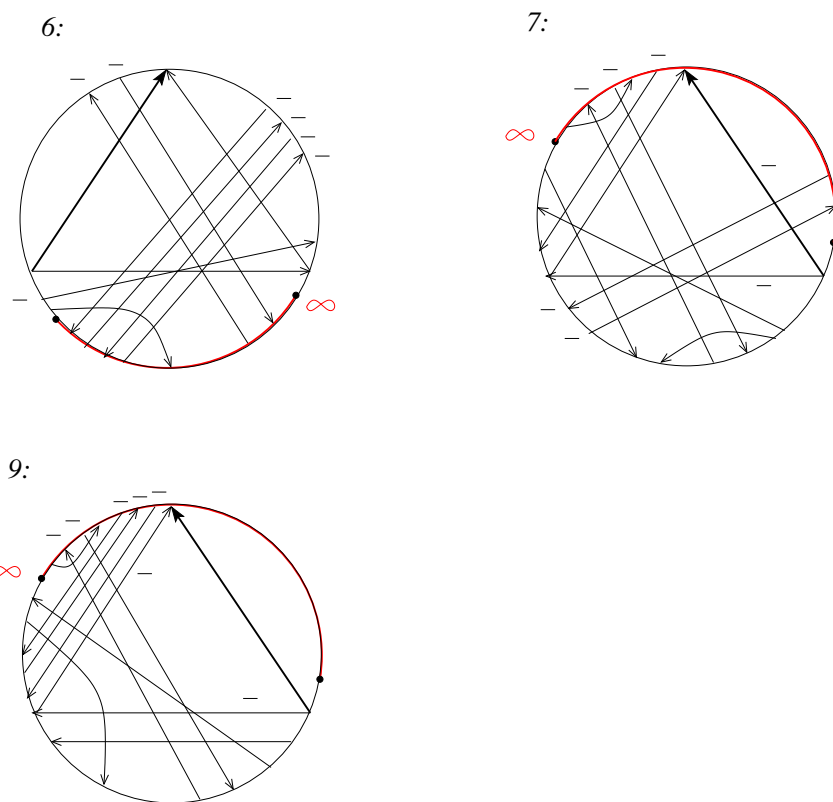


Figure 16: The remaining Gauss diagrams for the moves in $scan(-T\sigma_1)$

Corollary 1 $R_1(scan)$ distinguishes the above tangle T from its inverse $-T$ as an invariant which can be calculated with cubic complexity with respect to the number of crossings.

Proof. Evidently, if $T\sigma_1$ is not isotopic to $-T\sigma_1$ then T is not isotopic to $-T$. The calculation of the invariant $R_1(scan)$ is of complexity of degree at most 3 with respect to the number of crossings of the tangle. Indeed, the number of Seifert circles s (i.e. the number of circles in the plan which are obtained by smoothing all double points of $pr(T)$ with respect to the orientation) is not bigger than the number of crossings c . We can assume that the moving arc in $scan$ has at each moment at most $2s$ new crossings. Each crossing contributes at most once in a RIII-move and it is easy to see that we can change the diagram by an isotopy so that there are at most $2c$ RII-moves in $scan$. For each of the Reidemeister moves we have to calculate a weight of at most quadratic complexity with respect to $c + 2s$ (namely $W_2(d)$). Consequently, the whole $R_1(scan)$ is at most of cubic complexity with respect to the number of crossings c .

□

As already mentioned in the Introduction Bar-Natan has shown that there is no finite type invariant of degree smaller than 7 which can distinguish a 2-component string link from its inverse. It is easy to see that T and $-T$ can not be distinguished by the HOMFLYPT, Kauffman and Kuperberg invariants in the corresponding skein modules for 2-tangles in the 3-ball, because the corresponding skein modules are commutative and the skein relations and generators of the skein modules are invariant under orientation change of the 2-tangles, see e.g. [4], [35], [37]. It seems to be not known whether there is a primitive finite type invariant of degree at least 7, but which can nevertheless be calculated with complexity of degree 3. If there is no such invariant then it would follow that $R_1(scan)$ for a general string link T is not determined by any finite type invariants of T and in particular it is not determined by any quantum invariants (which can be decomposed into infinite series of finite type invariants).

The value in the example of $R_1(black - black, black - \infty)(scan(-T\sigma_1))$ is a *trinomial*. If the Viewnomial conjecture is true this would imply that $-T\sigma_1$ is not a 2-cable of any long knot.

So, it seems likely that $R_1(scan)$ can detect sometimes with cubic complexity with respect to the number of crossings that a 2-component string link is not a 2-cable of any long knot. (Sometimes the Alexander polynomial can

detect this too, but with complexity of degree 4. It is not easy to establish this in general. One has to find the JSJ-decomposition of the complement of the string link in the 3-ball. If T is a 2-cable of a non-trivial long knot then there is an incompressible embedded torus T^2 in $D^3 \setminus T$ and which intersects ∂D^3 in a cylinder C . $T^2 \setminus C$ bounds a properly embedded solid cylinder in D^3 with the tangle T inside it. The tangle in this solid cylinder has to be a 2-braid. This is the case if and only if the fundamental group of the complement of T in the solid cylinder is the free group F_2 .)

3.2 Applications of the 1-cocycle R_n in M for $n > 1$. Detecting the non-invertibility of knots

Let us consider now R_n . Gramain's loop is still defined in the same way for M_n , but at the end we have just to push a full twist of the n -strands back through the knot.

As already mentioned in the previous section there is only R_2 which is interesting for $n = 2$.

Example 3

$$\begin{aligned} R_2(\text{rot}(2 - \text{cable}(3_1^+), w = 3)) &= 36x^{12} - 72x^{10} + 56x^8 + 20x^5 - 20x^2 - 20 \\ R_2(\text{scan}(2 - \text{cable}(3_1^+), w = 3)) &= 36x^{11} + 20x^8 \end{aligned}$$

R_2 is the first non-trivial polynomial valued 1-cocycle for long knots. $R_2(\text{rot}(2 - \text{cable}(3_1^+), w = 3))$ and $R_2(\text{scan}(2 - \text{cable}(3_1^+), w = 3))$ are new polynomial invariants of the positive trefoil and which do not come from representation theory neither from generating functions of categorifications of known polynomial invariants! They can be calculated with cubic complexity with respect to the number of crossings and R_2 can distinguish the homology classes of loops in M_2 .

Notice that $R_2(\text{rot}(2 - \text{cable}(3_1^+), w = 3))$ vanishes at $x = 1$ (in fact, it is not very difficult to prove that this is the case for each knot). It is clear that R_2 depends strongly on the framing $w(K)$ because the string links $2 - \text{cable}(K), w(K)$ are not isotopic for different $w(K)$, but concrete examples have to be calculated with a computer.

The Fox-Hatcher loop has a nice combinatorial realization too: we go on K from ∞ to the first crossing. If we arrive at an under-cross then we move the branch of the over-cross over the rest of the knot up to the end

of K . If we arrive at an over-cross then we move the branch of the under-cross under the rest of the knot up to its end. We continue the process up to the moment when we obtain a diagram which is isotopic to our initial diagram of K , compare [23]. We can of course consider the analog loop for cables of long framed knots in M_n . It follows that the complexity of $R_n(fh(n - \text{cable}(K), w))$ is of degree 4 with respect to the number of crossings for each fixed n . Indeed, by moving an arc over or under the rest of the diagram each of the c crossings contributes at most with a weight of degree 2 and we have to move at most $2c$ arcs in the loop. Unfortunately, even for the 2-cable of 4_1 the calculation by hand is already too complicated. However, the example $2 - \text{cable}(3_1^+), w = 3$ shows that $R_n(fh(n - \text{cable}(K), w))$ is not always trivial too.

Let K be a non-trivial long knot and M_K its component in the moduli space. There is a well known action of the braid group B_n on M_K^n , see [20] and also [10], where M_K^n denotes the moduli space of the connected sum of n copies of the knot K . The generator σ_i acts by pushing the i -th copy of K through the $i + 1$ -th copy of K and the inverse σ_i^{-1} acts by pushing the $i + 1$ -th copy back through the i -th. The same action is still well defined for cables of framed knots. In particular, $R_2(\beta)$ is another polynomial knot invariant of K for each $\beta \in B_n$ when we apply R_2 to the 2-cable of the connected sum of long framed non-trivial knots K . Its calculation is of quartic complexity with respect to the numbers of crossings of K for each fixed braid β . Unfortunately, it is too difficult to calculate examples by hand.

Question 2 *Is $R_2(\beta)$ non-trivial for non-trivial braids?*

We could also define a polynomial valued bilinear form on $H_0(M_2)^2$ by evaluating R_2 on the loop which consists of pushing the 2-cable of a long framed knot K_1 through the 2-cable of a long framed knot K_2 and then pushing the 2-cable of K_2 through the 2-cable of K_1 . But again, without a computer program we do not know yet whether it is trivial or not.

Let R_3^1 be the 1-cocycle corresponding to the admissible coloring 1, with virtual closure $\sigma_1\sigma_2$ and red- ∞ , which has been introduced in the previous section. We consider *scan* with the red arc, see Fig. 17. The calculation by hand of $R_3^1(\text{scan})$ is rather laborious. Therefore we have calculated only the terms of the lowest degree in x_1 , *but which are already sufficient in order to distinguish 8_{17} from -8_{17} .*

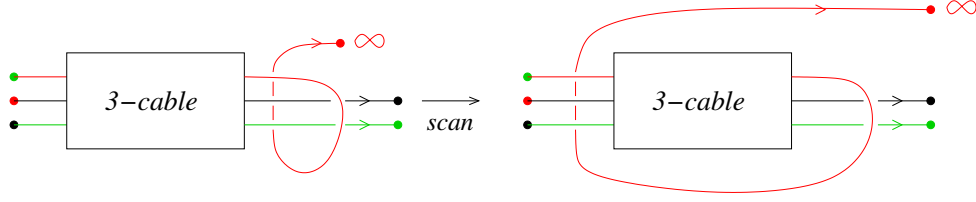


Figure 17: The scan of the 3-cable of the knot 8_{17}

Example 4 $R_3^1(scan(3 - cable(8_{17}), w = 0)) = \text{terms of degree } 0 \text{ and } -1$
 $R_3^1(scan(3 - cable(-8_{17}), w = 0)) = (\text{term of degree } -1) + 8x_1^{-2}$

Because of its great importance we give the calculation below in some detail .

Remember that d-or ml-crossings have to be of the type *red* \rightarrow *black* in order to contribute to R_3^1 and that in addition the crossing *ml* only contributes if the overcross of the crossing *d* in the R III move is *green* or *black*. f-crossings have to be of type *black* \rightarrow *black* or *black* \rightarrow *green*. r-crossings have to be of the type *green* \rightarrow *green* or *green* \rightarrow *black*.

The $(3 - cable(8_{17}), w = 0)$ is shown in Fig. 18 together with the ordered potential f-crossings $\{1, \dots, 11\}$, compare Definition 15. We show the Gauss diagram of the potential f- and r-crossings in Fig. 19. (For better visualizing the r-crossings are drawn in green.) We observe that the weight $W_1(f)$ of a f-crossing can only change in a R III move of type l_a , compare Fig. 13, with a black lowest branch in the move. But this can not happen in the scan-arc because the lowest branch is always red. There can't appear new f-crossings from R II moves in the scan-arc for the same reason. It follows that all the weights $W_1(f)$ are constant in the scan-arc. The calculation of $w(q)W_1(q)$ for each potential f-crossing $q \in \{1, \dots, 11\}$ gives now the sequence:

$0, -1, 2, -2, 1, -1, 1, 0, 0, 0, -1$. Going from red- ∞ along the black component we always come first to the undercross of a potential f-crossing. Consequently, the weights $W_2(d)$, $W_2(ml)$ and $W_2(ml) + w(hm)W_1(hm)$ are always of the form $W(0) = 0$ or $W(k) = w(1)W_1(1) + w(2)W_1(2) + \dots + w(k)W_1(k)$ for some $k \in \{1, \dots, 11\}$. An easy calculation gives now

$W(1) = 0, W(2) = -1, W(3) = 1, W(4) = -1, W(5) = 0, W(6) = -1, W(7) = 0, W(8) = 0, W(9) = 0, W(10) = 0, W(11) = -1$. The R II moves contribute to x_1^0 (from $W(8)$) respectively x_1^{-1} (from $W(6)$). Consequently, there are no contributions of degree strictly smaller than -1 at all

and the maximal possible degree of x_1 is 1. This happens exactly for ml in the R III moves with the crossing $hm = 3$ and $hm = 4$. But one easily sees that their contributions cancel out together.

The $(3 - \text{cable}(-8_{17}), w = 0)$ is shown in Fig. 20 together with the ordered potential f-crossings $\{1, \dots, 11\}$. We show the Gauss diagram of the potential f- and r-crossings in Fig. 21. The calculation of $w(q)W_1(q)$ for each potential f-crossing $q \in \{1, \dots, 11\}$ gives now the sequence:

2, -4, 2, -1, 1, -1, 0, 0, 0, -1, 0. This time we have

$$W(1) = 2, W(2) = -2, W(3) = 0, W(4) = -1, W(5) = 0, W(6) = -1, W(7) = -1, W(8) = -1, W(9) = -1, W(10) = -2, W(11) = -2.$$

The R II moves contribute to x_1^{-1} (from $W(4)$) respectively x_1^{-1} (from $W(8)$). Considerations analogue to those for 8_{17} show that the contributions with x_1^0 and the contributions with x_1^2 both cancel out. A somewhat longer calculation shows now that $8x_1^{-2}$ stays as the term of degree -2 .

□

But the invariant $R_3^1(\text{scan}(3 - \text{cable}(K), w))$ can still be refined in the following way: let t be an even natural number and let us add $t/2$ full-twists at the very end of the 3-cable of K but only *between the red and the black branch*, see Fig. 22. The t new crossings are never d-crossings or ml -crossings because they are never involved in Reidemeister moves in the scan-arc. They are never f-crossings or r-crossings because they don't have the right colors. In Fig. 23 we show the Gauss diagram of the t new crossings together with the only possibilities for crossings of type d and ml which contribute. It follows that for each of them the linking number l becomes $l + t$. Consequently, the invariant is now of the form

$$R_3^1(\text{scan}(3 - \text{cable}(K), w, t)) = t^2 P_2(x_1) + t P_1(x_1) + R_3^1(\text{scan}(3 - \text{cable}(K), w)),$$

where $P_2(x_1)$ and $P_1(x_1)$ are some new Laurent polynomials. Notice that $P_2(x_1)$ is completely determined by the contributions of the crossings of type ml alone and that we don't even have to calculate the linking numbers $l(ml)$, compare Definitions 12 and 14. We use the t^2 -part of the invariant to distinguish 8_{17} from -8_{17} even faster.

Example 5 $R_3^1(\text{scan}(3 - \text{cable}(8_{17}), w = 0, t)) = t^2(\text{terms of degree } \geq -1) + t P_1(x_1) + R_3^1(\text{scan}(3 - \text{cable}(8_{17}), w))$

$$R_3^1(\text{scan}(3 - \text{cable}(-8_{17}), w = 0, t)) = t^2(x_1^{-2} + \text{terms of higher degree}) + t Q_1(x_1) + R_3^1(\text{scan}(3 - \text{cable}(-8_{17}), w))$$

Indeed, there are no contributions of moves at all with x_1^{-2} in the case of

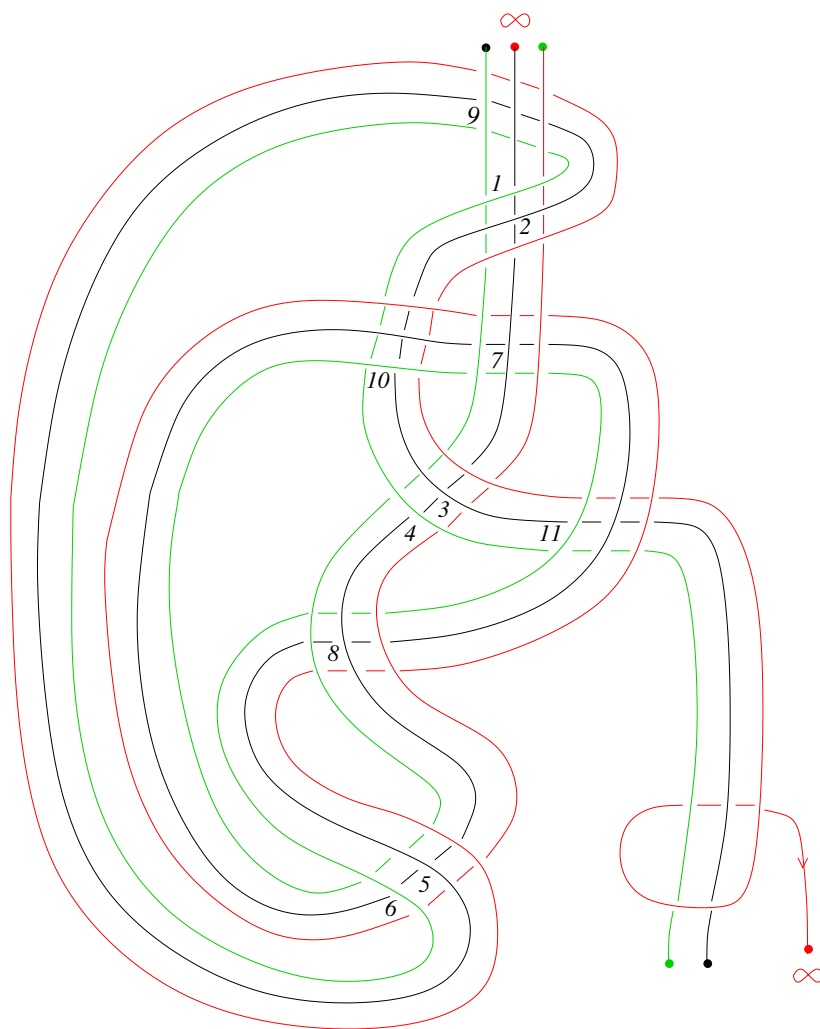


Figure 18: The potential f- and r-crossings for the 3-cable of 8_{17}

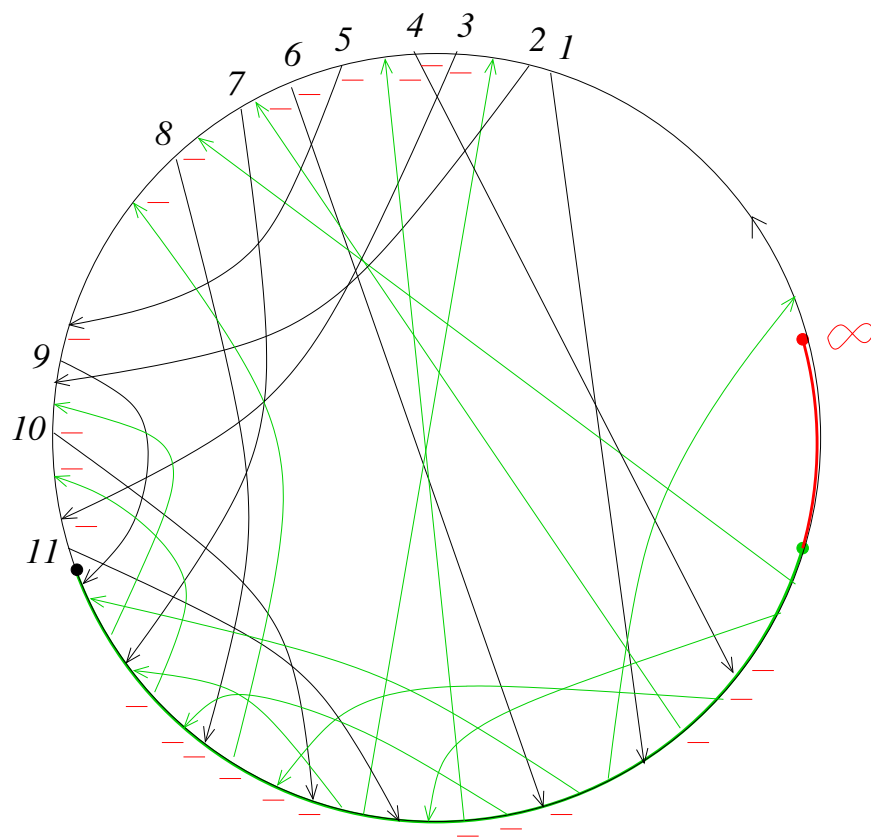


Figure 19: The Gauss diagram of the potential f- and r-crossings for the 3-cable of 8_{17}

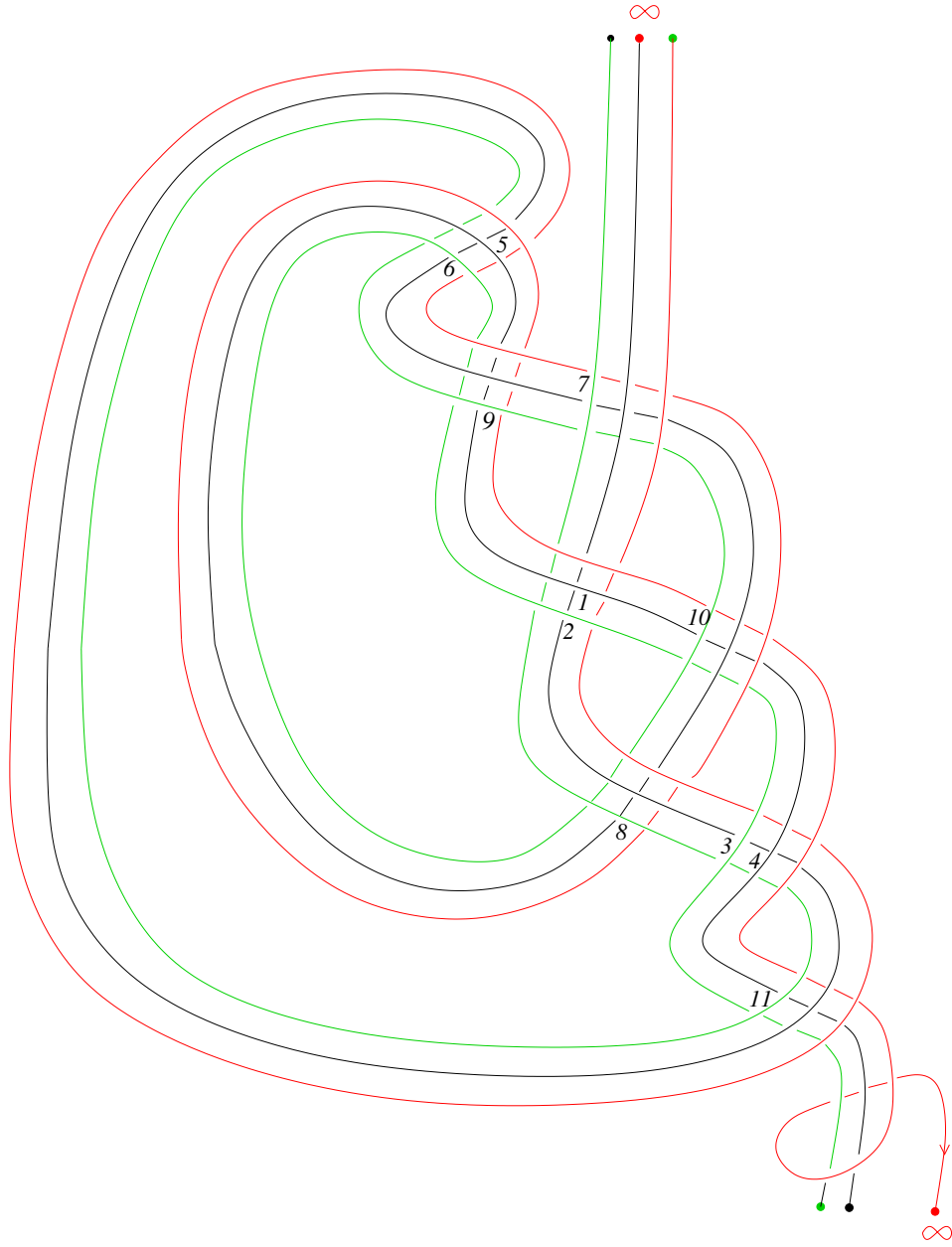


Figure 20: The potential f- and r-crossings for the 3-cable of -8_{17}

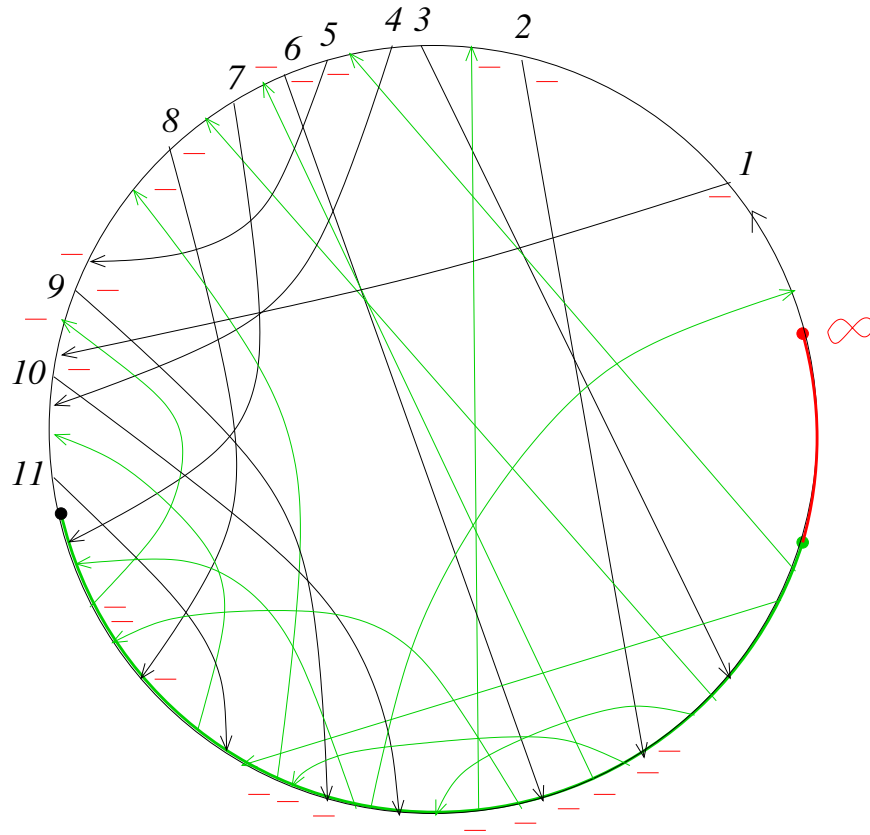


Figure 21: The Gauss diagram of the potential f- and r-crossings for the 3-cable of -8_{17}

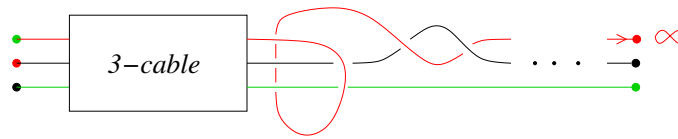


Figure 22: The scan of the 3-cable with $t/2$ full-twists between the red and the black branch

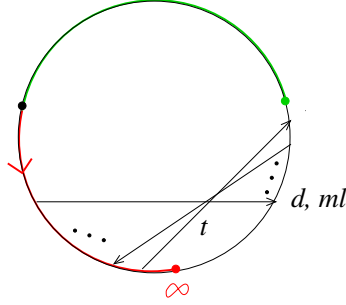


Figure 23: The Gauss diagram of the t new crossings

8_{17} as was shown in the previous example. Consequently, there is no term with x_1^{-2} in $P_2(x_1)$ in this case.

One sees immediately from the sequence of $W(k)$ in the case of -8_{17} that only the crossings ml for $hm = 2$, $hm = 3$, $hm = 10$ and $hm = 11$ could contribute to $t^2 x_1^{-2}$. But $W_1(hm = 11) = 0$ and hence the R III move with $hm = 11$ does not contribute. In the remaining three cases $W_1(hm) \neq 0$ and hence the coefficient of x_1^{-2} in $P_2(x_1)$ is odd! This is already sufficient but an easy calculation of the signs gives now that this coefficient is $+1$, compare Definitions 7 and 12.

□

It follows from results of Hatcher [23] that $M_n(K)$ is a contractible space for each n if K is the trivial knot. Consequently, $[R_n] = 0$ in this case.

Lemma 1 *Let (K, w) be a long framed non-trivial torus knot. Then the non-trivial classes $[rot(n - cable(K), w)]$ and $[fh(n - cable(K), w)]$ are linearly dependent in $H_1(M_n; \mathbb{Q})$ for each $n > 0$.*

Proof. Hatcher [23] has proven that for $n = 1$ the moduli space M_K deformation retracts onto a circle and more precisely a certain non-trivial integer multiple of the loop $rot(K)$ is homotopic to some non-trivial integer multiple of the loop $fh(K)$. (The homotopy class of $rot(K)$ does not depend on the framing and changing the framing adds multiples of $rot(K)$ to $fh(K)$.) We approximate $rot(K, w)$ and $fh(K, w)$ by loops in M_K^{reg} by using Whitney tricks (compare Question 1). We replace now the framed long knot by a n -cable which we can imagine on a band which projects to the plan by an immersion. The same generic homotopy as for the knot applies still to the band besides that a Reidemeister I move of the knot is now replaced by a

Reidemeister I move of the band together with a negative full-twist of the band if the crossing from the cusp is positive and with a positive full-twist of the band if the crossing from the cusp is negative. There can of course occur Reidemeister I moves in the homotopy because a loop can become tangential to $\Sigma_{cusp}^{(1)}$ or can pass through $\Sigma_{trans-cusp}^{(2)}$ or $\Sigma_{cusp-deg}^{(2)}$ (compare Proposition 1). But the homotopy starts and ends with two loops of bands (with a common band as starting point) which all projects to the plane as immersions and which have all the same writhe = framing. It follows that the homotopy adds the same number of positive and negative full-twists to the bands. But full-twists can be moved along the bands (in a unique way up to homotopy because a full-twist can not move over infinity) and moving a full-twist commutes with any regular isotopy of a band. Therefore we can cancel out the positive and the negative full-twists two by two and we obtain a homotopy from a multiple of $rot(n - cable(K), w)$ to a multiple of $fh(n - cable(K), w)$ and the conclusion of the lemma follows.

□

Let us call the invariants $R_n^i(fh(n - cable(K), w))/R_n^i(rot(n - cable(K), w))$ as well as $R_n(fh(n - cable(K), w))/R_n(rot(n - cable(K), w))$ the *rational knot functions*.

The lemma together with the fact that R_n^i is a 1-cocycle implies immediately the following corollary.

Corollary 2 *If (K, w) is a framed non-trivial torus knot then the rational knot function $R_n^i(fh(n - cable(K), w))/R_n^i(rot(n - cable(K), w)) \in \mathbb{Q}^*$ for each $n > 1$, each choice of a virtual closure to a circle, of a point at infinity and of a admissible coloring i , whenever $R_n^i(rot(n - cable(K), w)) \neq 0$.*

We conjecture that in fact the inverse is true too even in a broader sens.

Conjecture 2 *(Rational knot functions conjecture)*

Let (K, w) be a framed long knot.

(1) K is the unknot if and only if $R_n(fh(n - cable(K), w)) = R_n(rot(n - cable(K), w)) = 0$ for each $n > 1$.

(2) K is a non-trivial torus knot if and only if

$R_n(fh(n - cable(K), w))/R_n(rot(n - cable(K), w)) \in \mathbb{Q}^$ for each $n > 1$, whenever $R_n(rot(n - cable(K), w)) \neq 0$. Moreover, the values $R_n(fh(n - cable(K), w))/R_n(rot(n - cable(K), w)) \in \mathbb{Q}^*$ determine the type of the torus knot.*

(3) *The rational knot functions $R_n(fh(n - \text{cable}(K), w))/R_n(\text{rot}(n - \text{cable}(K), w))$, for $n > 1$, detect whether or not the simplicial volume of $S^3 \setminus K$ is 0.*

(Compare [27] for the Volume conjecture and [33] for a generalization using the simplicial volume.) Unfortunately, we are missing a computer program in order to calculate lots of examples and to formulate a more precise conjecture for the part (3). (There are simply too many ways to extract 0 from a rational number which is seen as a rational function.) It is likely that for iterated torus knots and for connected sums of torus knots the above rational functions will already no longer be constant (because the two loops are no longer linearly dependent and the calculation of R_n^i on them has different complexity). However, we have to extract 0 from them. If we extract in the same way a number in the case of a hyperbolic knot (or a satellite which contains a hyperbolic piece in the JSJ-decomposition of its complement in S^3) then the result should be different from 0.

A priori, we have an enormous amount of new knot invariants: for any knot K we can chose a framing $w(K)$, a natural number $n > 1$, a n -cycle in the symmetric group S_n , a point at infinity $m \in \{1, \dots, n\}$ and an admissible coloring i of the corresponding 1-cocycle R_1 and we obtain a rational knot function $R_n^i(fh(n - \text{cable}(K), w))/R_n^i(\text{rot}(n - \text{cable}(K), w))$. G. Kuperberg [30] has observed that if finite type invariants fail to distinguish oriented knots then they fail automatically to distinguish all non-oriented knots as well. Our invariants can sometimes distinguish the orientation of a knot. So at least there is a chance that they perhaps distinguish all knots in 3-space. An important point is of course to find out up to which extend our invariants are related amongst themselves.

As already mentioned, changing the framing $w(K)$ adds multiples of $\text{rot}(K)$ to $fh(K)$ for $n = 1$ and hence $R_1(fh(K))/R_1(\text{rot}(K))$ changes just by an integer. However, this is certainly no longer the case for $n > 1$, because changing the framing $w(K)$ changes the isotopy type of the n -cable of K .

If K is a non-trivial torus knot, then $R_n^i(fh(n - \text{cable}(K), w))/R_n^i(\text{rot}(n - \text{cable}(K), w)) \in \mathbb{Q}^*$ depends of course only on the type of K and on the framing $w(K)$.

Question 3 *Are there any relations between the rational knot functions of the same framed knot $(K, w(K))$, if K is not a torus knot?*

Let us finish this section with some vague questions and speculations about further developments.

Our construction is of combinatorial nature and of complexity of degree at most 4 for each fixed n . This is an advantage, because the invariants can be really calculated. But it is also a disadvantage, because the physical origin of our results stays completely mysterious and there are no evident connections to other fields in mathematics like e.g. representation theory or differential geometry.

Question 4 *We can consider our 1-cocycle as an integration of a discrete differential form over a discrete loop. For better understanding it would be very important to transform this into real analysis. Is there a connection with differential or even Riemannian geometry of the infinite-dimensional space M_n for $n > 1$? More precisely, can the class $[R_n^i]$ be represented by integrating a closed differential real polynomial valued 1-form over loops in M_n (in the spirit, but quite different, of the Jones polynomial for links in 3-manifolds by Witten's Feynmann integrals of the Chern-Simons functional over some infinite-dimensional space of $SU(2)$ -connections, see [42])? But notice that the 1-form should strongly depend on the choice of the abstract closure and of the point at infinity for the points in M_n . If such a 1-form exists then its "stationary phase approximation", with the critical points of the integrand corresponding to the Reidemeister moves, should coincide up to normalization with our combinatorial 1-cocycle R_n^i of integer polynomials.*

Notice also that each R_n^i is constant on each component of the loop space ΩM_n but can have different values on different components.

4 Proof

Our main results are based on very complicated combinatorics and the interested reader has certainly a hard time to check all the details. We apologize for this. But we believe that there will be conceptually better proofs in the future (compare Question 4).

4.1 Generalities and reductions by using singularity theory

We consider the moduli space M of all string links in $\mathbb{C} \times \mathbb{R}$ with a fixed projection $pr : \mathbb{C} \times \mathbb{R} \rightarrow \mathbb{C}$. A generic arc s in M intersects $\Sigma_{tri}^{(1)}$, $\Sigma_{tan}^{(1)}$ and

$\Sigma_{cusp}^{(1)}$ transversally in a finite number of points and it does not intersect at all strata of higher codimension. To each intersection point with $\Sigma_{tri}^{(1)}$ and $\Sigma_{tan}^{(1)}$ we associate a contribution in $\mathbb{Z}[x, x^{-1}]$. We sum up with signs (coming from the co-orientation) the contributions over all intersection points in s and we obtain $R_1(s)$.

We use now the strata from $\Sigma^{(2)}$ to show the invariance of $R_1(s)$ under all generic homotopies of s in M which fix the endpoints of s . A homotopy is *generic* if it intersects $\Sigma^{(1)}$ transversally besides for a finite number of points in s where s has an ordinary tangency with $\Sigma^{(1)}$, it intersects $\Sigma^{(2)}$ transversally in a finite number of points and it doesn't intersect at all $\Sigma^{(i)}$ for $i > 2$.

We see immediately that $R_1(s)$ is invariant by passing through a tangency of s with $\Sigma^{(1)}$. Indeed, the two intersection points have identical contributions but they enter with different signs and cancel out. In order to show the invariance under generic homotopies we have to study now normal 2-discs for the strata in $\Sigma^{(2)} \subset M$. For each type of stratum in $\Sigma^{(2)}$ we have to show that $R_1(m) = 0$ for the boundary m of the corresponding normal 2-disc in M . We call m a *meridian*. $\Sigma_{quad}^{(2)}$ is by far the hardest case which leads to the tetrahedron equation. We look at the tetrahedron equation from the point of view of singularities of the projection of lines as explained in the Introduction.

Going along the meridian m of the positive quadruple crossing we see ordinary diagrams of positive 4-braids and exactly eight diagrams with an ordinary positive triple crossing. We show this in Fig. 24. (For simplicity we have drawn the positive triple crossings as triple points, but the branches do never intersect.) However, we have to study 24×48 different types of quadruple crossings.

The different local types of triple crossings are shown and numbered in Fig. 25. The sign in the figure indicates the side of the discriminant $\Sigma^{(1)}$ if the triple crossing is of global type r . If it is of global type l then all signs have to be changed to the opposite ones. Triple crossings come together in points of $\Sigma_{trans-self}^{(2)}$, but one easily sees that the global type of the triple crossings (i.e. its pointed Gauss diagram without the writhe) is always preserved. We make now a graph Γ for each global type of a triple crossing in the following way: the vertices's correspond to the different local types of triple crossings. We connect two vertices's by an edge if and only if the corresponding strata of triple crossings are adjacent to a stratum of $\Sigma_{trans-self}^{(2)}$. One easily sees that

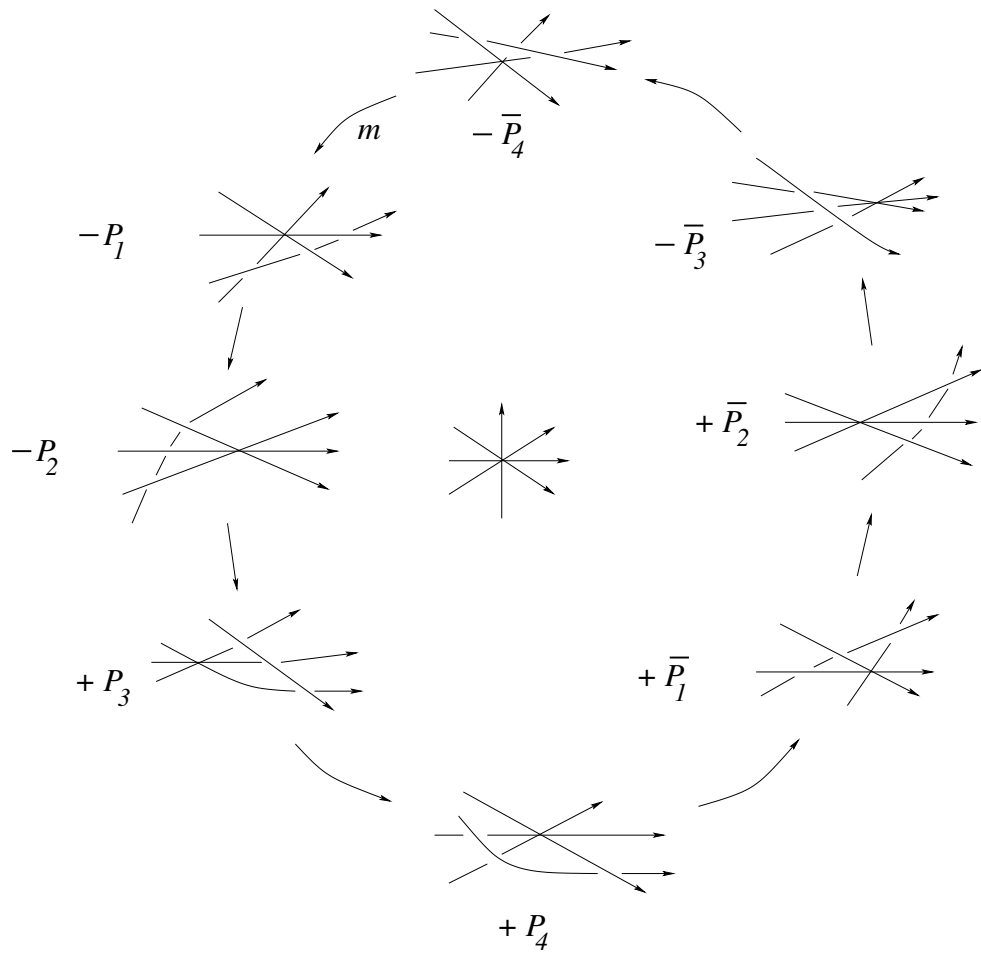


Figure 24: Unfolding of a positive quadruple crossing

the resulting graph is the 1-skeleton of the 3-dimensional cube I^3 (compare Section 4.5). In particular, it is connected. (Studying the normal discs to $\Sigma_{trans-self}^{(2)}$ in M one shows that if a 0-cochain is invariant under passing all $\Sigma_{tan}^{(1)}$ and just one local type of a stratum $\Sigma_{tri}^{(1)}$ then it is invariant under passing all remaining local types of triple crossings because Γ is connected.) The edges of the graph $\Gamma = skl_1(I^3)$ correspond to the types of strata in $\Sigma_{trans-self}^{(2)}$. The solution of the positive tetrahedron equation tells us what is the contribution to R_1 of a positive triple crossing (i.e. all three involved crossings are positive). The meridians of the strata from $\Sigma_{trans-self}^{(2)}$ give equations which allow us to determine the contributions of all other types of triple crossings as well as the contributions of self-tangencies. However, a global phenomenon occurs: each loop in Γ could give an additional equation. Evidently, it suffices to consider the loops which are the boundaries of the 2-faces from $skl_2(I^3)$. We call all the equations which come from the meridians of $\Sigma_{trans-self}^{(2)}$ and from the loops in $\Gamma = skl_1(I^3)$ the *cube equations* (Section 4.5). (Notice that a loop in Γ is more general than a loop in M . For a loop in Γ we come back to the same local type of a triple crossing but not necessarily to the same whole diagram of T .)

We need only the following strata from $\Sigma^{(3)}$ in order to simplify the proof of the invariance of R_1 in generic homotopies which pass through strata from $\Sigma^{(2)}$:

- (1) one degenerate quadruple crossing where exactly two branches have an ordinary self-tangency in the quadruple point, denoted by $\Sigma_{trans-trans-self}^{(3)}$ (see Fig. 26).
- (2) one self-tangency in an ordinary flex with a transverse branch passing through the tangent point, denoted by $\Sigma_{trans-self-flex}^{(3)}$ (see Fig. 27).
- (3) the transverse intersection of a stratum from $\Sigma^{(1)}$ with a stratum of $\Sigma_{trans-self}^{(2)}$

Again, for each fixed global type of a quadruple crossing we form a graph with the local types of quadruple crossings as vertices's and the adjacent strata of $\Sigma_{trans-trans-self}^{(3)}$ as edges. One easily sees that the resulting graph Γ has exactly 48 vertices's and that it is again connected. Luckily, we don't need to study the unfolding of $\Sigma_{trans-trans-self}^{(3)}$ in much detail. It is clear that

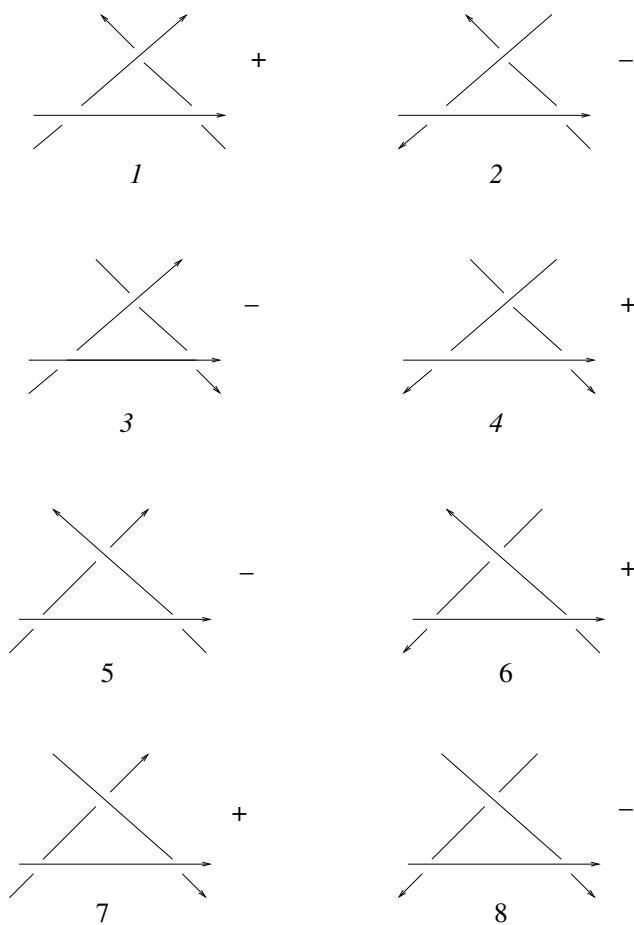


Figure 25: Local types of a triple crossing

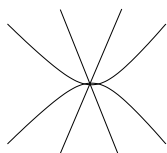


Figure 26: A quadruple crossing with two tangential branches

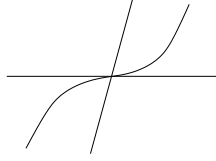


Figure 27: A self-tangency in a flex

each meridional 2-sphere for $\Sigma_{trans-trans-self}^{(3)}$ intersects $\Sigma^{(2)}$ transversally in a finite number of points, namely exactly in two strata from $\Sigma_{quad}^{(2)}$ and in lots of strata from $\Sigma_{trans-self}^{(2)}$ and from $\Sigma^{(1)} \cap \Sigma^{(1)}$ and there are no other intersections with strata of codimension 2. If we know now that $R_1(m) = 0$ for the meridian m of one of the quadruple crossings, that $R_1(m) = 0$ for all meridians of $\Sigma_{trans-self}^{(2)}$ (i.e. R_1 satisfies the cube equations) and for all meridians of $\Sigma^{(1)} \cap \Sigma^{(1)}$ (i.e. R_1 is invariant under passing simultaneous Reidemeister moves at different places in the diagram) then $R_1(m) = 0$ for the other quadruple crossing too. It follows that for each of the fixed 24 global types (see Fig. 28, where in each case we have four possibilities for the point at infinity) the 48 tetrahedron equations reduce to a single one, which is called the *positive global tetrahedron equation*. There is no further reduction possible because we are searching for non symmetric solutions and which depend non-trivially from the point at infinity!

In the cube equations there are also two local types of edges, corresponding to the two different local types of a Reidemeister II move with given orientations, compare Fig. 29. We reduce them to a single type of the edge by using the strata from $\Sigma_{trans-self-flex}^{(3)}$. The meridional 2-sphere for $\Sigma_{trans-self-flex}^{(3)}$ intersects $\Sigma^{(2)}$ transversally in exactly two strata from $\Sigma_{trans-self}^{(2)}$, which correspond to the two different types of the edge, and in lots of strata from $\Sigma_{self-flex}^{(2)}$ and from $\Sigma^{(1)} \cap \Sigma^{(1)}$. Hence, again the invariance under passing one of the two local types of strata from $\Sigma_{trans-self}^{(2)}$ together with the invariance under passing all strata from $\Sigma_{self-flex}^{(2)}$ and $\Sigma^{(1)} \cap \Sigma^{(1)}$ guaranties the invariance under passing the other local type of $\Sigma_{trans-self}^{(2)}$ too.

The unfolding (i.e. the intersection of a normal disc with the stratification of M) of e.g. the edge 1 – 5 of Γ is shown in Fig. 30 (compare [18]). The intersection of a meridional 2-sphere for $\Sigma^{(1)} \cap \Sigma_{trans-self}^{(2)}$ with $\Sigma^{(2)}$ consists

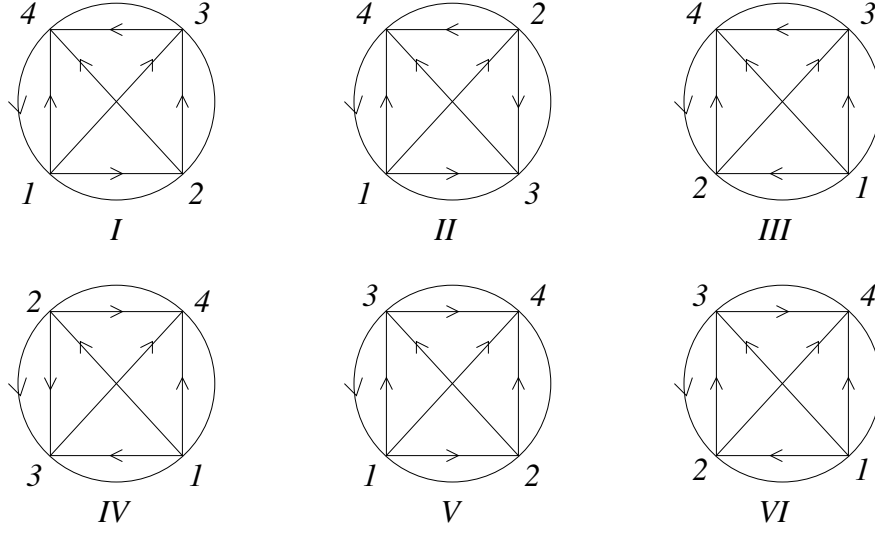


Figure 28: The global types of quadruple crossings

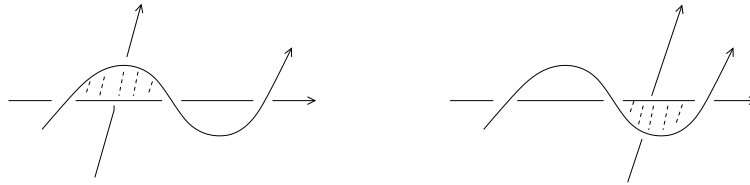


Figure 29: Two different local types of an edge 1-7 in the cube equations and which come together in $\Sigma_{trans-self-flex}^{(3)}$

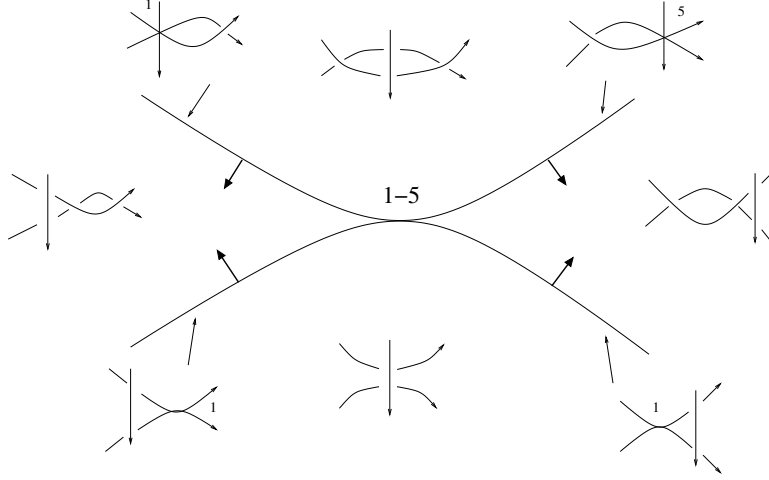


Figure 30: The unfolding of a self-tangency with a transverse branch corresponding to the edge 1 – 5

evidently of the transverse intersections of the stratum $\Sigma^{(1)}$ with all the strata of codimension 1 in the unfolding of $\Sigma_{trans-self}^{(2)}$. It follows again that it is sufficient to prove the invariance under passing $\Sigma^{(1)} \cap \Sigma^{(1)}$ only for positive triple crossings and only for one of the two local types of self-tangencies with a given orientation.

The remaining part of the paper is now organized as follows: we show the invariance of R_1 under generic homotopies which pass through the strata from Proposition 1 in the following Subsections: 4.2: (3) and (6), 4.3: (4), 4.5: (1), 4.6: (2) and the cube equations, 4.7: (5) besides for $\Sigma_{trans-cusp, cusp=[ml]=0, [d]=1}^{(2)}$ and the scan property, 4.8: the invariance of R_n^i for $n > 1$.

4.2 Reidemeister II moves in a cusp and in a flex

As a warm-up we consider first the less important strata. All weights and contributions were defined in Section 2.1.

Let's start with $\Sigma_{cusp-deg}^{(2)}$. A meridian for one type is shown in Fig. 31. There is a single Reidemeister II move p which could a priori contribute if it has the right global type. It follows easily from the Polyak-Viro formula, see [34], that in this case $W_2(p) = v_2(K)$. However, evidently the linking number $l(d) = 0$ and hence the move does not contribute.

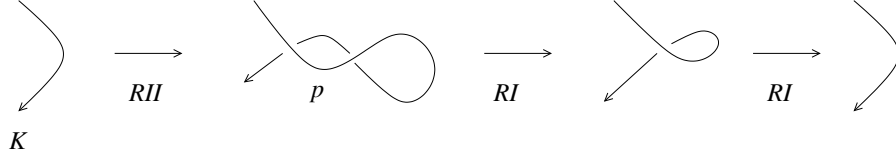


Figure 31: A meridian for a degenerated cusp

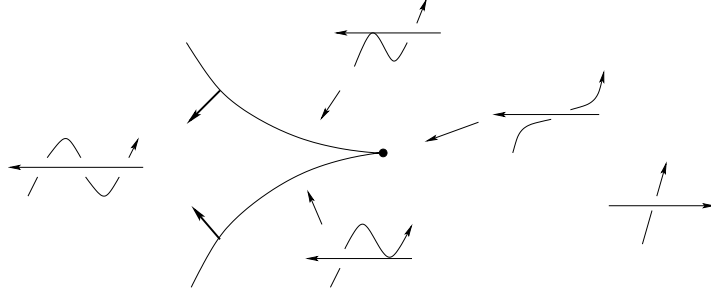


Figure 32: The unfolding for the self-tangency in a flex

The considerations for all other types of $\Sigma_{cusp-deg}^{(2)}$ are completely analogous.

We show the unfolding and a meridian for one type of $\Sigma_{self-flex}^{(2)}$ in Fig. 32. There are exactly two Reidemeister II moves, p_1 and p_2 . The third crossings, which are not in the Reidemeister moves, are never f-crossings in the case of long knots. If one is a r-crossing for one of the two moves then the other is a r-crossing for the other move with exactly the same f-crossing. Consequently, $W_2(p_1) = W_2(p_2)$. The linking numbers $l(d)$ are the same for both R II moves but their signs are different and they cancel out. The calculations for all the other types of $\Sigma_{self-flex}^{(2)}$ are completely analogous.

4.3 Simultaneous Reidemeister moves

An example of a meridian of $\Sigma^{(1)} \cap \Sigma^{(1)}$ is shown in Fig. 33. It is clear that e.g. the f-crossings for p_1 do not change when the meridian m crosses the discriminant at p_2 .

Let's consider the quadratic weight $W_2(p)$ (compare Definition 6). Here p could be the crossing d or ml . Evidently $W_1(hm)$ does not change.

Lemma 2 $W_2(p)$ is a relative isotopy invariant for each Reidemeister move of type I, II or III, i.e. $W_2(p)$ is invariant under any isotopy of the rest of

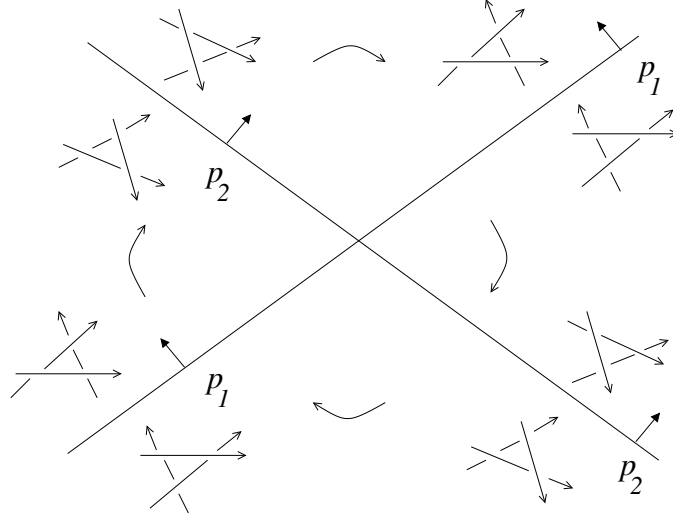


Figure 33: Meridian of two simultaneous Reidemeister III moves

the diagram outside of $D_p^2 \times \mathbb{R}$, where $D_p^2 \subset \mathbb{C}$ is a small disk around p .

The lemma implies that $W_2(p)$ doesn't change under a homotopy of an arc which passes through $\Sigma^{(1)} \cap \Sigma^{(1)}$. Evidently, the linking numbers $l(d)$ and $l(ml)$ don't change neither and hence the contributions to R_1 cancel out in the meridian m .

Proof. It is obvious that $W_2(p)$ is invariant under Reidemeister moves of type I and II. The latter comes from the fact that both new crossings are simultaneously crossings of type f or r and that they have different writhe. As was explained in Section 4.1 the graph Γ implies now that it is sufficient to prove the invariance of $W_2(p)$ only under positive Reidemeister moves of type III. There are two global types and for each of them there are three possibilities for the point at infinity. We give names 1, 2, 3 to the crossings and a, b, c to the points at infinity and we show the six cases in Fig. 34 and Fig. 35. Evidently, we have only to consider the mutual position of the three crossings in the pictures because the contributions with all other crossings do not change. We say that two crossings *intersect* if the corresponding arrows in the Gauss diagram intersect.

r_a : there is only 3 which could be a f -crossing but it does not contribute with another crossing in the picture to $W_2(p)$.

r_b : no r -crossing at all.

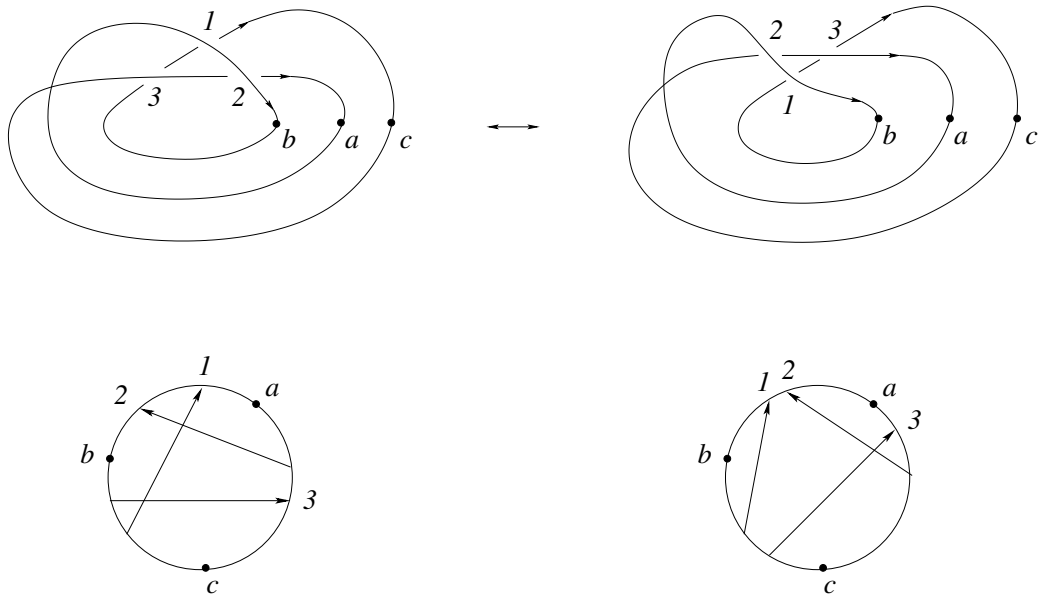


Figure 34: $RIII$ of type r

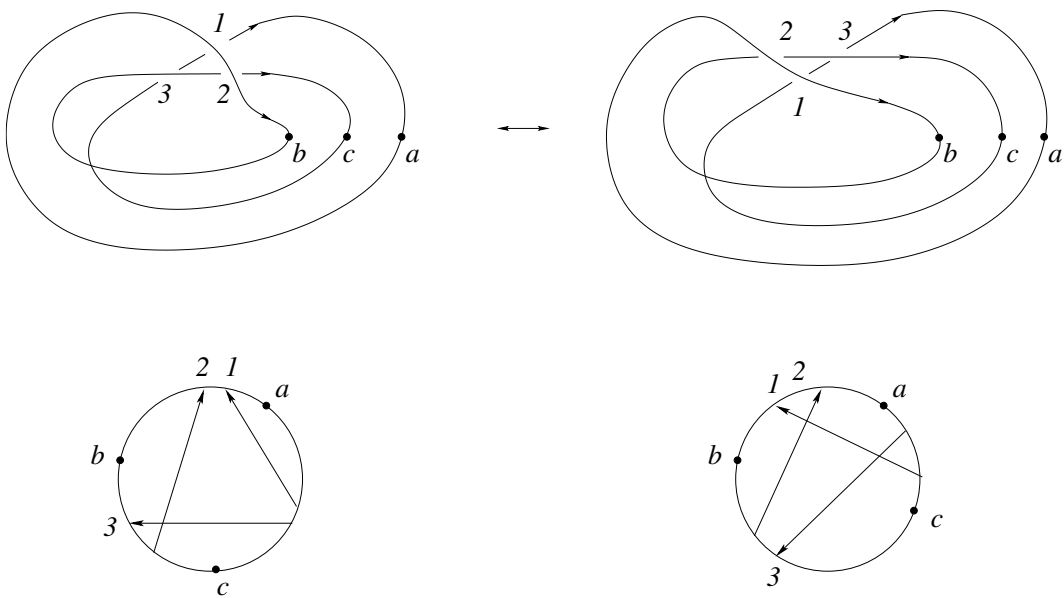


Figure 35: $RIII$ of type l

r_c : only 2 could be a f-crossing. In that case it contributes on the left side exactly with the r-crossing 1 and on the right side exactly with the r-crossing 3.

l_a : no f-crossing at all.

l_b : 1 and 2 could be f-crossings but non of them contributes with the crossing 3 to $W_2(p)$.

l_c : 1 and 3 could be f-crossings. But the foots of 1 and 3 are arbitrary close. Consequently, they can be f-crossings only simultaneously! In that case 3 contributes with 2 on the left side and 1 with 2 on the right side.

Consequently, we have proven that $W_2(p)$ is invariant.

□

4.4 Refined tetrahedron equation for string links

This section contains the heart of this paper.

As explained in Section 4.1 it suffices to consider global positive quadruple crossings with a fixed point at infinity. We naturally identify crossings in an isotopy outside Reidemeister moves of type I and II. The following lemma is of crucial importance.

Lemma 3 *The f-crossings for d of the eight adjacent strata of triple crossings (compare Fig. 24) have the following properties:*

- (1) *the f-crossings in P_2 are identical with those in \bar{P}_2*
- (2) *the f-crossings in P_1 , \bar{P}_1 , P_4 and \bar{P}_4 are all identical*
- (3) *the f-crossings in P_3 are either identical with those in \bar{P}_3 or there is exactly one new f-crossing in \bar{P}_3 with respect to P_3 . In the latter case the new crossing is always exactly the crossing $hm = 34$ in P_1 and \bar{P}_1*
- (4) *the new f-crossing in \bar{P}_3 appears if and only if P_1 (and hence also \bar{P}_1) is of one of the two global types r_a or l_c .*
- (5) *the distinguished crossing d in P_3 and \bar{P}_3 is always the crossing ml in P_1 and \bar{P}_1*

Proof. We have checked the assertions of the lemma in all twenty four cases (denoted by the global type of the quadruple crossing together with the point at infinity) using Fig. 36-47. These figures are our main instrument. Notice that the crossing hm in P_1 and \bar{P}_1 is always the crossing 34 and that d is of type 0 if ∞ is on the right side of it in the figures. The distinguished

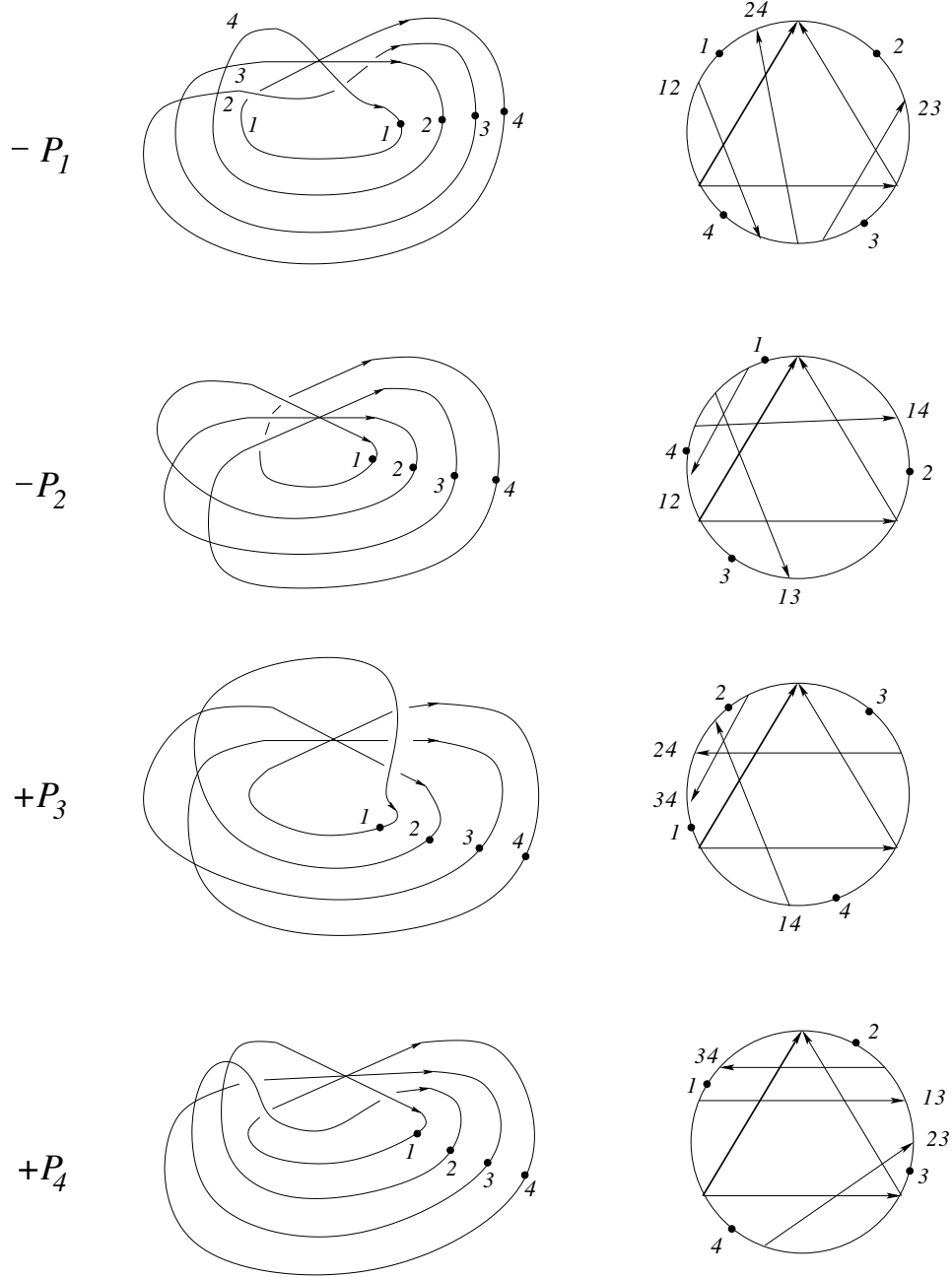


Figure 36: first half of the meridian for global type I

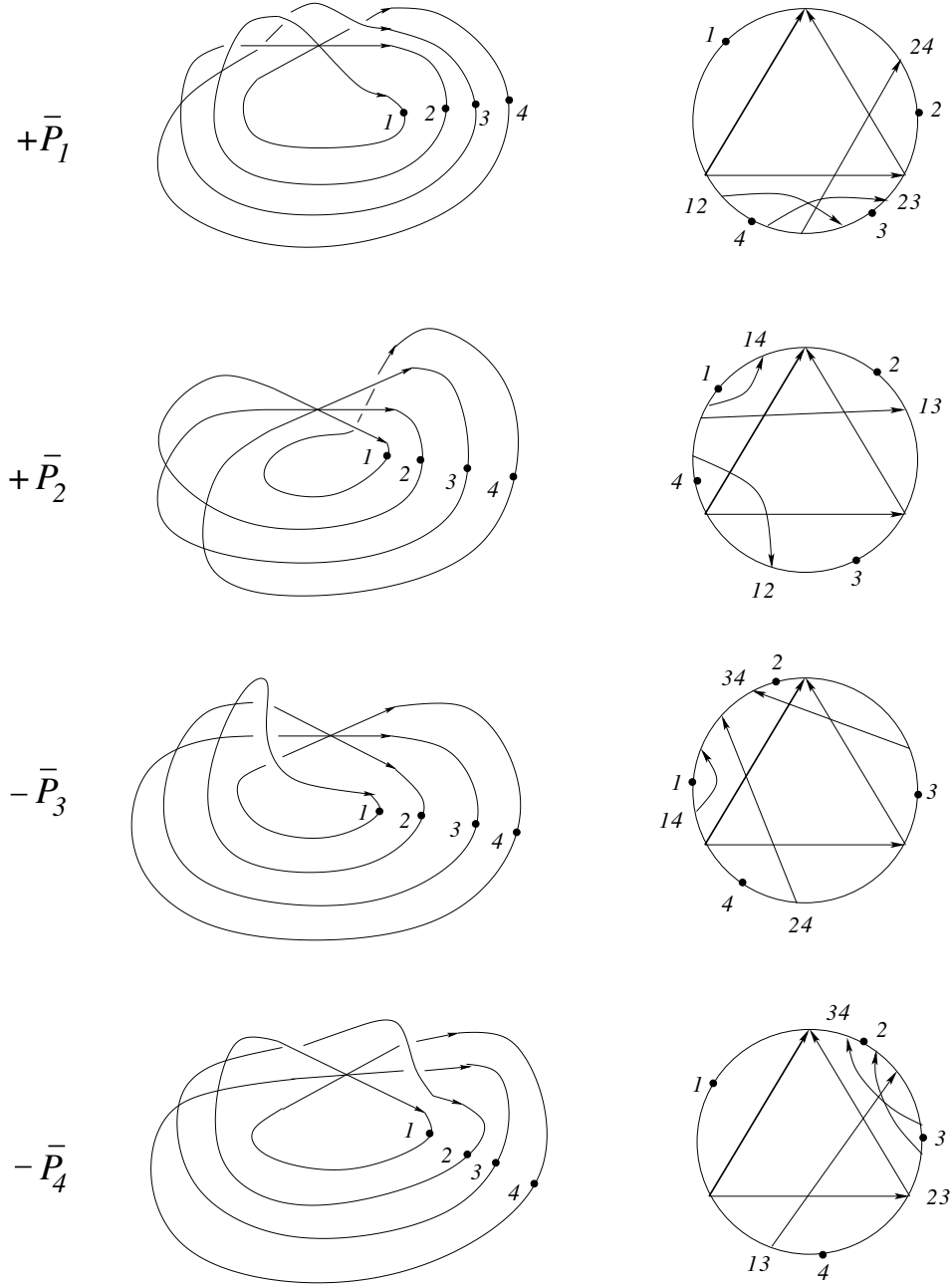


Figure 37: second half of the meridian for global type I

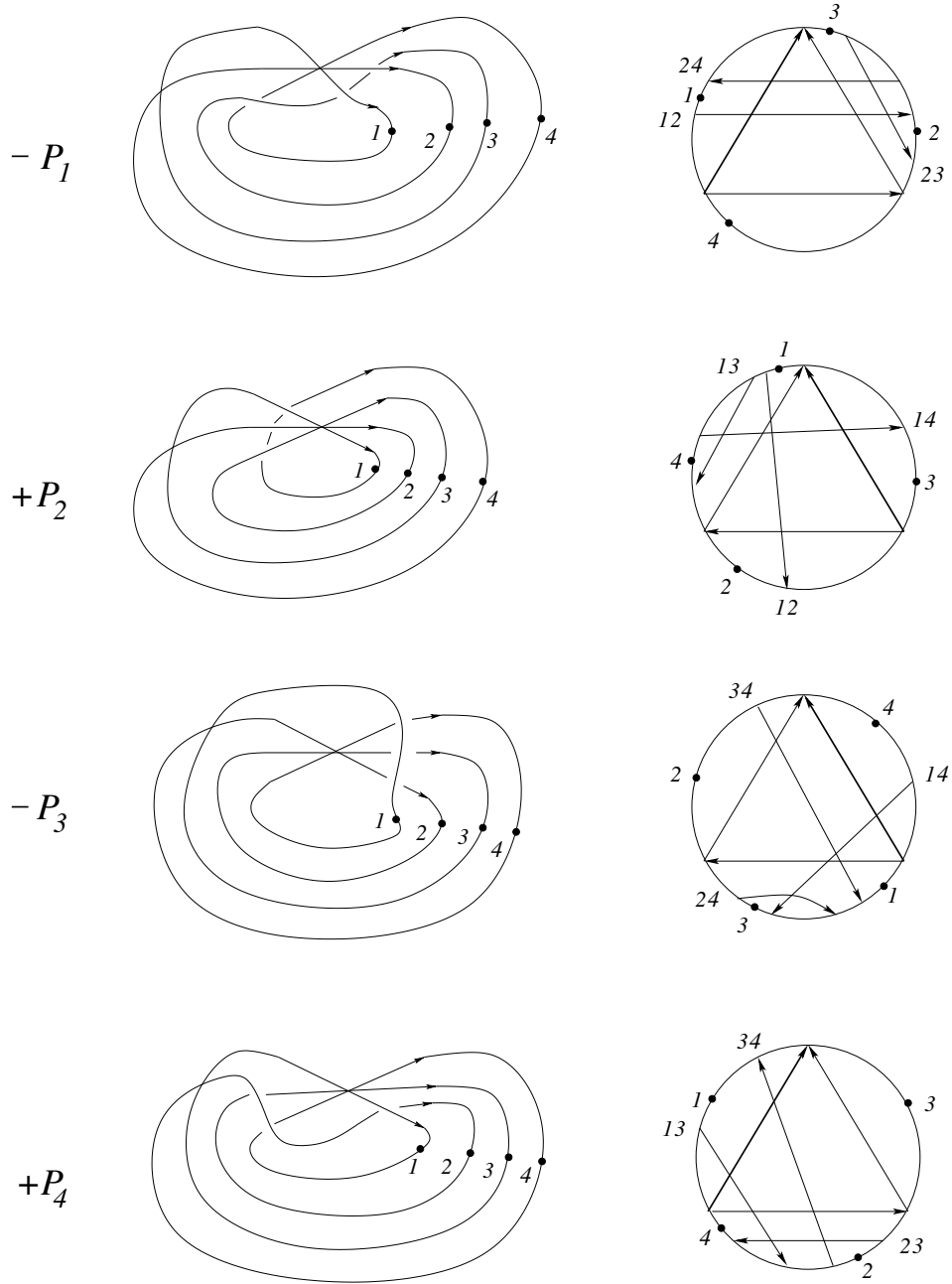


Figure 38: first half of the meridian for global type II

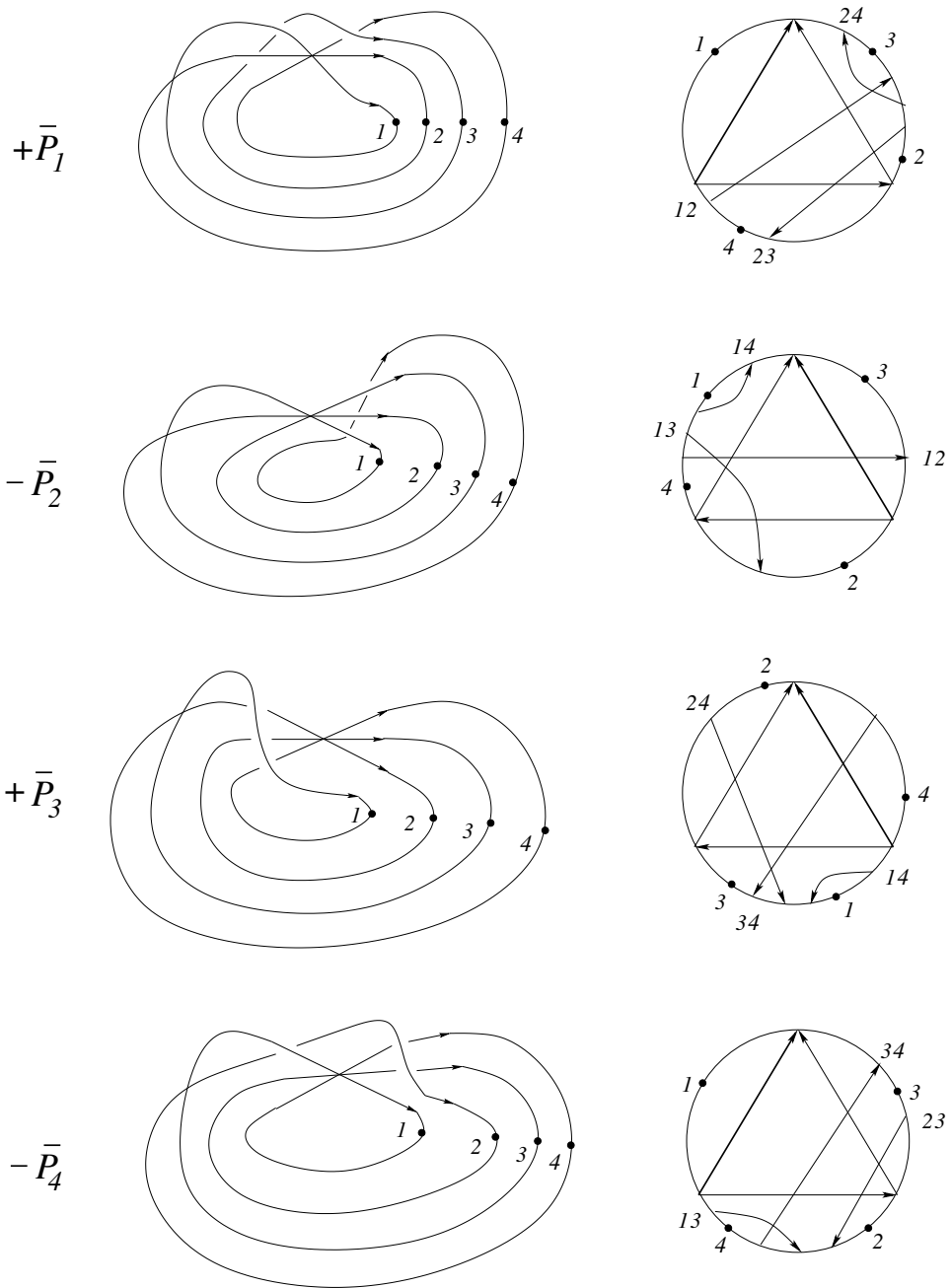


Figure 39: second half of the meridian for global type II

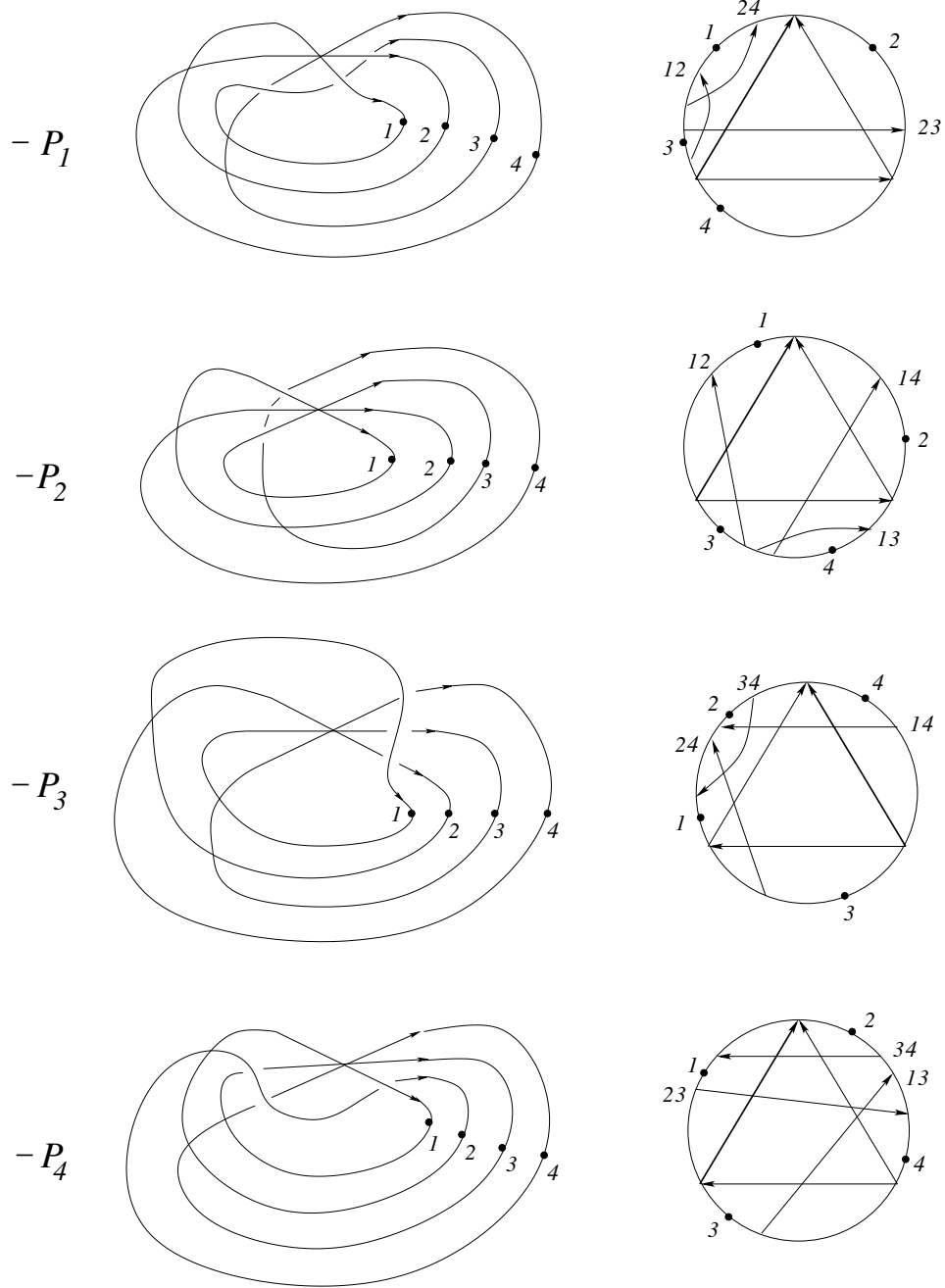


Figure 40: first half of the meridian for global type III

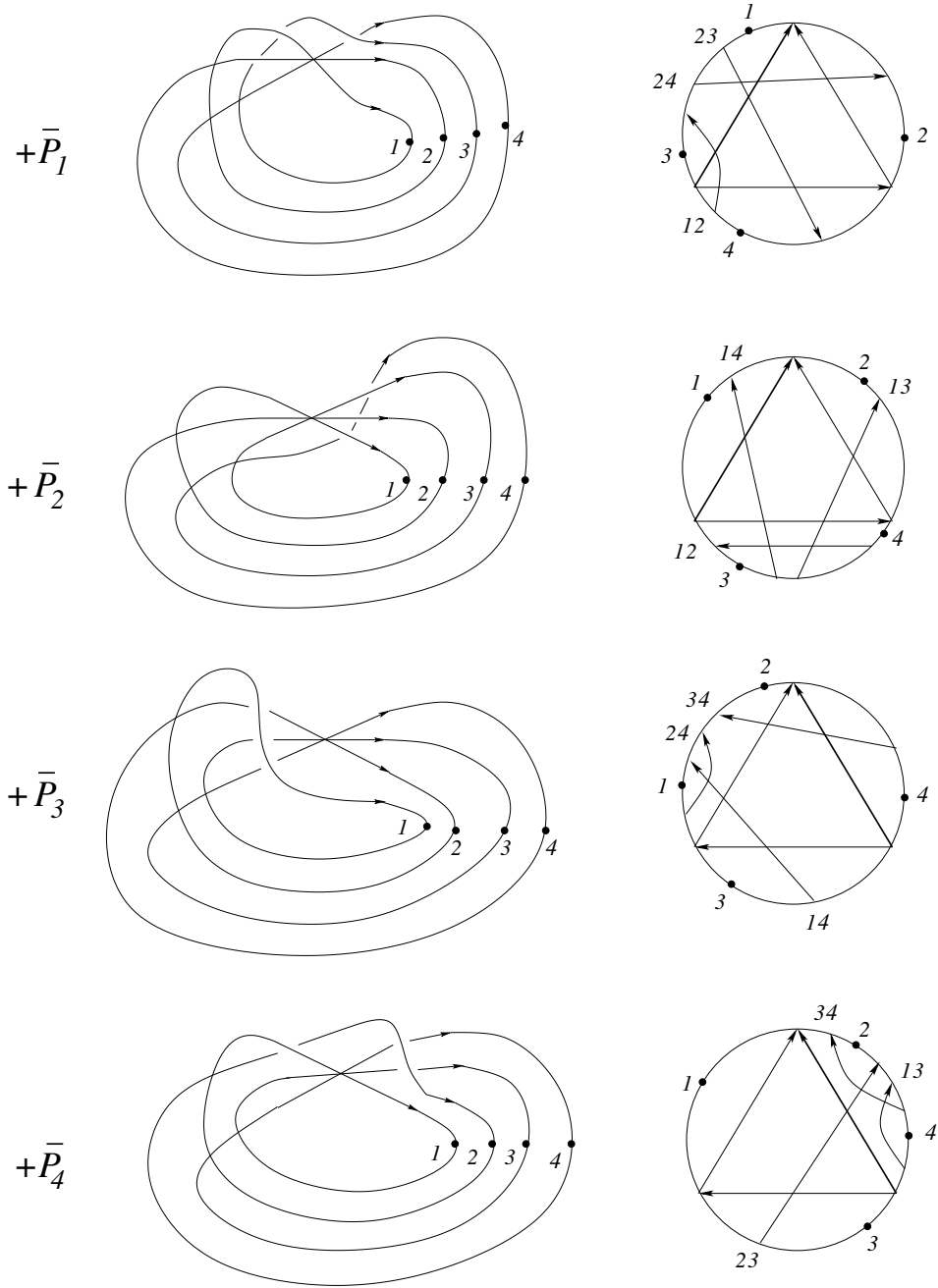


Figure 41: second half of the meridian for global type III

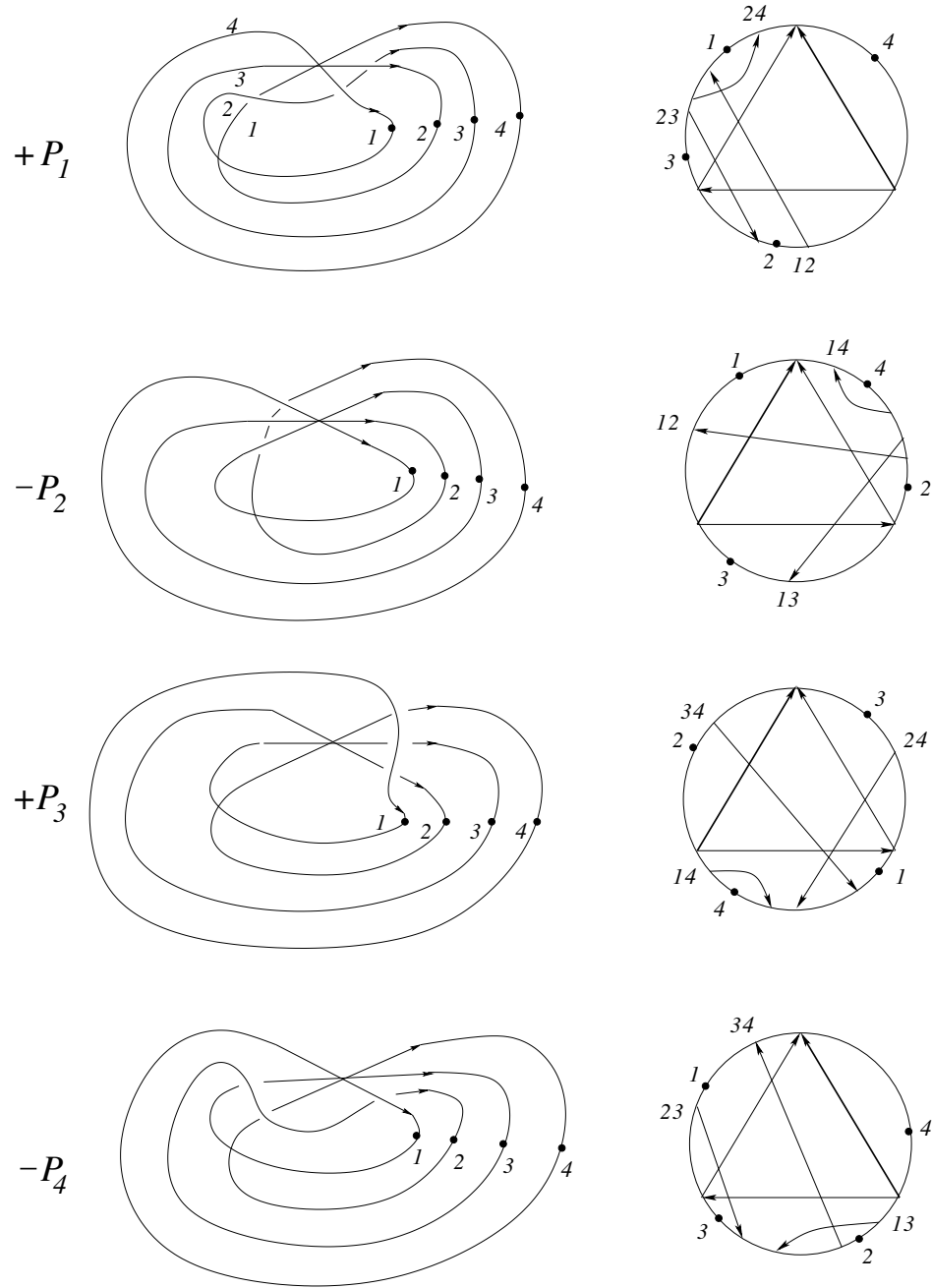


Figure 42: first half of the meridian for global type IV

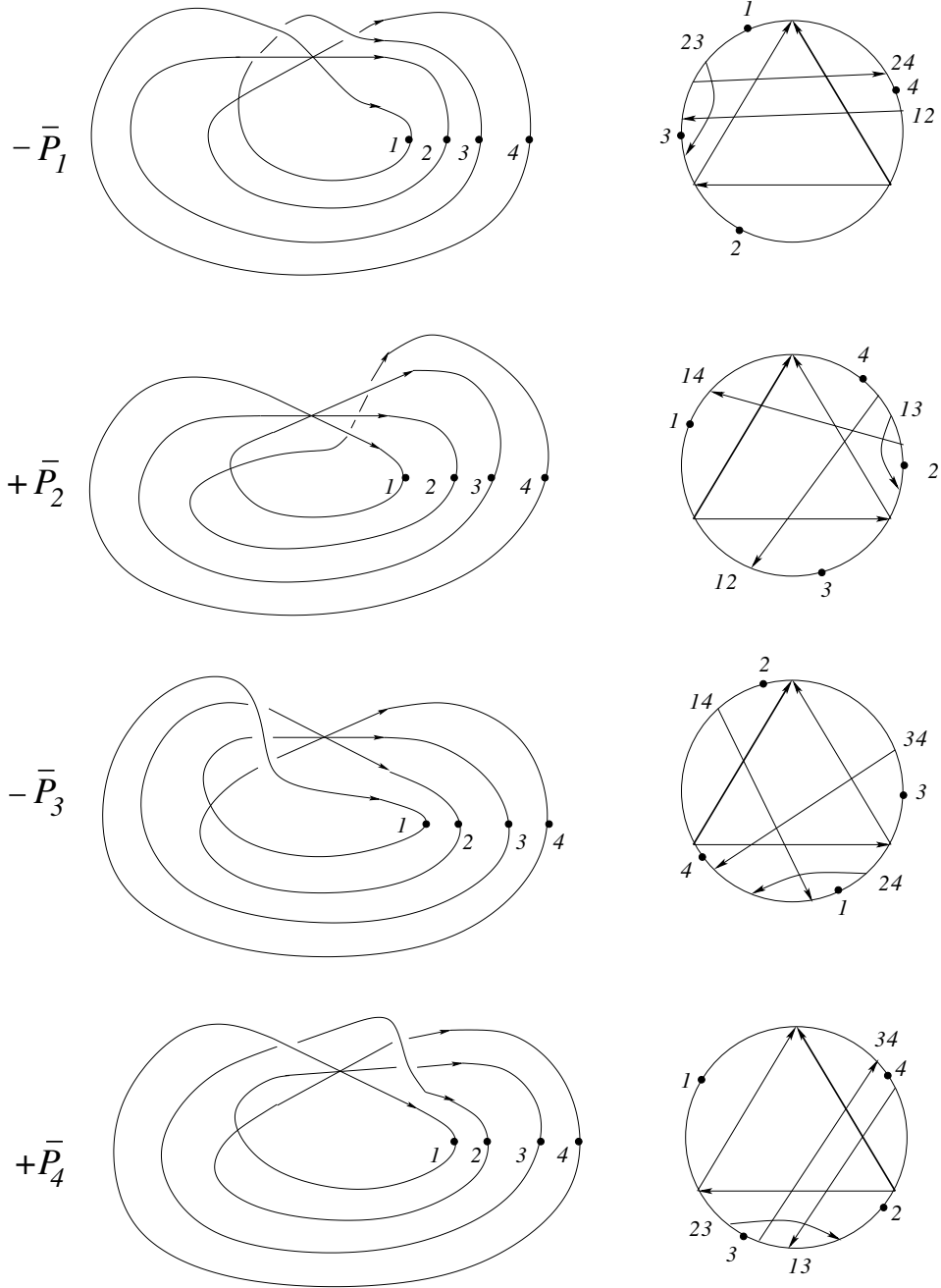


Figure 43: second half of the meridian for global type IV

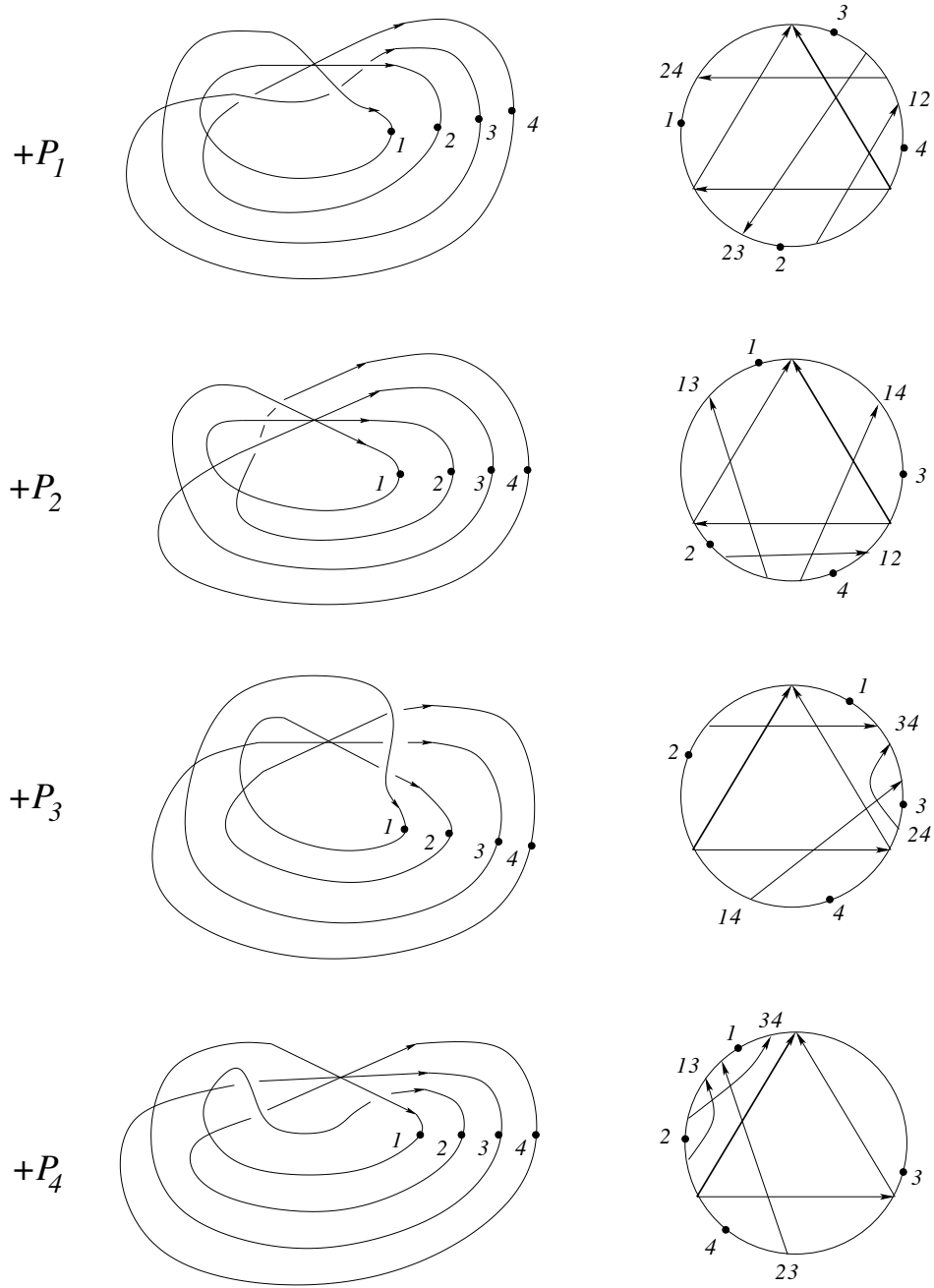


Figure 44: first half of the meridian for global type V

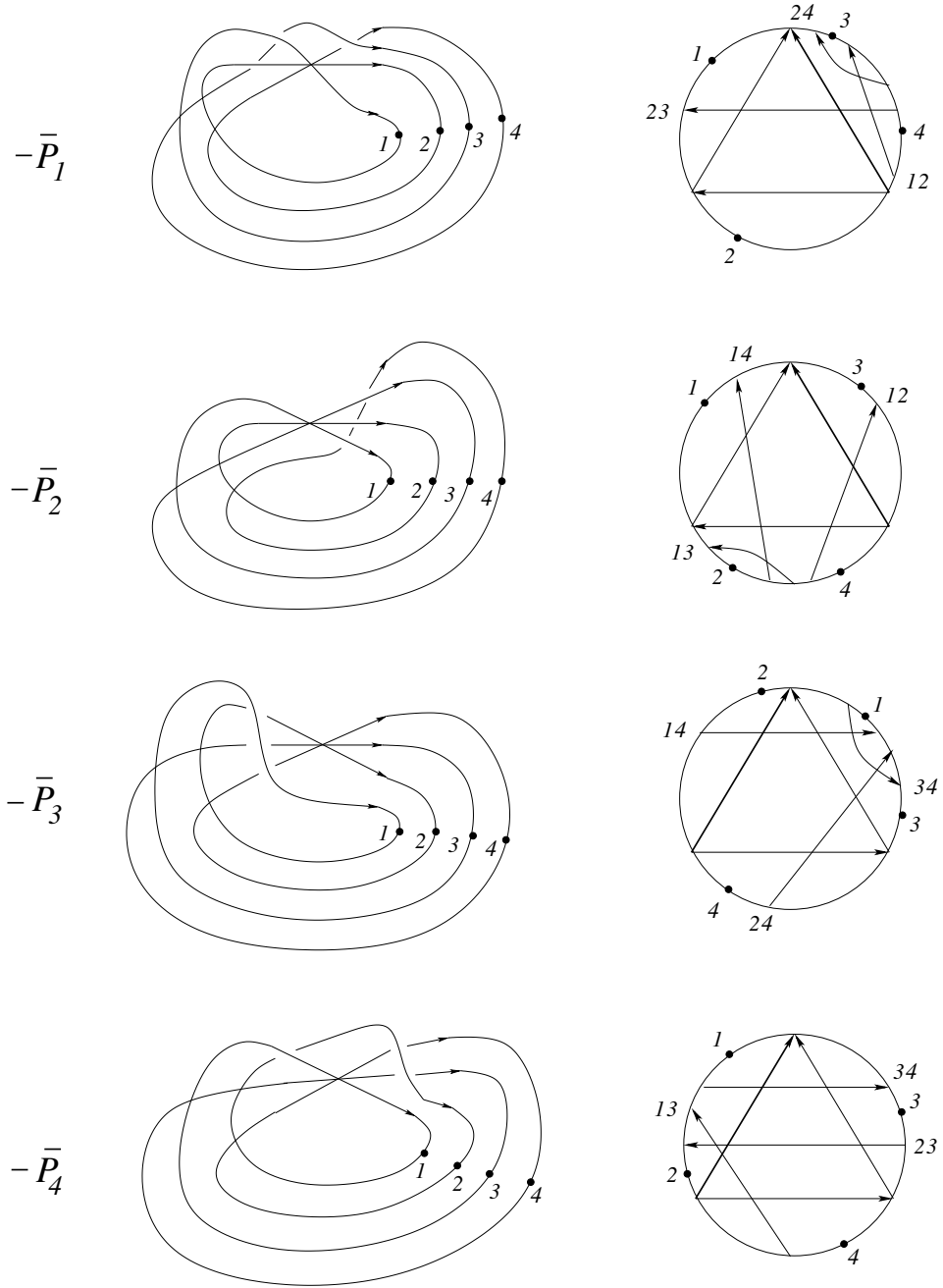


Figure 45: second half of the meridian for global type V

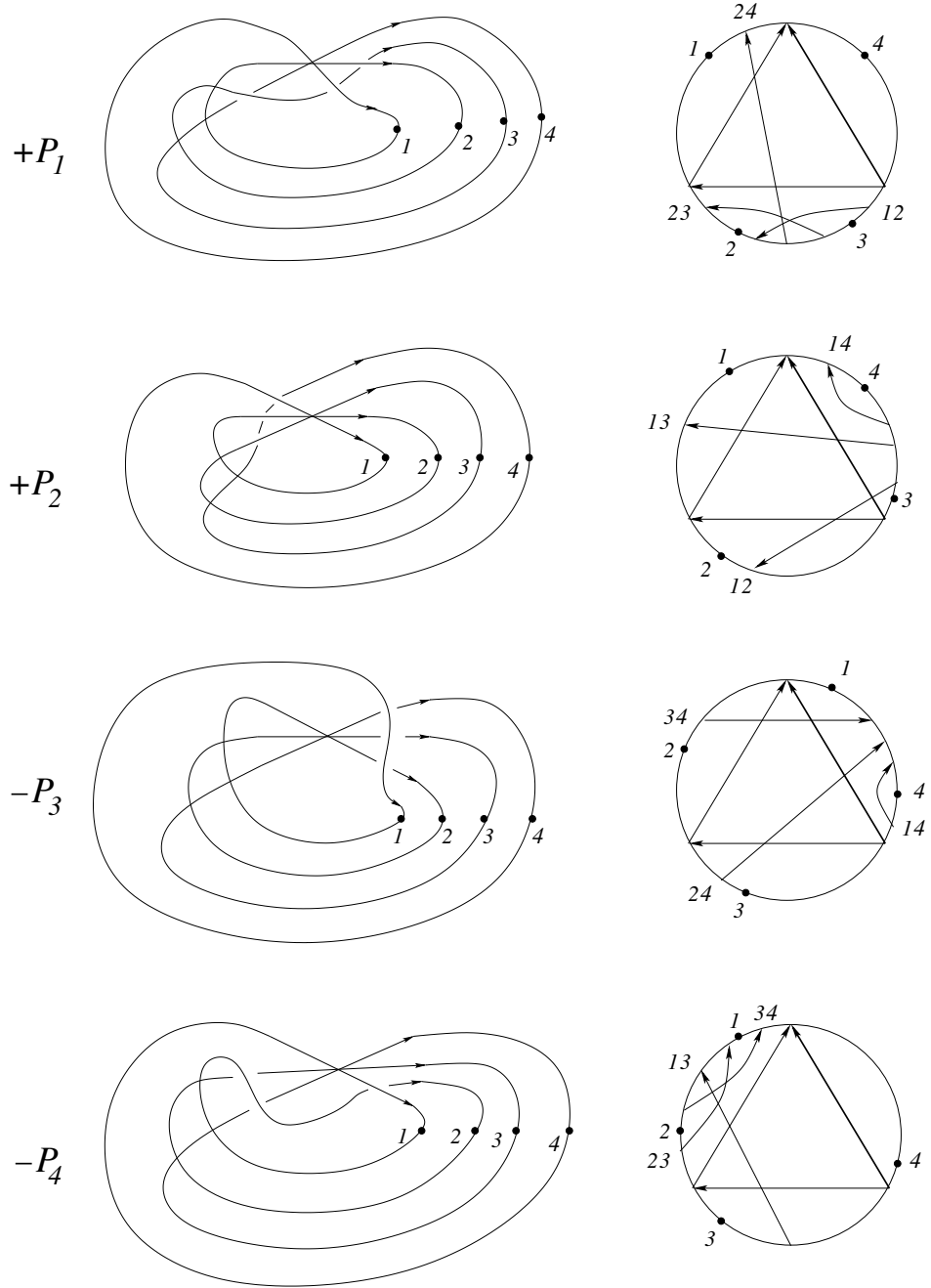


Figure 46: first half of the meridian for global type VI

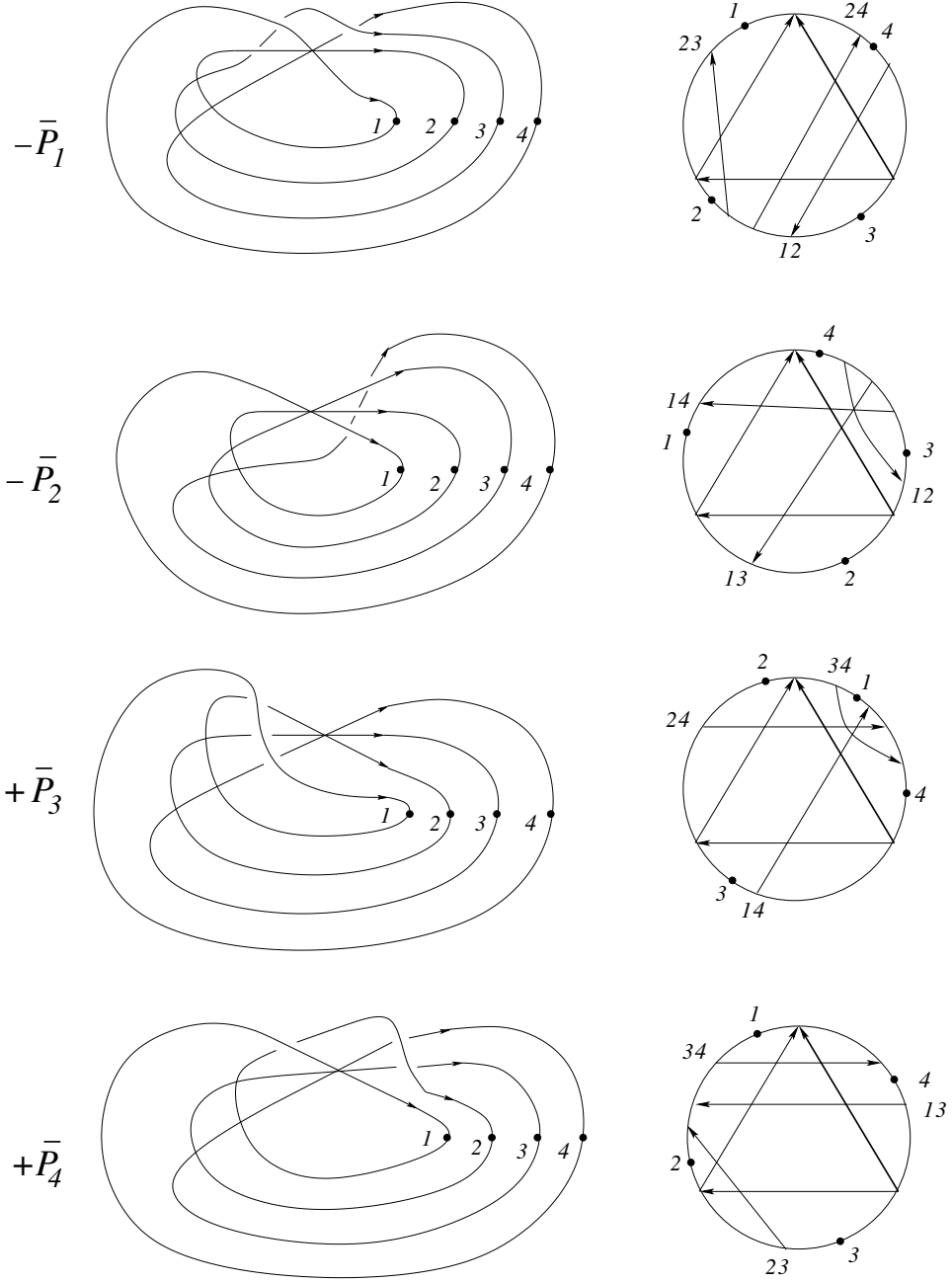


Figure 47: second half of the meridian for global type VI

crossing d in P_3 is always the crossing 13 which is always the crossing ml in P_1 too.

We consider just some examples. In particular we show that it is necessary to add the "degenerate" configuration in Fig. 7 and we left the rest of the verification to the reader.

The f-crossings are:

case I_1 . non at all

case I_2 . non at all

case I_3 . In P_1, \bar{P}_1 : 34 (both are the degenerate case). In P_4, \bar{P}_4 : 34 (the third configuration and the first configuration in Fig. 7). In P_2, \bar{P}_2 : 34. In P_3 : non. In \bar{P}_3 : 34.

case I_4 . In $P_1, \bar{P}_1, P_4, \bar{P}_4$: 34, 24, 23. In P_2, \bar{P}_2 : non. In P_3 : 23, 24. In \bar{P}_3 : 23, 24, 34.

case VI_3 : In P_2 : 12, 13, 14. In \bar{P}_2 : 12, 13, 14 (12 shows that the fourth configuration in Fig. 7 is necessary too).

case VI_1 : In P_3 : non. In \bar{P}_3 : 34 (shows that the global type l_c is necessary too). \square

It turns out that Lemma 3 could be used to define already a solution of the global tetrahedron equation. However, this solution is not controllable under moving cusps, compare Section 4.7. This forces us to go one step further and to introduce quadratic weights.

Let us consider now the quadratic weight $W_2(c)$. If a f-crossing is one of the six crossings from the positive quadruple crossing than its contribution to $W_2(c)$ is $+W_1(f)$.

We make the following conventions of notations: $W_2(d)$ and $W_1(hm)$ for P_i or \bar{P}_i are shortly denoted by $W_2(P_i)$ and $W_1(P_i)$ respectively $W_2(\bar{P}_i)$ and $W_1(\bar{P}_i)$. If a f-crossing is denoted by the names of the two branches ij , which define the f-crossing, then $W_1(ij)$ is the sum over all those r-crossings different from the six crossings of the quadruple crossing (i.e. this are the r-crossings which are not drawn in the figures). Consequently, $W_1(f)$ is the sum of $W_1(ij)$ and a correction term which comes from the r-crossings amongst the six crossings of the positive quadruple crossing.

In the case that the f-crossings in P_3 and \bar{P}_3 are not the same we get now $W_2(\bar{P}_3) = W_2(P_3) + W_1(f)$

where f is the new f-crossing in \bar{P}_3 . But luckily the new f-crossing f is always just the crossing $hm = 34$ in P_1 (compare the previous lemma).

The following lemma is a "quadratic refinement" of the previous lemma.

Lemma 4 (*Weights $W_2(d)$*)

- (1) $W_2(P_1) = W_2(\bar{P}_1) = W_2(P_4) = W_2(\bar{P}_4)$
- (2) $W_2(P_2) = W_2(\bar{P}_2)$
- (3) Let P_i for some $i \in \{1, 2\}$ be of one of the global types r_a or l_c . Then $W_1(P_i) = W_1(\bar{P}_i)$.
- (4) If the f -crossings in P_3 and \bar{P}_3 coincide then $W_2(P_3) = W_2(\bar{P}_3)$
- (5) Let f be the new f -crossing in \bar{P}_3 with respect to P_3 and let $f = hm$ be the corresponding crossing in P_1 . Then $W_2(\bar{P}_3) - W_2(P_3) = W_1(f)$ and $W_1(f) = W_1(P_1) = W_1(\bar{P}_1)$.
- (6) Let P_i for some $i \in \{3, 4\}$ be of one of the global types r_a or l_c . Then either simultaneously $W_1(P_3) = W_1(\bar{P}_3)$ and $W_1(P_4) = W_1(\bar{P}_4)$ or simultaneously $W_1(P_3) = W_1(\bar{P}_3) + 1$ and $W_1(\bar{P}_4) = W_1(P_4) + 1$.

Proof. The proof is by inspection of all f -crossings, all r -crossings and all hm -crossings in all twenty four cases in the figures. We give it below in details. (Those strata which can never contribute are dropped.) We skip also the $W_1(ij)$ and $W_2(ij)$ contributions because they are always determined by ij and cancel out.

It shows in particular that it is necessary to add the degenerate configurations in Fig. 7 and Fig. 6.

I_1 : nothing at all

I_2 : $W_2(P_1) = W_2(\bar{P}_1) = W_2(P_4) = W_2(\bar{P}_4) = 0$. $W_2(P_2) = W_2(\bar{P}_2) = 0$.

I_3 : $W_2(P_1) = W_2(\bar{P}_1) = W_2(P_4) = W_2(\bar{P}_4) = 2$. $W_2(P_2) = W_2(\bar{P}_2) = 2$. $W_1(P_1) = W_1(\bar{P}_1) = 2$. $W_1(P_2) = W_1(\bar{P}_2) = 2$. $W_2(P_3) = 0$ and $W_2(\bar{P}_3) = W_2(\bar{P}_3, f) = 2$.

I_4 : $W_2(P_1) = W_2(\bar{P}_1) = W_2(P_4) = W_2(\bar{P}_4) = 4$. $W_1(P_1) = W_1(\bar{P}_1) = 1$. $W_1(P_3) = W_1(\bar{P}_3) = 1$. $W_1(P_4) = W_1(\bar{P}_4) = 2$. $W_2(\bar{P}_3) - W_2(P_3) = W_2(\bar{P}_3, f) = 1$.

II_1 : $W_1(P_2) = W_1(\bar{P}_2) = 0$.

II_2 : $W_2(P_1) = W_2(\bar{P}_1) = W_2(P_4) = W_2(\bar{P}_4) = 2$. $W_1(P_3) = 1$ and $W_1(\bar{P}_3) = 0$. $W_1(P_4) = 1$ and $W_1(\bar{P}_4) = 2$.

II_3 : $W_2(P_1) = W_2(\bar{P}_1) = W_2(P_4) = W_2(\bar{P}_4) = 0$. $W_2(P_2) = W_2(\bar{P}_2) = 0$.

II_4 : $W_2(P_1) = W_2(\bar{P}_1) = W_2(P_4) = W_2(\bar{P}_4) = 3$. $W_1(P_1) = W_1(\bar{P}_1) = 2$. $W_1(P_2) = W_1(\bar{P}_2) = 2$. $W_2(\bar{P}_3) - W_2(P_3) = W_2(\bar{P}_3, f) = 2$. $W_1(P_4) = W_1(\bar{P}_4) = 1$.

$$III_1: W_1(P_3) = W_1(\bar{P}_3) = W_1(P_4) = W_1(\bar{P}_4) = 0.$$

$$III_2: W_2(P_1) = W_2(\bar{P}_1) = W_2(P_4) = W_2(\bar{P}_4) = 0. \quad W_2(P_2) = W_2(\bar{P}_2) = 0. \\ W_1(P_3) = W_1(\bar{P}_3) = 0.$$

$$III_3: W_2(P_2) = W_2(\bar{P}_2) = 3. \quad W_1(P_2) = W_1(\bar{P}_2) = 1.$$

$$III_4: W_2(P_1) = W_2(\bar{P}_1) = W_2(P_4) = W_2(\bar{P}_4) = 2. \quad W_1(P_1) = W_1(\bar{P}_1) = 2. \\ W_2(P_2) = W_2(\bar{P}_2) = 2. \quad W_1(P_2) = W_1(\bar{P}_2) = 2. \quad W_2(\bar{P}_3) - W_2(P_3) = W_2(\bar{P}_3, f) = 2.$$

$$IV_1: W_1(P_1) = W_1(\bar{P}_1) = 0. \quad W_2(\bar{P}_3) - W_2(P_3) = W_2(\bar{P}_3, f) = 0. \\ W_1(P_3) = W_1(\bar{P}_3) = 1. \quad W_1(P_4) = W_1(\bar{P}_4) = 0.$$

$$IV_2: W_2(P_2) = W_2(\bar{P}_2) = 3.$$

$$IV_3: W_1(P_1) = W_1(\bar{P}_1) = 1. \quad W_1(P_2) = W_1(\bar{P}_2) = 1. \quad W_2(P_2) = W_2(\bar{P}_2) = 2. \\ W_2(\bar{P}_3) - W_2(P_3) = W_2(\bar{P}_3, f) = 1.$$

$$IV_4: W_2(P_1) = W_2(\bar{P}_1) = W_2(P_4) = W_2(\bar{P}_4) = 0. \quad W_2(P_2) = W_2(\bar{P}_2) = 0. \\ W_1(P_3) = W_1(\bar{P}_3) = 1. \quad W_2(P_3) = W_2(\bar{P}_3) = 1.$$

$$V_1: W_1(P_1) = W_1(\bar{P}_1) = 0. \quad W_1(P_2) = W_1(\bar{P}_2) = 0. \quad W_2(\bar{P}_3) - W_2(P_3) = W_2(\bar{P}_3, f) = 0.$$

$$V_2: \text{nothing at all}$$

$$V_3: W_2(P_1) = W_2(\bar{P}_1) = W_2(P_4) = W_2(\bar{P}_4) = 0. \quad W_2(P_2) = W_2(\bar{P}_2) = 0. \\ W_2(P_3) = W_2(\bar{P}_3) = 0.$$

$$V_4: W_2(P_1) = W_2(\bar{P}_1) = W_2(P_4) = W_2(\bar{P}_4) = 4. \quad W_2(P_3) = W_2(\bar{P}_3) = 4. \\ W_2(P_4) = W_2(\bar{P}_4) = 4. \quad W_1(P_3) = 3. \quad W_1(\bar{P}_3) = 2. \quad W_1(P_4) = 1. \quad W_1(\bar{P}_4) = 2.$$

$$VI_1: W_1(P_1) = W_1(\bar{P}_1) = 0. \quad W_1(P_2) = W_1(\bar{P}_2) = 0. \quad W_1(P_4) = W_1(\bar{P}_4) = 0. \\ W_2(\bar{P}_3) - W_2(P_3) = W_2(\bar{P}_3, f) = 0.$$

$$VI_2: W_1(P_3) = 1. \quad W_1(\bar{P}_3) = 0. \quad W_1(P_4) = 0. \quad W_1(\bar{P}_4) = 1.$$

$$VI_3: W_2(P_2) = W_2(\bar{P}_2) = 4.$$

$$VI_4: W_2(P_1) = W_2(\bar{P}_1) = W_2(P_4) = W_2(\bar{P}_4) = 0. \quad W_2(P_2) = W_2(\bar{P}_2) = 0. \\ W_2(P_3) = W_2(\bar{P}_3) = 0.$$

□

We take now into account also $W_2(ml)$.

Lemma 5 (*Weights with $W_2(ml)$*)

We have to consider only the triple crossings of global type r_a and l_c .

- (1) $ml = 12$ in $P_3, P_4, \bar{P}_3, \bar{P}_4$.
(2) $13 = d$ in P_3, \bar{P}_3 and $13 = ml$ in P_1, \bar{P}_1 .
(3) The f -crossings for ml in P_2 and in \bar{P}_2 are the same. $W_2(ml)$ in P_2 is always equal to $W_2(ml)$ in \bar{P}_2 . $W_1(hm)$ in P_2 is always equal to $W_1(hm)$ in \bar{P}_2 .
(4) The f -crossings for ml in P_1 and in \bar{P}_1 are the same. $W_2(ml)$ in P_1 is always equal to $W_2(ml)$ in \bar{P}_1 .
(5) $W_2(P_3) = W_2(ml)$ in P_1 .
(6) the sum of $x^{W_2(ml)+W_1(hm)} - x^{W_2(ml)}$ over $+P_3 - \bar{P}_3 + P_4 - \bar{P}_4$ is 0. (Here it can happen that only $+P_3 - \bar{P}_3$ or $+P_4 - \bar{P}_4$ are of the right global type r_a or l_c .)

Proof. (1) and (2) are evident. By inspection of the f -crossings and the r -crossings we have

I_3 : $W_2(ml) = 0$ in P_1 and in \bar{P}_1 . $W_2(ml) = 0$ in P_2 and in \bar{P}_2 . $W_1(hm) = 2$ in P_2 and in \bar{P}_2 .

I_4 : $W_2(ml) = 3$ in P_1 and in \bar{P}_1 . $W_2(P_3) = 3 = W_2(ml)$ in P_1 . P_3 : $x^{W_2(12)+W_1(23)+1} - x^{W_2(12)}$, \bar{P}_3 : $x^{W_2(12)+W_1(23)+1+W_1(24)+2} - x^{W_2(12)+W_1(24)+2}$, P_4 : $x^{W_2(12)+W_1(23)+1+W_1(24)+2} - x^{W_2(12)+W_1(23)+1}$, \bar{P}_4 : $x^{W_2(12)+W_1(24)+2} - x^{W_2(12)}$.

II_1 : $W_2(ml) = 1$ in P_2 and in \bar{P}_2 . $W_1(hm) = 0$ in P_2 and in \bar{P}_2 .

II_2 : P_3 : $x^{W_2(12)+W_1(23)+1} - x^{W_2(12)}$, \bar{P}_3 : $x^{W_2(12)+W_1(23)+1+W_1(24)} - x^{W_2(12)+W_1(24)+1}$, P_4 : $x^{W_2(12)+W_1(23)+1+W_1(24)} - x^{W_2(12)+W_1(23)+1}$, \bar{P}_4 : $x^{W_2(12)+W_1(24)+1} - x^{W_2(12)}$.

II_4 : $W_2(ml) = 0$ in P_2 and in \bar{P}_2 . $W_1(hm) = 2$ in P_2 and in \bar{P}_2 . P_4 : $x^{W_2(12)+W_1(34)+2+W_1(24)+1} - x^{W_2(12)+W_1(34)+2}$, \bar{P}_4 : $x^{W_2(12)+W_1(34)+2+W_1(24)+1} - x^{W_2(12)+W_1(34)+2}$.

III_1 : P_3 : $x^{W_2(12)+W_1(23)} - x^{W_2(12)}$, \bar{P}_3 : $x^{W_2(12)+W_1(23)+W_1(24)} - x^{W_2(12)+W_1(24)}$, P_4 : $x^{W_2(12)+W_1(23)+W_1(24)} - x^{W_2(12)+W_1(23)}$, \bar{P}_4 : $x^{W_2(12)+W_1(24)} - x^{W_2(12)}$.

III_2 : P_3 : $x^{W_2(12)+W_1(23)} - x^{W_2(12)}$, \bar{P}_3 : $x^{W_2(12)+W_1(23)} - x^{W_2(12)}$.

III_3 : $W_2(ml) = 3$ in P_2 and in \bar{P}_2 . $W_1(hm) = 1$ in P_2 and in \bar{P}_2 .

III_4 : $W_2(ml) = 0$ in P_1 and in \bar{P}_1 . $W_2(P_3) = 0 = W_2(ml)$ in P_1 . $W_2(ml) = 0$ in P_2 and in \bar{P}_2 . $W_1(hm) = 2$ in P_2 and in \bar{P}_2 .

IV_1 : $W_2(ml) = 1$ in P_1 and in \bar{P}_1 . $W_2(P_3) = 1 = W_2(ml)$ in P_1 . P_3 : $x^{W_2(12)+W_1(23)+1} - x^{W_2(12)}$, \bar{P}_3 : $x^{W_2(12)+W_1(23)+W_1(24)+1} - x^{W_2(12)+W_1(24)}$, P_4 : $x^{W_2(12)+W_1(23)+W_1(24)+1} - x^{W_2(12)+W_1(23)+1}$, \bar{P}_4 : $x^{W_2(12)+W_1(24)} - x^{W_2(12)}$.

IV_3 : $W_2(ml) = 0$ in P_1 and in \bar{P}_1 . $W_2(ml) = 0$ in P_2 and in \bar{P}_2 . $W_1(hm) = 1$ in P_2 and in \bar{P}_2 .

IV_4 : P_3 : $x^{W_2(12)+W_1(23)} - x^{W_2(12)}$, \bar{P}_3 : $x^{W_2(12)+W_1(23)} - x^{W_2(12)}$.

V_1 : $W_2(ml) = 0$ in P_1 and in \bar{P}_1 . $W_2(ml) = 0$ in P_2 and in \bar{P}_2 . $W_1(hm) = 0$ in P_2 and in \bar{P}_2 .

V_4 : P_3 : $x^{W_2(12)+W_1(23)+3} - x^{W_2(12)}$, \bar{P}_3 : $x^{W_2(12)+W_1(23)+2+W_1(24)+2} - x^{W_2(12)+W_1(24)+2}$,
 P_4 : $x^{W_2(12)+W_1(23)+3+W_1(24)+1} - x^{W_2(12)+W_1(23)+3}$, \bar{P}_4 : $x^{W_2(12)+W_1(24)+2} - x^{W_2(12)}$.

VI_1 : $W_2(ml) = 0$ in P_1 and in \bar{P}_1 . $W_2(P_3) = 0 = W_2(ml)$ in P_1 .
 $W_2(ml) = 0$ in P_2 and in \bar{P}_2 . $W_1(hm) = 0$ in P_2 and in \bar{P}_2 . P_4 : $x^{W_2(12)+W_1(34)+W_1(24)} - x^{W_2(12)+W_1(34)}$, \bar{P}_4 : $x^{W_2(12)+W_1(34)+W_1(24)} - x^{W_2(12)+W_1(34)}$.

VI_2 : P_3 : $x^{W_2(12)+W_1(23)+1} - x^{W_2(12)}$, \bar{P}_3 : $x^{W_2(12)+W_1(23)+1+W_1(24)} - x^{W_2(12)+W_1(24)+1}$,
 P_4 : $x^{W_2(12)+W_1(23)+1+W_1(24)} - x^{W_2(12)+W_1(23)+1}$, \bar{P}_4 : $x^{W_2(12)+W_1(24)+1} - x^{W_2(12)}$.

□

We have to incorporate now the linking numbers $l(d)$ and $l(ml)$ in the case of positive triple crossings. First we observe that on the positive side of a positive triple crossing the crossings hm and ml do not intersect the crossing d and that exactly one of the crossings d or hm intersects the crossing ml on either side of the triple crossing, compare Fig. 34 and Fig. 35. It follows that $l(d)$ and $(l(ml) - w(ml))$ is exactly the sum of the writhe of those crossings which intersect d respectively ml (without counting any degenerations) in the Gauss diagram with the triple crossing. (Remember that $l(d)$ and $l(ml)$ do not take into account the homological types of the intersecting crossings.) The correction term $\epsilon(p)w(hm)(w(ml) - w(d)) = 0$ for positive triple crossings and $\eta(p) = 1$ for the global type l_c and $\eta(p) = -1$ for the global type r_a . We denote the linking number of a crossing ij for a stratum P_k or \bar{P}_k by $l(ij)(P_k)$ respectively $l(ij)(\bar{P}_k)$.

Lemma 6 (*Linking numbers*)

(1) P_1 and P_4 share the same $l(14)$ if and only if they have the same global type r or l (this happens exactly for the global types I, II, IV, VI of the quadruple crossing)

(2) \bar{P}_1 and \bar{P}_4 share the same $l(14)$ if and only if they have the same global type r or l

(3) P_1 and \bar{P}_4 share the same $l(14)$ if and only if they have different global types

(4) $l(14)(P_1) = l(14)(\bar{P}_1) + 2$ for the global types I, II

- (5) $l(14)(P_1) = l(14)(\bar{P}_1) - 2$ for the global types IV, VI
- (6) $l(14)(P_1) = l(14)(P_4) - 2$ for the global type III
- (7) $l(14)(P_1) = l(14)(P_4) + 2$ for the global type V
- (8) $12 = ml$ exactly for the strata $P_3, \bar{P}_3, P_4, \bar{P}_4$ and they share always the same $l(ml)$
- (9) $23 = ml$ exactly for the strata P_2, \bar{P}_2 and they share always the same $l(ml)$
- (10) $24 = d$ exactly for the strata P_2, \bar{P}_2 and they share always the same $l(d)$
- (11) $13 = d$ exactly for the strata P_3, \bar{P}_3 and they share always the same $l(d)$. $13 = ml$ exactly for the strata P_1, \bar{P}_1 : $l(ml = 13)(P_1) = l(ml = 13)(\bar{P}_1) + 2 = l(d = 13)(P_3) + 1$ if P_3 is of type r and $l(ml = 13)(P_1) = l(ml = 13)(\bar{P}_1) - 2 = l(d = 13)(P_3) - 1$ if P_3 is of type l
- (12) 34 is never d or ml .

Proof.

The inspection of Fig. 36-47 proves all assertions immediately.

□

Let γ be an oriented generic arc in M which intersects $\Sigma^{(1)}$ only in positive triple crossings. The restriction in Definition 12 to only positive triple crossings leads to the following definition:

Definition 16 *The evaluation of the 1-cochain R_1 on γ is defined by*

$$\begin{aligned}
R_1(s) = & \sum_{p \in \Sigma_{tri}^{(1)}, [d]=0} sign(p) 4l(d) x^{W_2(d)} \\
& + \sum_{p \in \Sigma_{tri}^{(1)}(l_c)} sign(p) (l(ml) - w(ml))^2 \times \\
& (x^{W_2(ml)+W_1(hm)} - x^{W_2(ml)}) \\
& - \sum_{p \in \Sigma_{tri}^{(1)}(r_a)} sign(p) (l(ml) - w(ml))^2 \times \\
& (x^{W_2(ml)+W_1(hm)} - x^{W_2(ml)})
\end{aligned}$$

Proposition 3 *Let m be the meridian for a positive quadruple crossing. Then $R_1(m) = 0$.*

Proof. The distinguished crossing d is the same for P_1, \bar{P}_1, P_4 and \bar{P}_4 and which share the same $W_2(d)$ as follows from (1) in Lemma 4. The contribution of P_1 cancels out with that of P_4 and the contribution of \bar{P}_1 cancels out with that of \bar{P}_4 for the global types I, II, IV, VI as follows from Lemma 6 parts (1), (2), (4) and (5). The contribution of \bar{P}_1 cancels out with that of P_4 and the contribution of P_1 cancels out with that of \bar{P}_4 for the global types III, V as follows from Lemma 6 parts (3), (6), and (7). It follows now from (2) in Lemma 4, (3) in Lemma 5 and (9) and (10) in Lemma 6 that the contributions of $23 = ml$ respectively $24 = d$ in P_2 and \bar{P}_2 cancel out. The same is true for $13 = d$ in P_3 and \bar{P}_3 if they share the same f-crossings, as follows from (4) in Lemma 4 and (11) in Lemma 6.

It follows from (4) in Lemma 3 that $13 = ml$ in P_1 and \bar{P}_1 does not contribute if P_3 and \bar{P}_3 share the same f-crossings, because P_1 and \bar{P}_1 have not the right global type. They contribute only if 34 is a f-crossing for \bar{P}_3 . In this case we write shortly W_2 for $W_2(13 = d) = W_2(13 = ml)$, W_1 for $W_1(34 = hm)$ and l for $l(13 = ml)$ but without the crossings involved in the quadruple crossing. We consider the six cases using Lemma 5 and Lemma 6 (compare also Fig. 36-47):

$$I: (l+3)^2(x^{W_2+W_1} - x^{W_2}) - (l+1)^2(x^{W_2+W_1} - x^{W_2}) + 4(l+2)x^{W_2} - 4(l+2)(x^{W_2+W_1} - x^{W_2}) = 0$$

$$II: l^2(x^{W_2+W_1} - x^{W_2}) - (l+2)^2(x^{W_2+W_1} - x^{W_2}) - 4(l+1)x^{W_2} + 4(l+1)(x^{W_2+W_1} - x^{W_2}) = 0$$

$$III: l^2(x^{W_2+W_1} - x^{W_2}) - (l+2)^2(x^{W_2+W_1} - x^{W_2}) - 4(l+1)x^{W_2} + 4(l+1)(x^{W_2+W_1} - x^{W_2}) = 0$$

$$IV: (l+2)^2(x^{W_2+W_1} - x^{W_2}) - l^2(x^{W_2+W_1} - x^{W_2}) + 4(l+1)x^{W_2} - 4(l+1)(x^{W_2+W_1} - x^{W_2}) = 0$$

$$V: (l+2)^2(x^{W_2+W_1} - x^{W_2}) - l^2(x^{W_2+W_1} - x^{W_2}) + 4(l+1)x^{W_2} - 4(l+1)(x^{W_2+W_1} - x^{W_2}) = 0$$

$$VI: (l+1)^2(x^{W_2+W_1} - x^{W_2}) - (l+3)^2(x^{W_2+W_1} - x^{W_2}) - 4(l+2)x^{W_2} + 4(l+2)(x^{W_2+W_1} - x^{W_2}) = 0$$

It follows from (6) in Lemma 4 that we can have only simultaneously $W_1(P_3) = W_1(\bar{P}_3) + 1$ and $W_1(\bar{P}_4) = W_1(P_4) + 1$. It follows now from (6) in Lemma 5 and (8) in Lemma 6 that the contributions of $12 = ml$ cancel always out together in P_3, \bar{P}_3, P_4 and \bar{P}_4 .

□

Remark 4 *Let us summarize the combinatorial structure of the tetrahedron equation which leads to $R_1(m) = 0$ for the meridian m of a positive quadruple crossing.*

(1) *The strata $P_1, \bar{P}_1, P_4, \bar{P}_4$ share the same distinguished crossing d and their contributions with d cancel out.*

(2) *All contributions of P_2 and \bar{P}_2 cancel out.*

(3) *The strata P_3 and \bar{P}_3 contribute non trivially with d if and only if P_1 and \bar{P}_1 are of global type r_a or l_c and in this case the contributions of P_3 and \bar{P}_3 with d cancel out with those of P_1 and \bar{P}_1 with ml . The linking numbers enter here in a non trivial way.*

(4) *The contributions of P_3 and \bar{P}_3 with ml cancel always out with those from P_4 and \bar{P}_4 with ml too.*

It follows immediately from this combinatorial structure that we can restrict R_1 to only those crossings d and ml with given colors of foots and heads (but of course the same for d and ml).

The lack of symmetry of R_1 is apparent: $-P_2 + \bar{P}_2$, where the triple crossing is on the top, does never contribute at all, but $+P_3 - \bar{P}_3$, where the triple crossing is on the bottom, can contribute highly non trivially both for d and for ml . Its contribution for d cancels out with the contribution for ml in P_1, \bar{P}_1 and its contribution with ml cancels out with the contribution for ml in P_4, \bar{P}_4 .

Remark 5 *It seems that the coefficients of R_1 can be generalized to 2-variable polynomials by considering in addition a second type of f -crossings, called h -crossings, together with a new variable y : the head of the h -crossing of type 1 is in the arc from the foot of the crossing c to the point at infinity. In order to define the r -crossings of the h -crossings we use the second formula of Polyak-Viro for $v_2(K)$ (compare Fig. 10). Now, also the crossing hm contributes exactly for the global types r_b and l_a . The solution of the tetrahedron equation is still non symmetric because only the global type r_c does never contribute. The new 1-cocycle doesn't have any longer a scan property. Its specialization for $y = 1$ coincides with R_1 . But the verifications for the tetrahedron equation and the cube equations become so complicated that we will perhaps come back to them only in a separate paper.*

There are of course also "dual" solutions R_1 by using symmetries as taking mirror images, the orientation change and the rotation by π around the imaginary axes $i\mathbb{R} \times 0 \subset \mathbb{C} \times \mathbb{R}$ for the definition of the weights W_1 and W_2 . But the linking numbers l are always defined in the same way.

There is at least one other situation where our approach should work well too.

Remark 6 *The case of knots which are closed braids in the solid torus is also interesting (i.e. conjugacy classes of braids). We consider the natural projection into the annulus. There are two canonical loops in the moduli space which are induced by the natural rotations of the solid torus. Hatcher has proven that the rational homology classes of these loops are linearly dependent if and only if the braid is periodic. It is well known that the braid is periodic if and only if its closure is a torus knot, see [6]. There is no longer a point at infinity but we have now the homological type of a crossing c defined by the homology class of D_c^+ in the solid torus, compare Definition 3 and also [15]. The linking numbers l are defined in exactly the same way as previously, namely as sums of the writhe of crossings. We can still use the same combinatorial structure of the tetrahedron equation as described in Remark 4 because positive quadruple crossings can be represented by braids. The result are polynomial valued 1-cocycles R_1 for closed n -braids. (There are no moving cusps and no local knots here and we do not need colorings.) We will perhaps come back to this in another paper.*

4.5 Cube equations

We have to consider now all other local types of triple crossings together with the self-tangencies. We know already the contributions for the local type 1, the positive triple crossings, from our solution of the tetrahedron equation and we will determine the contributions of all other local types from the cube equations. The local types of triple crossings were shown in Fig. 25. The diagrams which correspond to the edges of the graph Γ (compare Section 4.1) are shown in Fig. 48. The projection of a triple crossing p into the plan separates the plan near p into three couples of a region and its dual. The regions correspond exactly to the three edges adjacent to the vertex corresponding to the local type of the triple crossing (we can forget about the three dual regions because of $\Sigma_{trans-self-flex}^{(3)}$ as was explained in Section 4.1). We show the corresponding graph Γ now in Fig. 49. The unfolding of e.g. the edge 1 – 5 was shown in Fig. 30 (compare [18]).

Observation 1 *The diagrams corresponding to the two vertices's of an edge differ just by the two crossings of the self-tangency which replace each other*

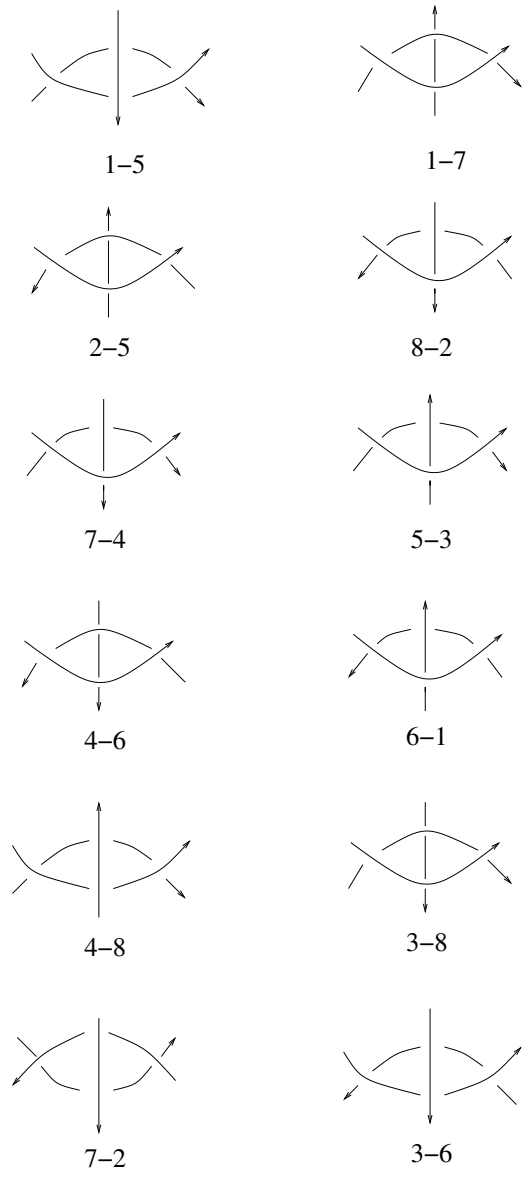


Figure 48: The twelve edges of the graph Γ

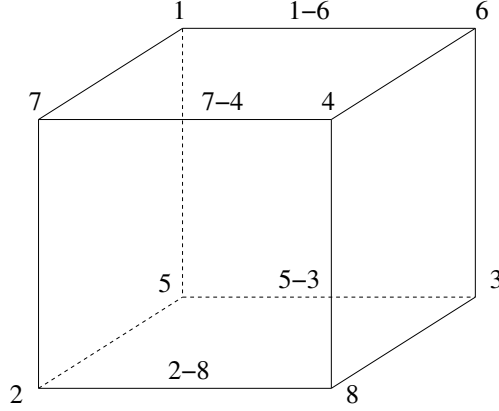


Figure 49: The graph Γ

in the triangle as shown in Fig. 50. Consequently, the two vertices of an edge have always the same global type and always different local types and the two crossings which are interchanged can only be simultaneously f -crossings for d . Moreover, the two self-tangencies in the unfolding (of an edge) can contribute non trivially to R_1 only if they have different weights $W_2(d)$ or different linking numbers $l(d)$. The first happens exactly for the edges "1-5", "4-8", "3-6" and "7-2" (where the crossings of the self-tangencies are the crossings ml of the triple crossings). The latter happens exactly for the edges "1-6", "3-5", "4-7" and "2-8" (where the third branch passes between the two branches of the self-tangency).

It follows that we have to solve the cube equations for the graph Γ exactly six times: one solution for each global type of triple crossings. We show the Gauss diagrams for some edges of Γ in Fig. 51 up to Fig. 58 and we will check the solution of the cube equations for these edges. The remaining cases are completely analogous and are left to the reader.

We will denote by l the linking number of a crossing $l(c)$ without counting the other involved crossings in the stratum $\Sigma_{trans-self}^{(2)}$. Notice that the calculations of $l(d)$ and $l(ml) - w(ml)$ depend now in a more subtly way on the local type of the triple crossings and it is not just the algebraic number of generic crossings which intersect the given crossing in the triangle as in the case of positive triple crossings. We represent the meridian m of $\Sigma_{trans-self}^{(2)}$ in the following way: we create first the self-tangency and then we move the transverse branch from the left to the right and we eliminate again the

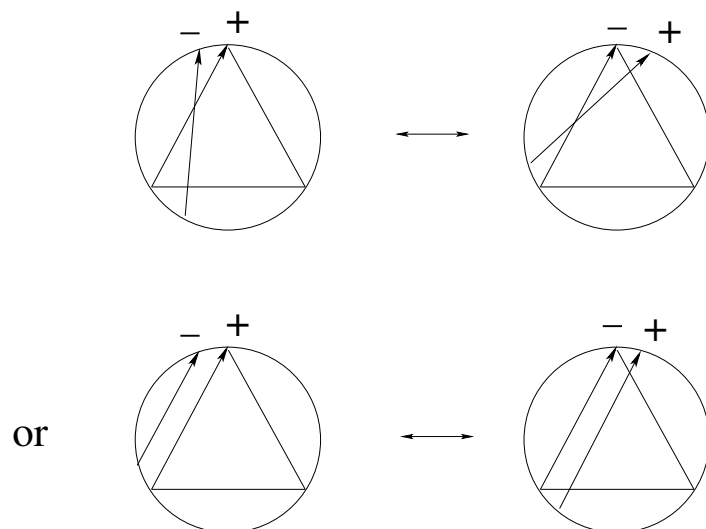


Figure 50: Two crossings replace each other for an edge of Γ

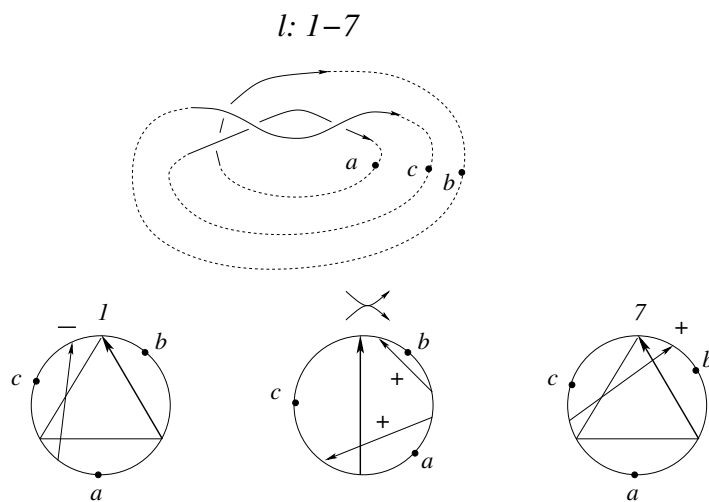


Figure 51: $l1 - 7$

$l:1-5$

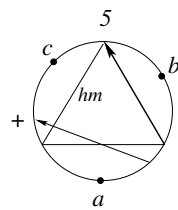
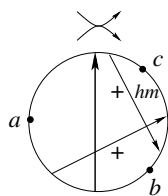
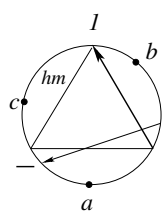
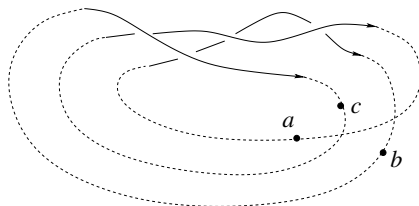


Figure 52: $l1 - 5$

$l:1-6$

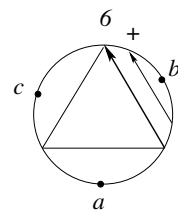
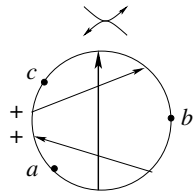
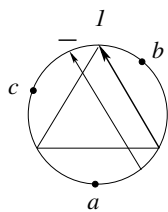
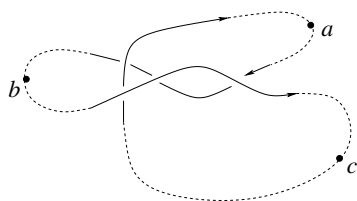


Figure 53: $l1 - 6$

$l: 7-2$

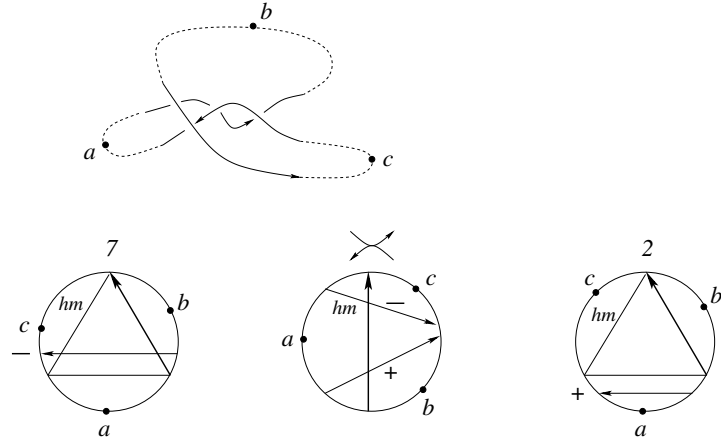


Figure 54: $l7 - 2$

$l: 7-4$

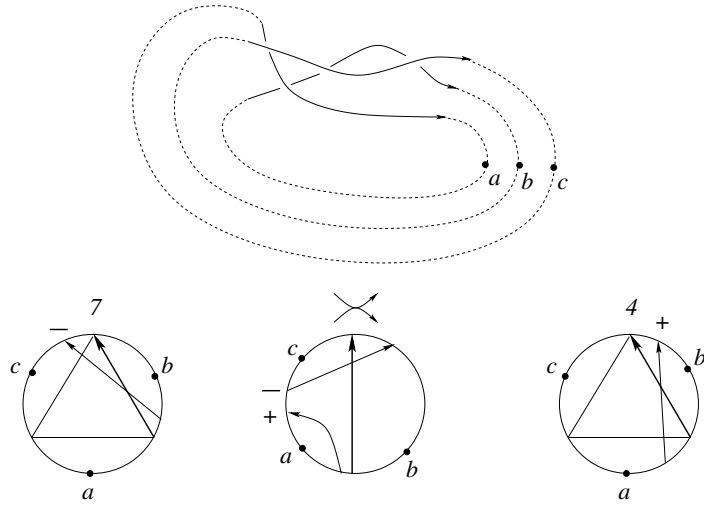


Figure 55: $l7 - 4$

$r: 1-7$

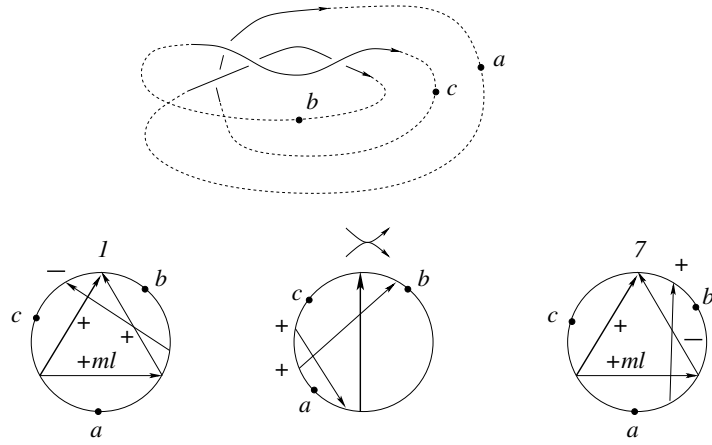


Figure 56: $r1 - 7$

$r: 1-5$

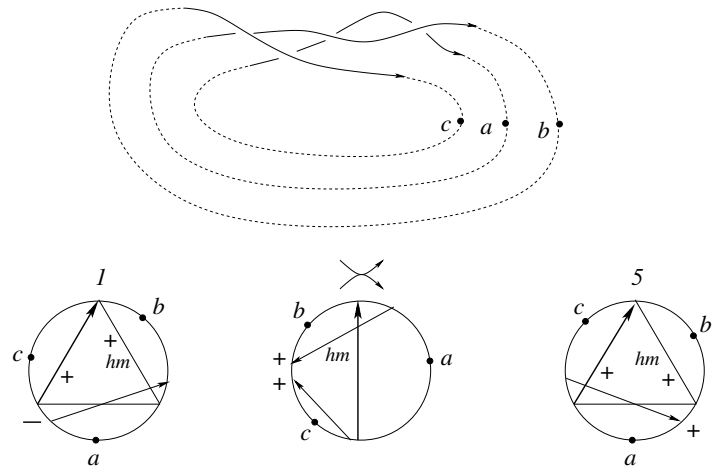


Figure 57: $r1 - 5$

$r: 1-6$

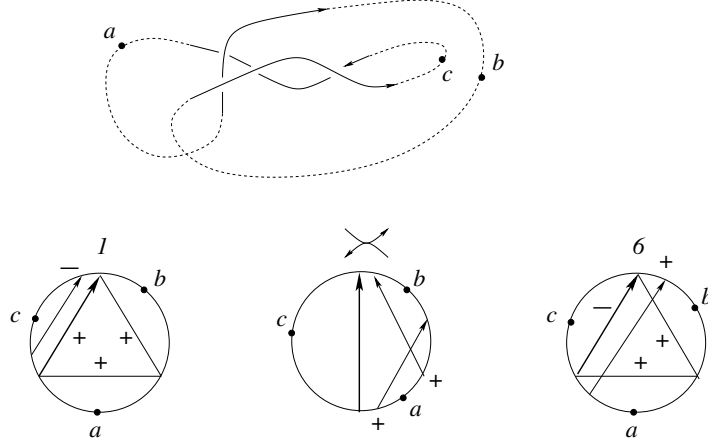


Figure 58: $r1 - 6$

self-tangency.

Proposition 4 *Let m be a meridian of $\Sigma_{trans-self}^{(2)}$ or a loop in Γ . Then $R_1(m) = 0$ for the contributions given in Definition 12.*

Proof. First of all we observe that the two vertices of an edge (i.e. triple crossings) share the same f-crossings with respect to the crossing d . The f-crossings could only change if the foot of a f-crossing slides over the head of the crossing d . But this is not the case as it was shown in Fig. 50. Indeed, the foot of the crossing which changes in the triangle can not coincide with the head of d because the latter coincides always with the head of another crossing. The f-crossings of the crossings ml differ just by a crossing hm and this happens exactly when hm is a crossing of the self-tangency. The two triple crossings in an edge have always different signs as well as the two self-tangencies.

In the following it suffices of course to consider only the four crossings involved in an edge because the position of the triple crossings and the self-tangencies with respect to all other crossings do not change.

One easily sees that $\epsilon(p)w(hm)(w(ml) - w(d)) = 0$ in all cases besides for some local types of global type r_a which will be studied below.

We start with the solutions for triple crossings of global type l . In the figures we show the Gauss diagrams of the two triple crossings together with

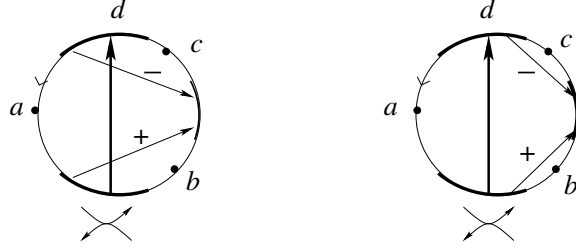


Figure 59: The two self-tangencies for the edge $l7 - 2$

the points at infinity and the Gauss diagram of just one of the two self-tangencies. The Gauss diagram of the second self-tangency is derived from the first one in the following way: the two arrows slide over the arrow d but their mutual position does not change. We show an example in Fig. 59. Notice that in the thick part of the circle there aren't any other heads or foots of arrows.

The fourth arrow which is not in the triangle is always almost identical with an arrow of the triangle. Consequently, in the case l_c it can not be a r-crossing with respect to hm . In the case l_b it could be a r-crossing with respect to some f-crossing. But the almost identical arrow in the triangle would be a r-crossing for the same f-crossing too. Their contributions cancel out, because they have different writhe.

It can happen for the type l_c that the crossing hm becomes a new f-crossing with respect to ml for the new triple crossing. This forces us to use the coefficient $w(hm)$ in Definition 12 for the weights for the new triple crossing.

The type l_a does never contribute.

The mutual position of the two arrows for a self-tangency does not change. Only the position with respect to the distinguished crossing d changes. It remains to consider the edges "1-5", "4-8", "2-7" and "3-6" for l_c , where one of the two self-tangencies has a new f-crossing with respect to the other self-tangency. But one sees immediately from the figures that this new f-crossing is exactly the crossing hm in the triple crossings. In this case, exactly one of the self-tangencies contributes with the factor $w(hm)x^{W_2(ml)+w(hm)W_1(hm)}$ and the other contributes with the factor $w(hm)x^{W_2(ml)}$.

We consider now some edges in detail.

edge "1-7": l_b : the contributions of the self-tangencies cancel out together. local types 1 and 7 contribute $4lx^{W_2(d)}$ and have the same linking number

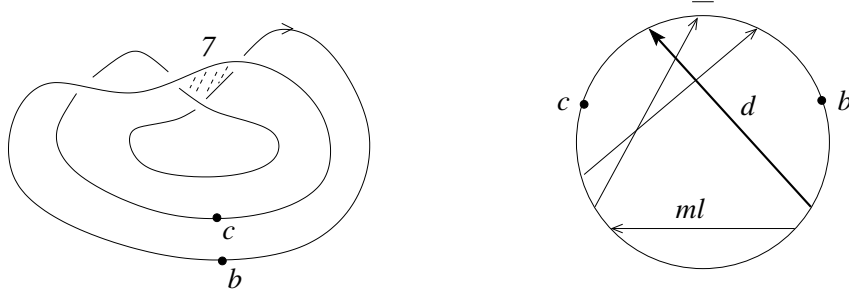


Figure 60: linking numbers for the local type 7 in $l1 - 7$

$$l(d) = l.$$

$$l_c: \text{local type 1 contributes } -(l-1)^2(x^{W_2(ml)+W_1(hm)} - x^{W_2(ml)})$$

$$\text{local type 7 contributes } (l-1)^2(-1)(x^{W_2(ml)+W_1(hm)-W_1(hm)} - x^{W_2(ml)+W_1(hm)})$$

, compare Fig. 60 for the linking number.

edge "1-5": l_b : local types 1 and 5 contribute $4(l-1)x^{W_2(d)}$ and have the same linking number $l(d)$, compare Fig. 61 for the linking number.

$$l_c: 8(l+1)x^{W_2(ml)+W_1(hm)} + (l-1)^2(x^{W_2(ml)+W_1(hm)} - x^{W_2(ml)}) - (l+2 - (-1))^2(x^{W_2(ml)+W_1(hm)} - x^{W_2(ml)}) - 8(l+1)x^{W_2(ml)} = 0, \text{ compare Fig. 61 for the linking number.}$$

$$\text{edge "1-6": } l_b: 4lx^{W_2(d)} + 4(l+2)x^{W_2(d)} - 4(l+2)x^{W_2(d)} - 4lx^{W_2(d)} = 0, \text{ compare Fig. 8 for the sign of the local type 6.}$$

$$l_c: l^2x^{W_2(ml)} - l^2x^{W_2(ml)} = 0.$$

$$\text{edge "7-2": } l_b: 4lx^{W_2(d)} + 4(l-2)x^{W_2(d)} - 4(l-2)x^{W_2(d)} - 4lx^{W_2(d)} = 0.$$

$$l_c: 4lx^{W_2(ml)} + (-1)(l-1)^2(x^{W_2(ml)-W_1(hm)} - x^{W_2(ml)}) - (-1)(l-1)^2(x^{W_2(ml)-W_1(hm)} - x^{W_2(ml)}) - 4lx^{W_2(ml)} = 0, \text{ compare Fig. 62 for the linking numbers.}$$

$$\text{edge "7-4": } l_b: 8(l-1)x^{W_2(d)} - 4(l-2)x^{W_2(d)} + 4(l+2)x^{W_2(d)} - 8(l+1)x^{W_2(d)} = 0.$$

$$l_c: -(-1)(l-1)^2(x^{W_2(ml)-W_1(hm)} - x^{W_2(ml)}) + (-1)(l-1)^2(x^{W_2(ml)-W_1(hm)} - x^{W_2(ml)}) = 0, \text{ compare Fig. 63 for the linking numbers.}$$

We proceed then in exactly the same way for the global type r . Exactly the same arguments as previously apply in the case r_b . In the case r_c there are no contributions at all. But notice the difference which comes from the fact that we have broken the symmetry: the global type r_a contributes both with ml and with d . Here sometimes the fourth crossing, which is not in the triangle, is a r -crossing with respect to hm for exactly one of the two triple crossings. If there could be confusion then we write the local type of the triple crossing in brackets behind the weight (remember that we haven't yet

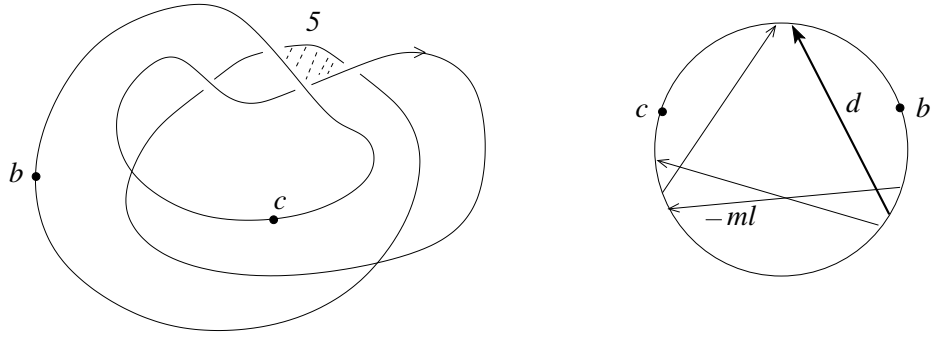


Figure 61: linking numbers for the local type 5 in $l1 - 5$

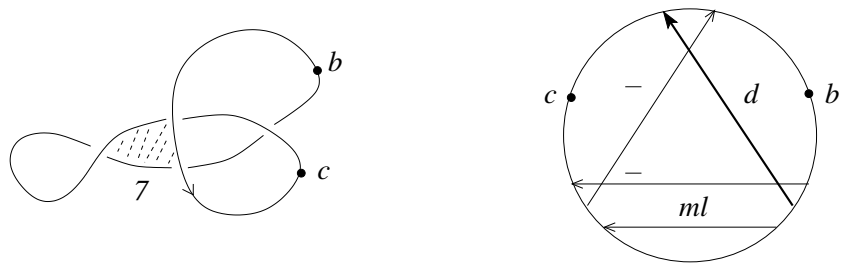


Figure 62: linking numbers for the local type 7 in $l7 - 2$

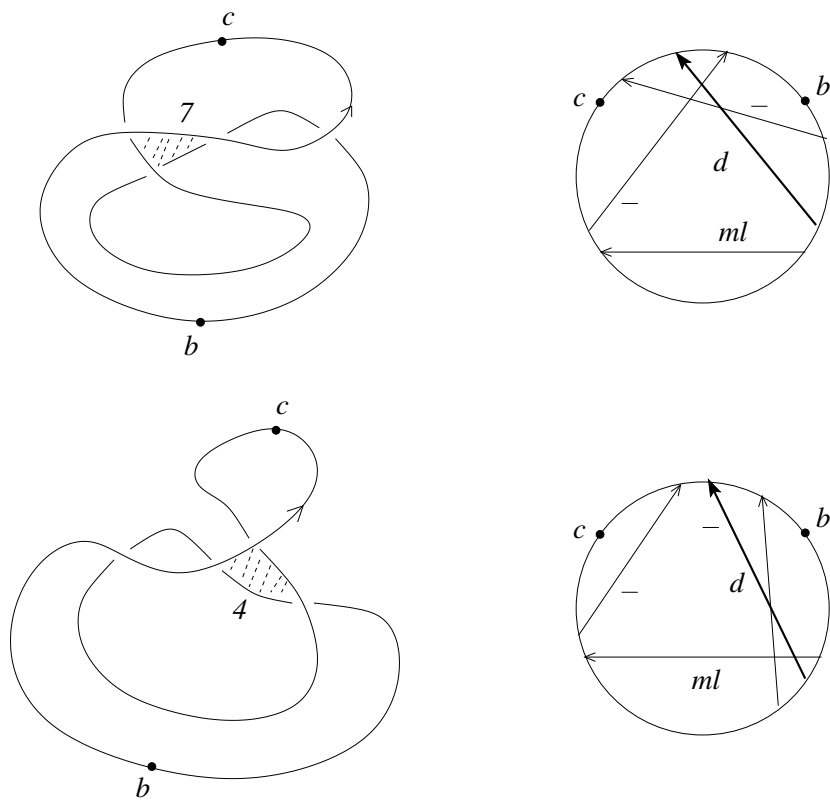


Figure 63: linking numbers for the local types 7 and 4 in $l7 - 4$

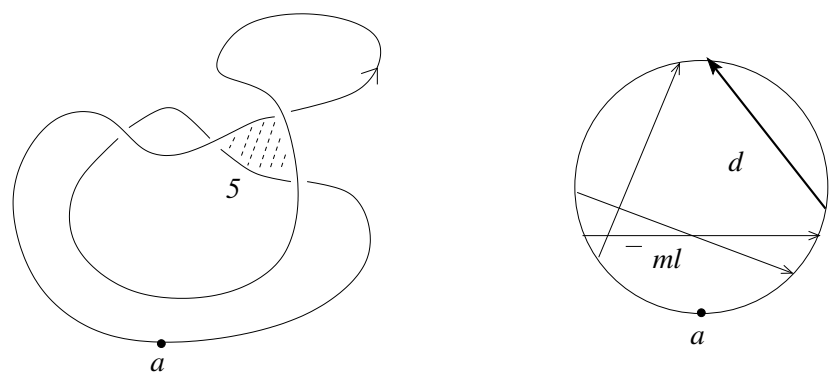


Figure 64: linking numbers for the local type 5 in $r1 - 5$

taken into account the correction term for the local type from Definition 12).

We examine now the figures for r_a (don't forget the degenerate configurations in the definition of the weights):

edge "1-7": type 1 and type 7 share the same $W_1(hm)$ and $W_2(d)$, but $W_2(ml)(7) = W_2(ml)(1) + W_1(hm)$

edge "1-5": $W_1(hm)(5) = W_1(hm)(1) + 1$, $W_2(d)(5) = W_2(d)(1) + 1$, they share the same $W_2(ml)$

edge "1-6": $W_1(hm)(6) = W_1(hm)(1) - 1$, $W_2(d)(6) = W_2(d)(1) - 1$, they share the same $W_2(ml)$

edge "7-4": $W_1(hm)(4) = W_1(hm)(7) - 1$, $W_2(d)(4) = W_2(d)(7) + 1$, they share the same $W_2(ml)$

edge "7-2": $W_1(hm)(2) = W_1(hm)(7) + 1$, $W_2(d)(2) = W_2(d)(7) - 1$, they share the same $W_2(ml)$

edge "5-2": same $W_1(hm)$, but $W_2(d)(2) = W_2(d)(5) - 2$ and $W_2(ml)(2) = W_2(ml)(5) + (W_1(hm) - 1)$

edge "5-3": $W_1(hm)(3) = W_1(hm)(5) - 1$, $W_2(d)(3) = W_2(d)(5) - 1$, they share the same $W_2(ml)$

edge "3-8": they share the same $W_1(hm)$ and $W_2(d)$, but $W_2(ml)(8) = W_2(ml)(3) + W_1(hm)$

edge "3-6": $W_1(hm)(6) = W_1(hm)(3) - 1$, $W_2(d)(6) = W_2(d)(3) - 1$, they share the same $W_2(ml)$

edge "4-8": $W_1(hm)(8) = W_1(hm)(4) + 1$, $W_2(d)(8) = W_2(d)(4) - 1$, they share the same $W_2(ml)$

edge "4-6": same $W_1(hm)$, but $W_2(d)(6) = W_2(d)(4) - 2$ and $W_2(ml)(6) = W_2(ml)(4) - (W_1(hm) + 1)$

edge "8-2": $W_1(hm)(8) = W_1(hm)(2) - 1$, $W_2(d)(8) = W_2(d)(2) + 1$, they share the same $W_2(ml)$.

The weights have to be the same for both vertices of an edge. This forces the constant correction term $\epsilon(p)w(hm)(w(ml) - w(d))$ for the weights given in Definition 12.

For the self-tangencies "8-2" as well as "1-6" both self-tangencies in the unfolding have the same $W_2(d)$ as the triple crossing in type 8 respectively type 1. In the self-tangencies "7-4" and "5-3" both have the same $W_2(d)$ as the triple crossing in type 7 respectively type 3. In the remaining cases $W_2(d)$ is either the same too for the two self-tangencies or they differ exactly by $W_1(hm)$ of the triple crossing.

We check now some edges of type r_a (where for shorter writing we do not mention the constant correction term which was already checked).

edge "1-7": $4(l-1)x^{W_2(d)} - 4(l-1)x^{W_2(d)} = 0$.
 $(-1)l^2(x^{W_2(ml)+W_1(hm)} - x^{W_2(ml)}) - (-1)(-1)l^2(x^{W_2(ml)+W_1(hm)-W_1(hm)} - x^{W_2(ml)+W_1(hm)}) = 0$.
 edge "1-5": $4lx^{W_2(d)} - 4lx^{W_2(d)} = 0$.
 $8(l+1)x^{W_2(ml)+W_1(hm)} - (-1)(l-1)^2(x^{W_2(ml)+W_1(hm)} - x^{W_2(ml)}) + (-1)(l+2 - (-1))^2(x^{W_2(ml)+W_1(hm)} - x^{W_2(ml)}) - 8(l+1)x^{W_2(ml)} = 0$, compare Fig. 64 for the linking numbers.
 edge "1-6": $4lx^{W_2(d)} - 4lx^{W_2(d)} + 4(l+2)x^{W_2(d)} - 4(l+2)x^{W_2(d)} = 0$.
 $-(-1)l^2(x^{W_2(ml)+W_1(hm)} - x^{W_2(ml)}) + (-1)l^2(x^{W_2(ml)+W_1(hm)} - x^{W_2(ml)}) = 0$.
 All the remaining cases are quit similar and we leave them to the reader.
 \square

4.6 Moving cusps and scan-property

We have to deal now with the irreducible strata of codimension two which contain a diagram with a cusp which moves over or under another branch. We can assume that in the local picture there is exactly one crossing, before the small curl from the cusp appears. Notice that in this case the local types 2 and 6 can evidently not occur as triple crossings. There are exactly sixteen possible local types. We list them in Fig. 65...Fig. 68, where we move the branch from the right to the left. For each local type we have exactly two global types, corresponding to the position of the point at infinity. It is very important that in $\Sigma_{r_a}^{(2)}$ only the local types 1, 3, 7 and 8 of triple crossings can occur, because these are exactly the local types for which the correction $\epsilon(p)w(hm)(w(ml) - w(d)) = 0$ (compare the previous subsection).

We give in the figure also the Gauss diagrams of the triple crossing and of one of the self-tangencies. Notice that in each Gauss diagram of a triple crossing one of the three arcs is empty besides just one head or foot of an arrow. Let us denote each stratum of $\Sigma_{trans-cusp}^{(2)}$ simply by the global type of the corresponding triple crossing.

The following lemma reduces the number of cases which have to be considered.

Lemma 7 *If $R_1(m) = 0$ for $\Sigma_{trans-cusp}^{(2)}$ with one orientation of the moving branch then it is also 0 for the other orientation of the moving branch.*

Proof. It suffices to notice that the contributions of the two Reidemeister II moves shown in Fig. 69 obviously cancel out.

\square

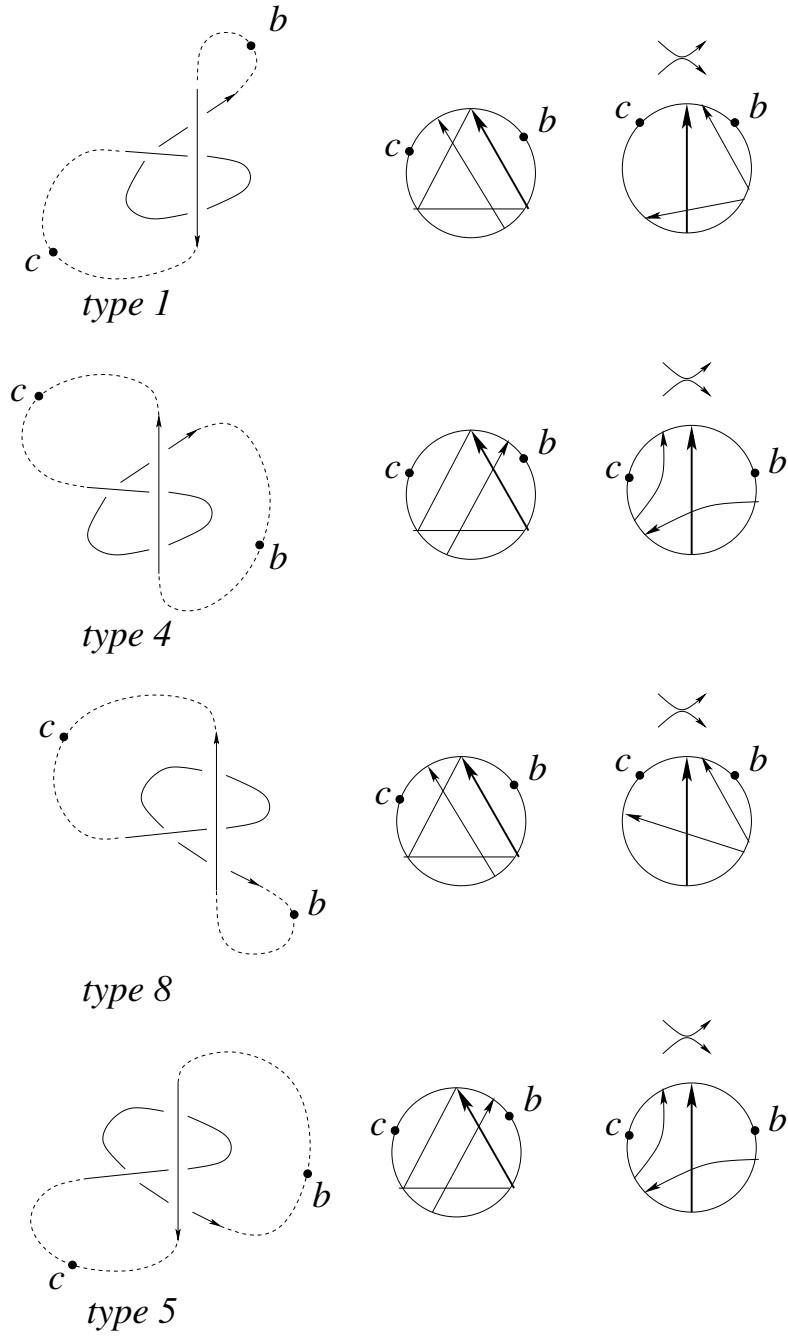


Figure 65: the strata $\Sigma_{l_c}^{(2)}$ and $\Sigma_{l_b}^{(2)}$

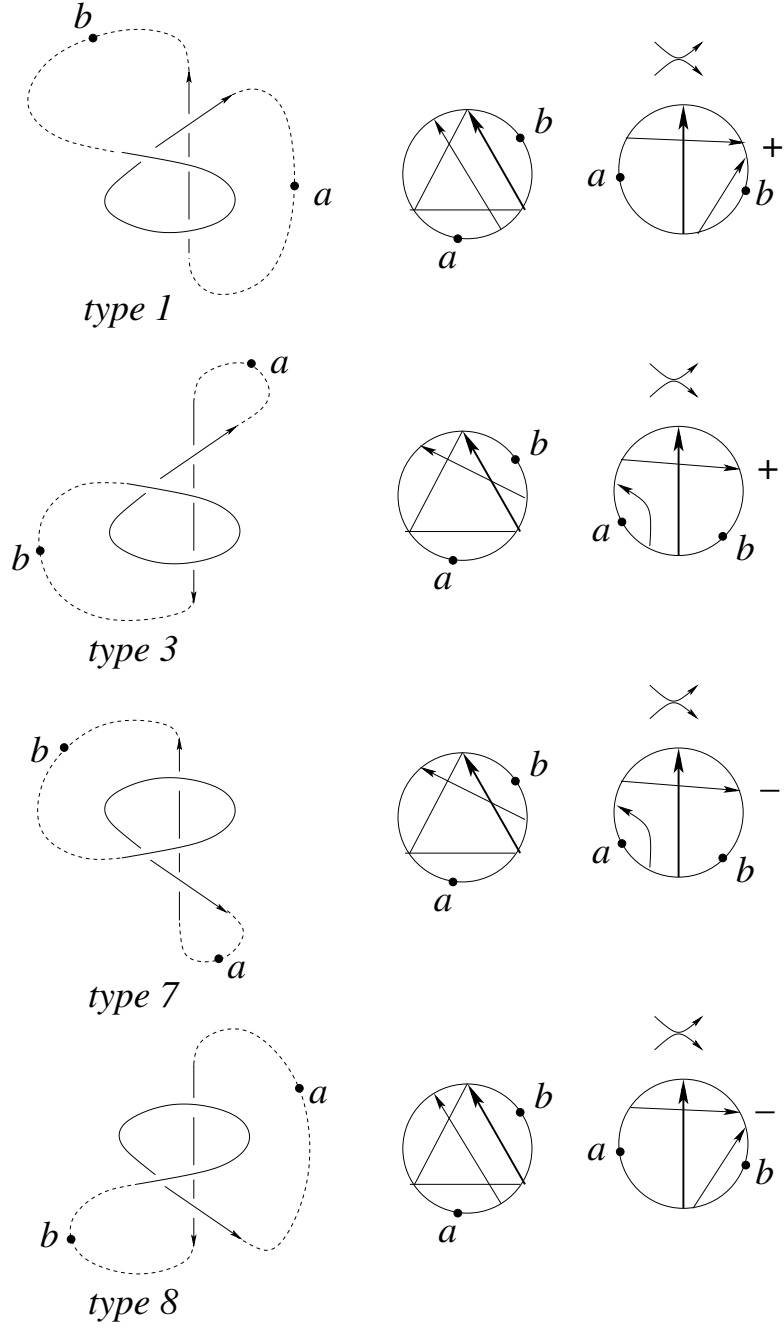


Figure 66: the strata $\Sigma_{l_a}^{(2)}$ and $\Sigma_{l_b}^{(2)}$

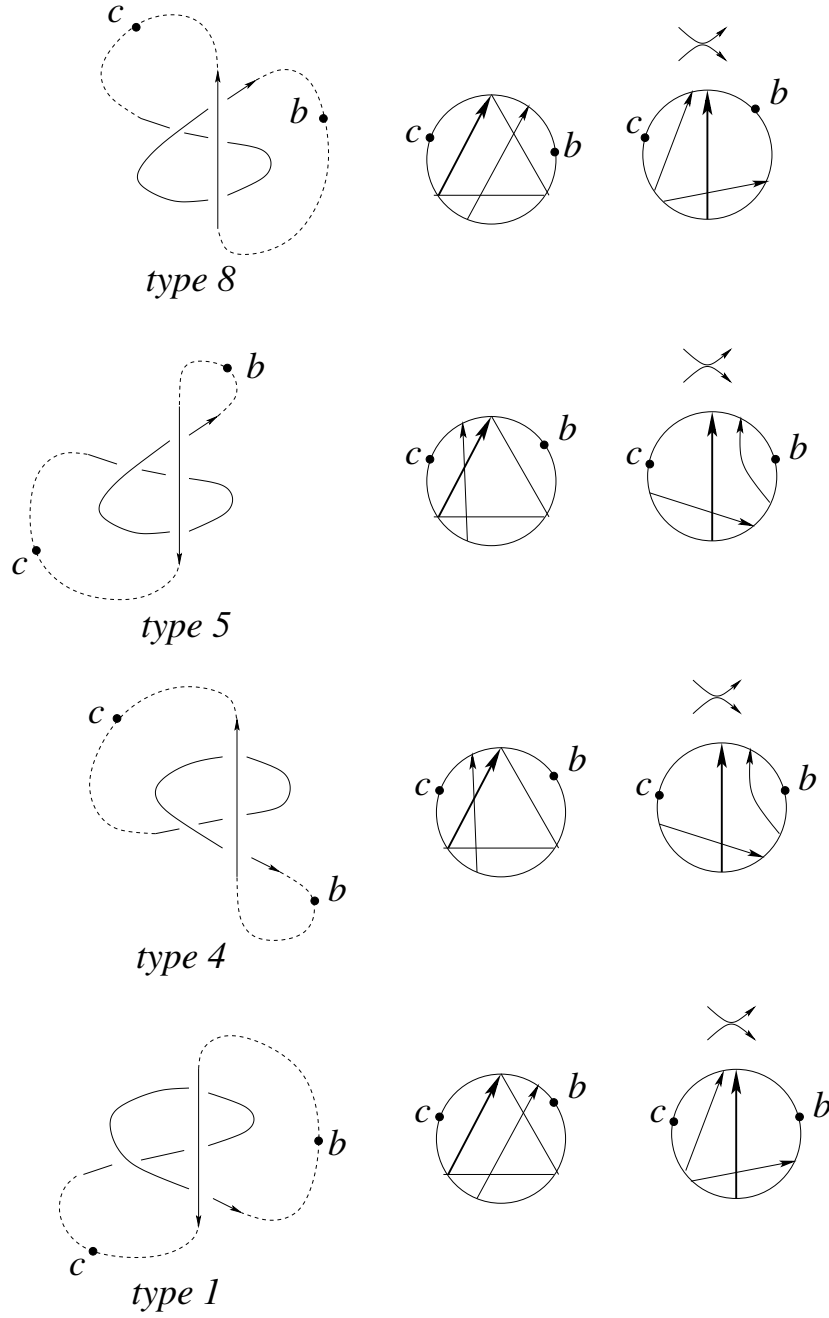


Figure 67: the strata $\Sigma_{r_b}^{(2)}$ and $\Sigma_{r_c}^{(2)}$

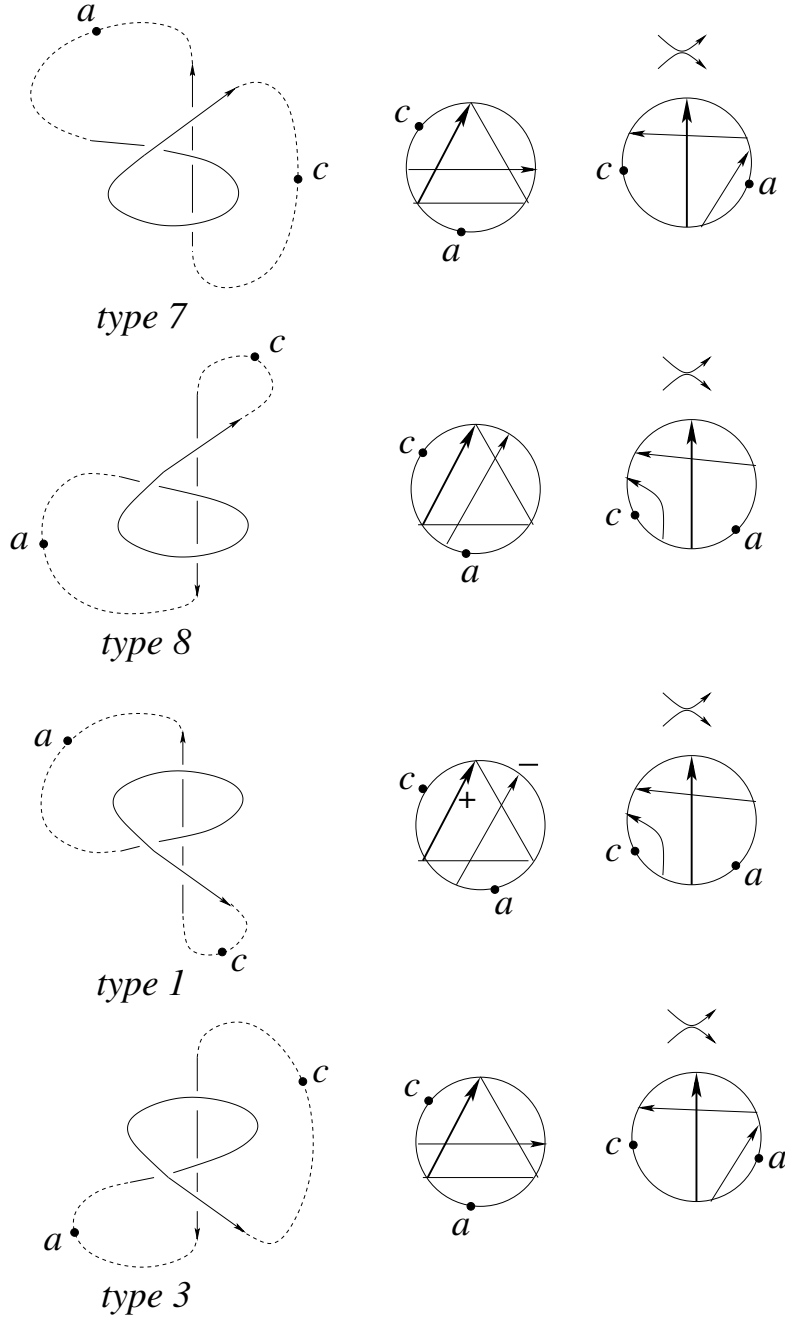


Figure 68: the strata $\Sigma_{r_a}^{(2)}$ and $\Sigma_{r_c}^{(2)}$

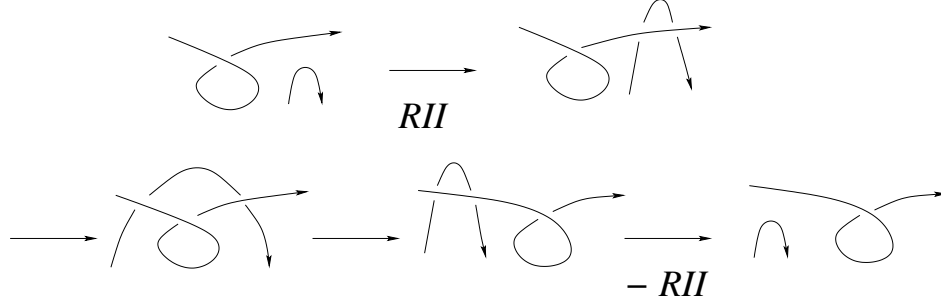


Figure 69: Two Reidemeister II moves with canceling contributions

Proposition 5 *Let m be a meridian of $\Sigma_{trans-cusp}^{(2)}$. Then $R_1(m) = 0$ for all strata of $\Sigma_{trans-cusp}^{(2)}$ besides for those of the types $\Sigma_{lc}^{(2)}$.*

Proof. Exactly for the type $\Sigma_{lc}^{(2)}$ only the triple crossing contributes to $R_1(m)$, namely by $(l(ml) - w(ml))^2(x^{W_2(ml)+W_1(hm)} - x^{W_2(ml)})$. Notice that $W_1(hm)$ can be non-trivial as well as $(l(ml) - w(ml))$. Consequently, R_1 does not necessarily vanish on this meridian.

Let us show that $R_1(m) = 0$ for $\Sigma_{ra}^{(2)}$ of local type 1.

We show the meridian of a stratum $\Sigma_{ra}^{(2)}$ of local type 1 in Fig. 70 and the Gauss diagram of the triple crossing in Fig. 71.

First of all we observe that $W_1(hm) = 0$. Indeed, d of the triple crossing contributes $+1$ and the negative crossing from the self-tangency contributes -1 and there are no other crossings at all which contribute to $W_1(hm)$. Moreover, as already mentioned $\epsilon(p)w(hm)(w(ml) - w(d)) = 0$. Hence $x^{W_2(ml)+W_1(hm)} - x^{W_2(ml)} = 0$ and the triple crossing does not contribute with ml . On the other hand, $W_2(d) = W_2(ml) + W_1(hm) = W_2(ml)$ for the triple crossing because there are no foots of arrows in the segment from the undercross to the overcross of hm (this is exactly the small curl). Let d' be the distinguished crossing of the self-tangencies. One easily sees (compare Fig. 68) that $W_2(d') = W_2(ml) + W_1(hm) = W_2(ml)$ too. It follows that the weights of degree 2 are all the same and they are simply denoted by W_2 . Moreover, the linking numbers $l(d)$ and $l(ml)$ are the same too.

The calculation of $R_1(m)$ gives now: $R_1(m) = 8(l+1)x^{W_2} - (-1)(l-1)^2(x^{W_2} - x^{W_2}) - 4(l+2)x^{W_2} - 4(l+2)x^{W_2} = 0$

All the remaining cases are completely analogous and are left to the reader.

□

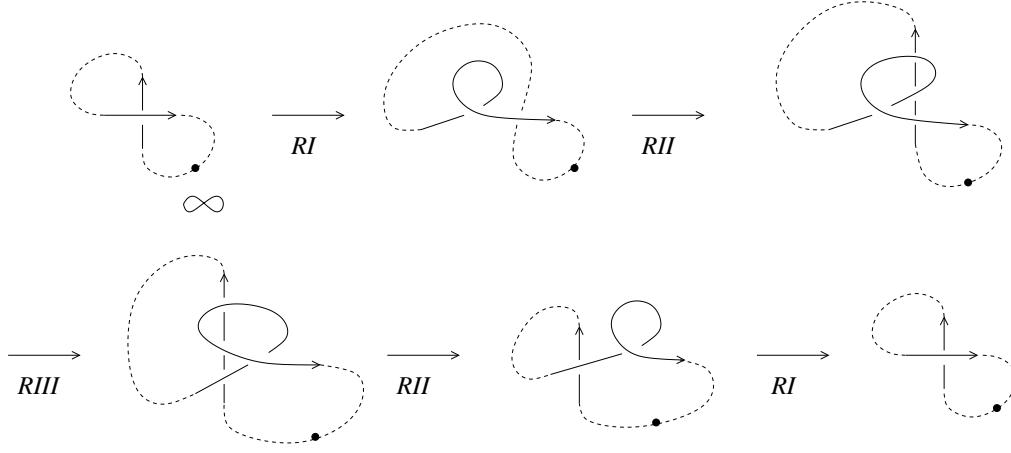


Figure 70: The meridian of a stratum $\Sigma_{r_a}^{(2)}$ of local type 1

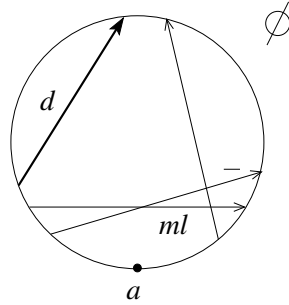


Figure 71: The triple crossing $\Sigma_{r_a}^{(2)}$ of local type 1 on the positive side

Remark 7 *It is necessary to use the quadratic weight W_2 for the construction of R_1 . Indeed, assume that we replace W_2 by a linear weight W (which is just the sum of the writhes of the f-crossings). This implies that we have to replace W_2 by W for the self-tangencies too and that we have to replace the linear weight W_1 for the types r_a and l_c by the constant weight 1 (forced by the tetrahedron equation). The calculation of $R_1(m)$ for $\Sigma_{r_a}^{(2)}$ of local type 1 would give now $R_1(m) = -(-1)(l-1)^2(x^{W_2+1} - x^{W_2}) \neq 0$.*

We have proven that $R_1(\gamma)$ is invariant under all generic homotopies of γ in M through the six types of strata of Proposition 1 besides $\Sigma_{l_c}^{(2)}$ and hence R_1 is a 1-cocycle in $M \setminus \Sigma_{l_c}^{(2)}$.

Lemma 8 *Let T be a diagram of a string link and let t be a Reidemeister*

move of type II for T . Then the contribution of t to R_1 does not change if a branch of T is moved under t from one side of t to the other.

Proof. Besides d of t there are two crossings involved with the branch which goes under t . Moving the branch under t from one side to the other slides the heads of the corresponding arrows over d , see e.g. Fig. 51 and Fig. 56. Consequently, the f-crossings do not change. Notice that the mutual position of the two arrows does not change. Consequently, there are no new r-crossings and $W_2(d)$ does not change neither. Evidently, $l(d)$ does not change and the assertion of the lemma follows.

□

We are now ready to prove the *scan-property* which was claimed in Theorem 1.

Proof. Let T be a diagram of a string link and let s be an isotopy which connects T with a diagram T' . We consider the loop

$-s \circ -scan(T') \circ s \circ scan(T)$ in M_T . This loop is contractible in M_T because s and $scan$ commute. Consequently, R_1 vanishes on this loop, because R_1 is a 1-cocycle. It suffices to prove now that each contribution of a Reidemeister move t in s cancels out with the contribution of the same move t in $-s$ (the signs of the contributions are of course opposite). The difference for the two Reidemeister moves is in a branch which has moved under t . It suffices to study the weights and the linking numbers. Evidently, the linking numbers have not changed because the branch has moved under the rest of the diagram. If t is a positive triple crossing now then the weights are the same just before the branch moves under t and just after it has moved under t . Indeed, this follows from the fact that for the positive global tetrahedron equation the contribution from the stratum $-P_2$ cancels always out with that from the stratum \bar{P}_2 (compare the Section 4.4). If we move the branch further away then the invariance follows from the already proven fact that the values of the 1-cocycles do not change if the loop passes through a stratum of $\Sigma^{(1)} \cap \Sigma^{(1)}$ (compare Section 4.3). We use now again the graph Γ . The meridian m which corresponds to an arbitrary edge of Γ is a contractible loop in M_T , no matter what is the position of the branch which moves under everything. Let's take an edge where one vertex is a triple crossing of local type 1. We know from Lemma 8 that the contributions of the self-tangencies in s do not depend on the position of the moving branch. Consequently the contribution of the other vertex of the edge doesn't change neither because the contributions from all four Reidemeister moves together sum up to 0.

Using the fact that the graph Γ is connected we obtain the invariance with respect to the position of the moving branch for all Reidemeister moves t of type III and II. It remains to observe that Reidemeister moves of type I evidently do not change $R_1(\text{scan}(T))$ and, as already mentioned, strata of type $\Sigma_{l_c}^{(2)}$ can not occur, because the branch moves under everything else.

□

Notice that R_1 does not have the scan-property for a branch which moves over everything else because the contributions of the strata P_3 and $-\bar{P}_3$ in the positive tetrahedron equation do not cancel out at all (compare Subsection 4.4). Of course, the "dual" 1-cocycle will have the scan property for a branch which moves over everything (compare Remark 5).

Question 5 *Does the 1-cocycle R_1 and son "mirror dual", which is obtained by taking in all definitions mirror images, represent always the same cohomology class in $H^1(M^{\text{reg}}; \mathbb{Z}[x, x^{-1}])$ up to normalization?*

We have proven that R_1 has the scan-property. It is not always trivial as shows the example in Section 3.1. This finishes the proof of Theorem 1.

4.7 Invariance of R_n^i for $n > 1$

We have to go again through the proof of the invariance of R_1 under generic homotopies of arcs in M but with taking into account the colorings. Remember that the linking numbers do not depend on the colorings. Therefore we have only to check the weights W_2 and W_1 .

Reidemeister II moves in a cusp and in a flex: the two respectively three involved crossings have all the same coloring and exactly the same arguments as for R_1 apply.

Simultaneous Reidemeister moves: Evidently, a simultaneous R II-move does not change anything because the two new crossings have the same homological and the same colored type. They are only simultaneously potential f-crossings as well as potential r-crossings. In the first case they have the same weight W_1 . But they have different signs and cancel out together.

For the simultaneous R III-moves we reexamine now Fig. 34 and Fig. 35 which were used in the proof of Lemma 2. Only the cases r_c and l_c have to be considered as in the proof of Lemma 2.

For r_c only the crossing 2 could be a potential f-crossing. The crossing 1 is a r-crossing for 2 if and only if its foot is C_3 and its head is C_2 or C_3 . On the other side of the triple crossing the crossing 3 is a r-crossing for 2 if and only if its foot is C_3 and its head is C_2 or C_3 . But the foots of 1 and 2 have always the same color. The head of 1 has the same color as the head of 2 which is C_2 or C_3 . The head of 3 has the same color as the foot of 2 which is C_2 . It follows that 1 and 3 can only be simultaneously r-crossings for 2 and hence the weights of R_n^i are invariant.

If 1 is a potential f-crossing in l_c then its foot is C_2 . The foot of 3 is always C_2 too. If 1 is a potential f-crossing then the head of 2 is C_2 or C_3 . Consequently, 2 is a r-crossing for 1 if and only if its foot is C_3 . But the head of 3 has the same color as the foot of 2. Consequently, 2 is a r-crossing for 1 if and only if 3 is a potential f-crossing too. In the latter case 2 is also a r-crossing for 3 and hence the weights of R_n^i are again invariant. (Notice that we really need here C_2 or C_3 for the heads of both the f-and r-crossings and there is no solution with only C_2 or only C_3 .)

Refined tetrahedron equation: We have shown in Lemma 3 that the f-crossings for d or ml in the corresponding strata are almost always identical. An exception is the new f-crossing in \bar{P}_3 which is exactly the crossing $hm = 34$ in P_1 and \bar{P}_1 . The crossing d in P_3 and \bar{P}_3 contributes only if it is of type $C_1 \rightarrow C_2$. In this case the crossing ml in P_1 and \bar{P}_1 is of the same type and hence $hm = 34$ has the foot C_2 . Consequently, it is a f-crossing if and only if the head of d in P_1 and \bar{P}_1 is C_2 or C_3 . The r-crossings of corresponding f-crossings can be different. But the difference comes just from passing adjacent strata of triple crossings in the meridian of the quadruple crossing. But we have already shown above in *Simultaneous Reidemeister moves* that this does not change the weights in R_n^i .

Cube equations: We use again Fig. 51 up to Fig. 58. For the type l_b the f-crossings and the r-crossings are always the same for the two triple crossings of an edge. For the type l_c there can be a new f-crossing for ml if hm is one of the crossings of the self-tangencies, compare "11-7". But the remaining two crossings are never r-crossings for hm and hence the weights of R_n^i are invariant.

For the type r_b the f-crossings and the r-crossings are again the same for the two triple crossings of an edge.

Let us consider the edge " r_a 1-7": d contributes if it is of type $C_1 \rightarrow C_2$. The crossing hm and the other crossing from the self-tangencies are now f-

crossings if and only if the head of ml is C_2 . The r-crossings for hm do not change. For the other crossing of the self-tangencies d is a r-crossing for the local type 1 and ml is a r-crossing for the local type 7. But both r-crossings are of type $C_1 \rightarrow C_2$ and hence the weight of R_n^i hasn't changed.

The crossing ml contributes if it is of type $C_1 \rightarrow C_2$. The crossing hm contributes if and only if its head is C_2 or C_3 . But then d is a r-crossing for the other crossing in the self-tangencies for the local type 1 and ml is a r-crossing for the other crossing in the self-tangencies for the local type 7 and the weights of R_n^i are invariant.

Let us consider the edge " r_a 1-5": d contributes if it is of type $C_1 \rightarrow C_2$. The crossing hm is a f-crossing if and only if the head of ml is C_2 . The crossing d is a r-crossing for hm for the local type 1 if and only if it is a r-crossing for hm for the local type 5 too. The other crossing from the self-tangencies is never a r-crossing for hm for the local type 5, but it could be a r-crossing for hm for the local type 1. However, it is of type $C_1 \rightarrow C_2$. Consequently, for a non-degenerate admissible coloring ($C_3 \neq C_1$) the weights of R_n^i are invariant, but for a degenerate admissible coloring we need the same correction term $\epsilon(p)w(hm)(w(ml) - w(d))$ as for R_1 (compare Definition 12 and the proof of Proposition 4). Exactly the same arguments apply also to the contributions of ml because hm is still the only f-crossing.

Let us consider the edge " r_a 1-6": hm is the only potential f-crossing and for the local type 1 only d can be a r-crossing for hm . For the local type 6 the crossing d and the other crossing from the self-tangencies are simultaneously r-crossings. But if hm is a f-crossing then d is of type $C_1 \rightarrow C_2$ or $C_1 \rightarrow C_3$. Consequently, for a non-degenerate admissible coloring the weights of R_n^i are invariant, but for a degenerate admissible coloring we need again the correction term $\epsilon(p)w(hm)(w(ml) - w(d))$.

All other cases are completely analogous and are left to the reader.

Moving cusps and scan-property: There are evidently at most two colors involved. Only the crossing ml could contribute in $\Sigma_{l_c}^{(2)}$. But its overcross and its undercross have the same color. Consequently, it does not contribute because we would have $C_1 = C_2$ (compare Remark 3).

Let us consider the stratum $\Sigma_{r_a}^{(2)}$ of local type 1. The f-and the r-crossings which contribute to W_2 are all identical in the R III-move and in the two R II-moves. It remains to observe that ml does not contribute because we have still $W_1(hm) = 0$. Indeed, if hm is a f-crossing for ml then its foot is C_2 and its head is C_2 or C_3 . The foot of d is C_1 and hence d is a r-crossing

for hm if and only if $C_1 = C_3$ (the degenerate case), compare Fig. 71. But the negative crossing from the self-tangency has also the foot C_1 and it has the head C_2 . Consequently, it is also a r-crossing for hm and we have still $W_1(hm) = 0$.

All other case are completely analogous and are left to the reader.

Notice that we need $C_2 \neq C_3$ in the definition of an admissible coloring only in order to prevent that adding a local knot on a component of the string link leads to a multiplication of the invariant by some factor, which would imply that the invariant is almost trivial because the position of the local knot on the component does matter (compare Proposition 2 and Remark 3).

The proof of Lemma 8 carries over for R_n^i without any changes. The corresponding f-crossings and r-crossings are identical in $-P_2$ and \bar{P}_2 and consequently the corresponding weights in R_n^i are still the same for the two strata. R_n^i satisfies the cube equations, as was already shown above. It follows that the proof of the scan-property carries over for R_n^i without any changes too.

We have proven that $R_n^i(\gamma)$ is invariant under all generic homotopies of an arc γ in M through the six types of strata of Proposition 1 and hence R_n^i is a 1-cocycle in M . Moreover, it has the scan-property and Examples 4 and 5 show that it can detect the non-invertibility of a knot. Example 3 shows that the cohomology class $[R_n^i]$ is not always trivial.

This finishes the proof of Theorem 2.

References

- [1] Bar-Natan D. : On the Vassiliev knot invariants, Topology 34 (1995) 423-472
- [2] Bar-Natan D. : Vassiliev homotopy string link invariants, J. Knot Theory Ramif. 4 (1995) 13-32
- [3] Bar-Natan D. : Some computations related to Vassiliev invariants, <http://www.math.toronto.edu/~drorbn/papers>
- [4] Berger A., Stassen I.: The skein relation for the (g_2, V) -link invariant, Comment. Math. Helv. 75 (2000) 134-155

- [5] Birman J. : Braids , Links and Mapping class groups, Annals of Mathematics Studies 82 , Princeton University Press (1974)
- [6] Birman J., Gebhardt V., Gonzáles-Meneses J.: Conjugacy in Garside groups III: Periodic braids, J. of Algebra 316 (2007) 746-776
- [7] Budney R., Conant J., Scannell K., Sinha D.: New perspectives on self-linking, Advances in Math. 191 (2005) 78-113
- [8] Budney R., Cohen F.: On the homology of the space of knots, Geometry & Topology 13 (2009) 99-139
- [9] Budney R. : Topology of spaces of knots in dimension 3, Proceedings London Math. Soc. 101 (2010) 477-496
- [10] Budney R. : An operad for splicing, arXiv: 1004.3908v4
- [11] Carter J.S., Saito M.: Reidemeister moves for surface isotopies and their interpretations as moves to movies, J. Knot Theory Ramif. 2 (1993) 251-284
- [12] Cooper D., Long D.: Representation theory and the A-polynomial of a knot, Chaos, Solitons & Fractals 9 (1998) 748-763
- [13] Duzhin S., Karev M.: Detecting the orientation of string links by finite type invariants, Functional Analysis and its Appl. 41 (2007) 208-216
- [14] Fiedler T. : Gauss Diagram Invariants for Knots and Links, Mathematics and Its Applications 532 , Kluwer Academic Publishers (2001)
- [15] Fiedler T. : Isotopy invariants for closed braids and almost closed braids via loops in stratified spaces, arXiv: math.GT/0606443 (48 pp)
- [16] Fiedler T. : Quantum one-cocycles for knots, arXiv: 1304.0970v2 (177 pp)

- [17] Fiedler T. : Singularization of knots and closed braids, arXiv: 1405.5562 v3 (165 pp)
- [18] Fiedler T., Kurlin V. : A one-parameter approach to knot theory, J. Math. Soc. Japan 62 (2010) 167-211
- [19] Fox R. : Rolling, Bull.Amer. Math. Soc. 72 (1966) 162-164
- [20] Gramain A.: Sur le groupe fondamental de l'espace des noeuds, Ann. Inst. Fourier 27 (1977) 29-44
- [21] Goussarov M., Polyak M., Viro O.: Finite type invariants of classical and virtual knots, Topology 39 (2000) 1045-1068
- [22] Hatcher A. : A proof of the Smale Conjecture, Ann. of Math. 117 (1983) 553-607
- [23] Hatcher A. : Topological moduli spaces of knots, arXiv: math.GT/9909095
- [24] Hatcher A., McCullough D.: Finiteness of classifying spaces of relative diffeomorphism groups of 3-manifolds, Geometry & Topology 1 (1997) 91-109
- [25] Johannson K. : Homotopy equivalences of 3-manifolds with boundary, Lecture Notes in Math. 761, Springer Berlin (1979)
- [26] Jones V.: Hecke algebra representations of braid groups and link polynomials, Ann. of Math. 126 (1987) 335-388
- [27] Kashaev R.: The hyperbolic volume of knots from the quantum dilogarithm, Lett. Math. Phys. 39 (1997) 269-275
- [28] Kashaev R., Korepanov I., Sergeev S.: Functional tetrahedron equation, Theoret. and Math. Phys. 117 (1998) 1402-1413
- [29] Kauffman L. : Knots and Physics, World Scientific, Singapore (1991)
- [30] Kuperberg G.: Detecting knot invertibility, J. Knot Theory Ramifications 5 (1996) 173-181

- [31] Mortier A.: Combinatorial cohomology of the space of long knots, *Alg. Geom. Top.* 15 (2015) 3435-3465
- [32] Mortier A.: Finite-type 1-cocycles, *J. Knot Theory Ramifications* 24 (2015) 30 pp.
- [33] Murakami H., Murakami J.: The colored Jones polynomials and the simplicial volume of a knot, *Acta Math.* 186 (2001) 85-104
- [34] Polyak M., Viro O.: Gauss diagram formulas for Vassiliev invariants, *Internat. Math. Res. Notes* 11 (1994) 445-453
- [35] Przytycki J.: Skein modules of 3-manifolds, *Bull. Polish Acad. Sci. Math.* 39 (1991) 91-100
- [36] Sakai K.: An integral expression of the first non-trivial one-cocycle of the space of long knots in \mathbb{R}^3 , *Pacific J. Math.* 250 (2011) 407-419
- [37] Turaev V.: The Conway and Kauffman modules of a solid torus, *J. Soviet. Math.* 52 (1990) 2799-2805
- [38] Turchin V. : Computation of the first non-trivial 1-cocycle in the space of long knots, (Russian) *Mat. Zametki* 80 (2006), no. 1, 105-114; translation in *Math. Notes* 80 (2006), no. 1-2, 101-108.
- [39] Vassiliev V. : Cohomology of knot spaces // in: *Theory of Singularities and its Applications*, *Advances in Soviet. Math.* 1 (1990) 23-69
- [40] Vassiliev V. : Combinatorial formulas of cohomology of knot spaces, *Moscow Math. Journal* 1 (2001) 91-123
- [41] Waldhausen F. : On irreducible 3-manifolds which are sufficiently large, *Ann. of Math.* 87 (1968) 56-88
- [42] Witten E.: Quantum field theory and the Jones polynomial, *Comm. Math. Phys.* 121 (1989) 351-399

Institut de Mathématiques de Toulouse, UMR 5219
Université Paul Sabatier
118, route de Narbonne
31062 Toulouse Cedex 09, France
fiedler@math.univ-toulouse.fr